Strengthening Historic Covered Bridges To Carry Modern Traffic

May 2007

U.S. Department
of Transportation
**Federal Highway
Administration**

FOREWORD

The National Historic Covered Bridge Preservation Program (NHCBP) includes preservation of covered bridges that are listed, or are eligible for listing, on the National Register of Historic Places. It also advocates research for better means of restoring and protecting historic covered bridges, using advanced technology. *Strengthening Historic Covered Bridges To Carry Modern Traffic* is aimed at the highest form of historic preservation: maintaining the bridge not only physically, but also functionally. While the builder's original form is preserved, the structure continues to serve as a real bridge and not a historical relic. The technology being investigated uses glass-fiber reinforced polymer (GFRP) products to increase the strength of the members with minimal increases in x-section. The study also looks at ways to mask the use of the GFRP components. This study is just the beginning of research on this topic. The concept will be refined and amplified in future projects. This report is intended primarily for engineers, contractors, researchers, consultants, bridge owners, and historic bridge preservationists to help them keep these historic structures in full service. This report does not supersede any other. This publication is the final version of the report.

This report corresponds to the TechBrief titled, "Strengthening Historic Covered Bridges To Carry Modern Traffic" (FHWA-HRT-07-041). This report is being distributed through the National Technical Information Service for informational purposes only. The content in this report is being distributed "as is" and may contain editorial or grammatical errors. This report is the result of work performed under the following contract number: DTFH61-00-C-00081.

Technical Report Documentation Page

1. Report No.	2. Government Accession No.	3. Recipient's Catalog No.
4. Title and Subtitle Strengthening Historic Covered Bridges To Carry Modern Traffic		5. Report Date: May 2007 6. Performing Organization Code 00108
7. Authors Samer Petro, P.E.; Hota GangaRao, P.E., Ph.D.; Emory Kemp, P.E., Ph.D.; Rex Cyphers, E.I.T.; Jeffrey Teagarden, E.I.T		8. Performing Organization Report No.
9. Performing Organization Name and Address Constructed Facilities Center, College of Engineering & Mineral Resources; and Institute for History of Technology & Industrial Archaeology, Eberly College; West Virginia University; Morgantown, WV 26506		10. Work Unit No. 11. Contract or Grant No. DTFH61-00-C-00081
12. Sponsoring Agency Name and Address Federal Highway Administration Office of Infrastructure R&D 6300 Georgetown Pike McLean, VA 22101-2296 Federal Highway Administration Office of Bridge Technology 400 7th Street, NW Washington, DC 20590		13. Type of Report and Period Covered Final: September 2000 to March 2004 14. Sponsoring Agency Code

15. Supplementary Notes
Contracting Officer's Technical Representatives (COTRs):
Sheila Rimal Duwadi, P.E. (HRDI-07) and John O'Fallon , P.E. (HRDI-07)

16. Abstract

In this research project, the Constructed Facilities Center (CFC) and the Institute for the History of Technology and Industrial Archaeology (IHTIA) of West Virginia University (WVU) teamed up to develop means and methods to strengthen wooden superstructure components of historic covered bridges, using glass-fiber reinforced polymer (GFRP) composite materials. The strengthening methodologies developed in this project were designed to conform to the Secretary of the Interior's Standard for Historic Preservation.

Specifically, tension and bending tests were conducted to establish the bond strength of GFRP rebars embedded in wood, and to establish the bending strength and stiffness of large-scale floor beams reinforced with GFRP pultruded plates and with GFRP rebars. In addition, methods were developed to enhance the shear capacity of large-scale floor beams reinforced with GFRP pultruded plates bonded on edge in narrow, prerouted vertical slots. The GFRP rebars were developed to be used specifically as axial reinforcement for truss members, while the GFRP were developed to increase the bending and shear capacity of floor beams. The test results showed bonded-in GFRP rebars performed very well in terms of pullout force and bond strength, and the strength and stiffness of GFRP-reinforced floor beams improved significantly. Although the shear strength was also expected to improve considerably with the addition of the GFRP plates placed on edge (resulting in a flitched beam), the shear capacity decreased slightly. The flitched beams tested were severely checked, which degraded their shear strength as compared to the solid control specimen. Further testing will continue in a succeeding study.

Additionally, during this research, several methods of concealing the reinforcement were investigated. One successful method took advantage of routing a member on the bottom face and bonding a GFRP plate with an integrated veil to match the wood grain and color of the original aged wood.

17. Key Words	18. Distribution Statement
covered bridge, glass-fiber reinforced polymer (GFRP), historic preservation, flitched beam, horizontal shear, GFRP plates, GFRP rebars, pultrusion, strengthening.	No restrictions. This document is available to the public through the National Technical Information Service, Springfield, VA 22161.

19. Security Classif. (of this report)	20. Security Classif. (of this page)	21. No of Pages	22. Price
Unclassified	Unclassified	116	

SI* (MODERN METRIC) CONVERSION FACTORS

APPROXIMATE CONVERSIONS TO SI UNITS

Symbol	When You Know	Multiply By	To Find	Symbol
		LENGTH		
in	inches	25.4	millimeters	mm
ft	feet	0.305	meters	m
yd	yards	0.914	meters	m
mi	miles	1.61	kilometers	km
		AREA		
in^2	square inches	645.2	square millimeters	mm^2
ft^2	square feet	0.093	square meters	m^2
yd^2	square yard	0.836	square meters	m^2
ac	acres	0.405	hectares	ha
mi^2	square miles	2.59	square kilometers	km^2
		VOLUME		
fl oz	fluid ounces	29.57	milliliters	mL
gal	gallons	3.785	liters	L
ft^3	cubic feet	0.028	cubic meters	m^3
yd^3	cubic yards	0.765	cubic meters	m^3
	NOTE: volumes greater than 1000 L shall be shown in m^3			
		MASS		
oz	ounces	28.35	grams	g
lb	pounds	0.454	kilograms	kg
T	short tons (2000 lb)	0.907	megagrams (or "metric ton")	Mg (or "t")
		TEMPERATURE (exact degrees)		
^oF	Fahrenheit	5 (F-32)/9 or (F-32)/1.8	Celsius	^oC
		ILLUMINATION		
fc	foot-candles	10.76	lux	lx
fl	foot-Lamberts	3.426	$candela/m^2$	cd/m^2
		FORCE and PRESSURE or STRESS		
lbf	poundforce	4.45	newtons	N
lbf/in^2	poundforce per square inch	6.89	kilopascals	kPa

APPROXIMATE CONVERSIONS FROM SI UNITS

Symbol	When You Know	Multiply By	To Find	Symbol
		LENGTH		
mm	millimeters	0.039	inches	in
m	meters	3.28	feet	ft
m	meters	1.09	yards	yd
km	kilometers	0.621	miles	mi
		AREA		
mm^2	square millimeters	0.0016	square inches	in^2
m^2	square meters	10.764	square feet	ft^2
m^2	square meters	1.195	square yards	yd^2
ha	hectares	2.47	acres	ac
km^2	square kilometers	0.386	square miles	mi^2
		VOLUME		
mL	milliliters	0.034	fluid ounces	fl oz
L	liters	0.264	gallons	gal
m^3	cubic meters	35.314	cubic feet	ft^3
m^3	cubic meters	1.307	cubic yards	yd^3
		MASS		
g	grams	0.035	ounces	oz
kg	kilograms	2.202	pounds	lb
Mg (or "t")	megagrams (or "metric ton")	1.103	short tons (2000 lb)	T
		TEMPERATURE (exact degrees)		
^oC	Celsius	1.8C+32	Fahrenheit	^oF
		ILLUMINATION		
lx	lux	0.0929	foot-candles	fc
cd/m^2	$candela/m^2$	0.2919	foot-Lamberts	fl
		FORCE and PRESSURE or STRESS		
N	newtons	0.225	poundforce	lbf
kPa	kilopascals	0.145	poundforce per square inch	lbf/in^2

*SI is the symbol for the International System of Units. Appropriate rounding should be made to comply with Section 4 of ASTM E380.
(Revised March 2003)

Table of Contents

List of Figures

List of Tables

List of Symbols

Δ	Deflection	V	Shear load, lbs
$\mu\varepsilon$	Microstrain	Q	First moment of area
E	Modulus of Elasticity	b	Beam width
EI	Flexural Rigidity	$\bar{y}$	Distance from centroid of area to neutral axis
I	Moment of Inertia	A	Area
I_T	Transformed Moment of Inertia	$\bar{y}_b$	Centroid of the entire beam
M_{Theo}	Theoretical Moment	$\bar{y}_i$	Centroid of each element in beam
M_{Exp}	Experimental Moment	A_i	Area of each element
MOE	Modulus of Elasticity of the Beam	b_i	Solid beam width
MOR	Modulus of Rupture	b_v	Notch width
n	Modular ratio	b_r	Reinforcement width
P	Load	h_i	Height of each element
τ	Shear stress	b_t	Transformed beam width
G	Shear Modulus	Q	First moment of area
g	Shear strain	d_i	Distance from the centroid of the element to the neutral axis

EXECUTIVE SUMMARY

In this research program, the Constructed Facilities Center (CFC) and the Institute for the History of Technology and Industrial Archaeology (IHTIA) of West Virginia University (WVU) teamed up to develop means and methods to strengthen wooden superstructure components of historic covered bridges using glass-fiber reinforced polymer (GFRP) composite materials. The strengthening methodologies developed during this research project were designed to conform with the Secretary of the Interior's Standard for the Treatment of Historic Properties.

Specifically, tension and bending tests were conducted to establish the bond strength of GFRP rebars embedded in wood and to establish the bending strength and stiffness of large-scale floor beams reinforced with GFRP pultruded plates and GFRP rebars. Additionally, methods were developed to enhance the shear capacity of large-scale floor beams reinforced with GFRP pultruded plates bonded on edge in prerouted narrow vertical slots. The GFRP rebars were developed for use specifically as reinforcement for truss members, while the GFRP plates were developed to enhance the bending and shear capacity of floor beams. The results showed bonded-in GFRP rebars performed very well for pullout force and bond strength, and the strength and stiffness of GFRP reinforced wooden beams improved significantly. Although the shear capacity was expected to improve significantly with the addition of the GFRP plates placed on edge (resulting in a flitched beam), the shear capacity decreased slightly. The flitched beams tested were severely checked, which reduced their shear strength in contrast to the solid control specimen. Further testing will continue.

Additionally, during this research, several methods of concealing the reinforcement were investigated. One successful method takes advantage of routing a member on the bottom face and bonding a GFRP plate with an integrated veil to match the grain and color of the original aged wood.

CHAPTER 1—INTRODUCTION

1.1. BACKGROUND

During the 1800s and most particularly after the Civil War, a great many covered wooden bridges were built almost entirely by hand throughout the United States. Many types and designs comprised the once abundant population of covered wooden bridges, of which fewer than 1000 remain as icons of nineteenth-century American bridge engineering and craftsmanship. Of great importance to historians, engineers, and the general public, most remaining covered bridges are listed or eligible to be listed on the National Register of Historic Places. In West Virginia, covered bridges are not only a part of the State's distinctive heritage, but also a tourist attraction to the region's most serene settings. Members of the National Society for the Preservation of Covered Bridges make annual trips to West Virginia and other States to see and photograph covered bridges.

Of the remaining covered bridges, some have been closed to vehicle traffic, while others are being moved to local fairgrounds or parks for use as pedestrian crossings. In some cases, new bridges have been built alongside existing covered bridges to divert traffic. As a matter of integrity, ideal preservation practice involves restoration and rehabilitation of existing covered bridges, thus allowing them to carry modern loads and at the same time preserving their historic and aesthetic values and national heritage.[1] Figure 1 is a photograph of what can be done to preserve the vibrant heritage of American civil engineering. This photograph shows the Barrackville, WV, covered bridge, the second oldest covered bridge still in service in that State. In 1987 a new bridge was built next to the Barrackville covered bridge to carry highway traffic, and the Barrackville covered bridge, restored in 1999, is used as a pedestrian bridge. Figure 2 is a drawing of the same bridge, depicting the Burr Arch construction patented by Theodore Burr in 1817.[2]

The Transportation Equity Act of the 21st Century (TEA-21) established the National Historic Covered Bridge Preservation Program (NHCBP). Under this program (which provides funding for research and development of improved means to restore and protect covered bridges and to assist States in rehabilitation, repair, and preservation of historic covered bridges), the Federal Highway Administration (FHWA) is funding the rehabilitation, restoration, and preservation of a large number of bridges. Unfortunately, a lack of acceptable modern technologies hinders the preservation of remaining historic structures if they are to continue to carry vehicular traffic.

This project of the Constructed Facilities Center (CFC) and the Institute for the History of Technology and Industrial Archaeology (IHTIA) of West Virginia University (WVU) was funded by FHWA to develop methodologies for the preservation of historic structures through the use of advanced composite materials and innovative techniques.

Figure 1. Photo. Barrackville Covered Bridge, Barrackville, WV.

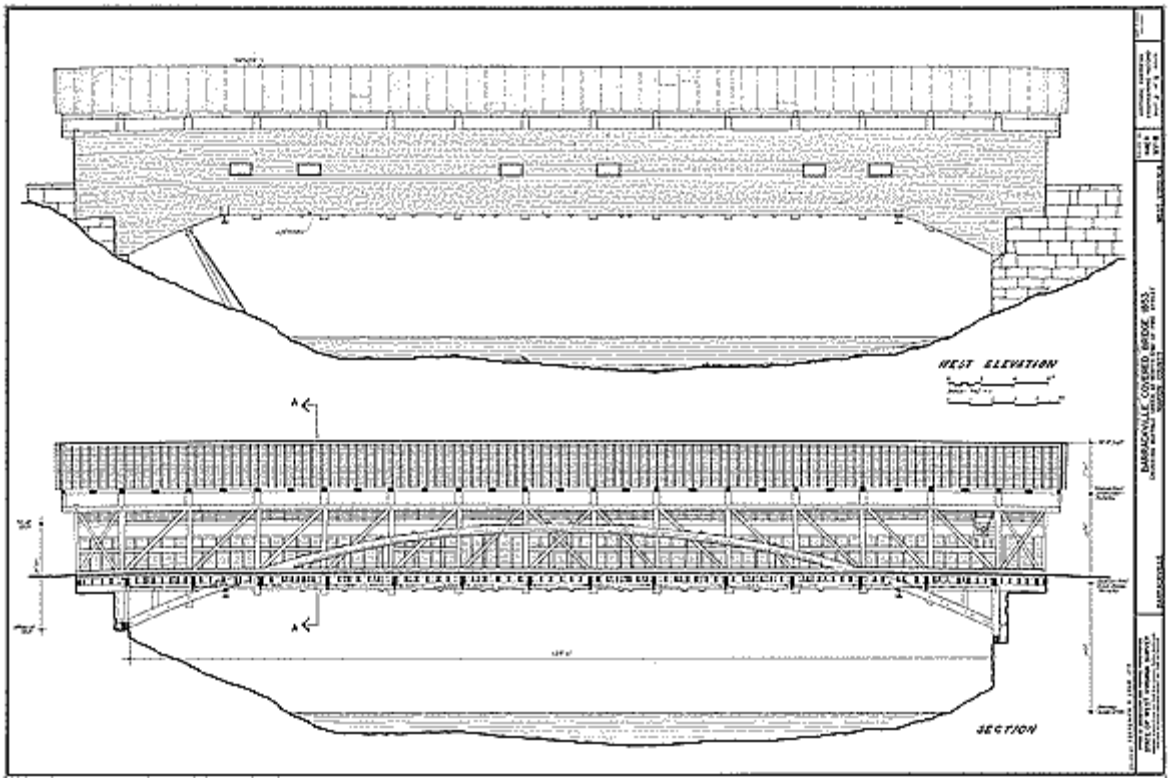

Figure 2. Illustrations. Drawings of Barrackville Covered Bridge.

1.2. OBJECTIVES AND SCOPE OF WORK

1.2.1 Objectives

The primary goals of this project are to develop means and methods to strengthen timber superstructure components of historic covered bridges without compromising the structural and material integrity of the original structure and its heritage. The specific objectives are to:

- Develop methods to strengthen truss and arch members.
- Develop methods to strengthen floor beams.
- Develop simple analytical models to predict moment and shear capacities of strengthened members.
- Conduct a state-of-the-art literature review and compile an annotated bibliography.

1.2.2. Scope of Work

This research offers a new approach to preserving historic covered bridges: strengthening them to carry modern traffic. Chapter 2 provides a look at current and past methods being used to rehabilitate and preserve covered bridges. Innovative methods for strengthening that were developed and tested in the laboratory for tension and bending members are described in chapter 3. Chapter 4 presents the results of experimental tests, and chapter 5, the conclusions and recommendations. Appendix A presents a description of some of the preliminary testing, while appendix B presents an annotated bibliography.

1.3. RESEARCH SIGNIFICANCE

Common preservation or repair methods for historic timber structures and covered bridges often use steel fasteners, additional timber members, and steel components.[11] These techniques are less than desirable for historic structures because they result in an adulteration of a structure's history and are not compatible with the highest standards of preservation.[2]

The goal of this research is to develop methods and techniques that comprehend historic preservation as part art and part science. In the view of the author(s), the proposed methods of internally strengthening truss members and floor beams using advanced composite materials, as described in this report and discussed at length in the following chapters, will serve to improve the member's load carrying capacity and yet maintain its authenticity. The reason for this approach is the preservation of the authentic historic structure for future generations.

CHAPTER 2—LITERATURE REVIEW

2.1. INTRODUCTION

A detailed literature review was conducted to determine what methods are currently being used and what methods are being developed to preserve and strengthen historic covered bridges. More than 50 recent journal articles and technical papers reviewed were culled from sources such as the MountainLynx (WVU Library and statewide library system), Compendex, and Applied Science & Technology databases, and the Internet. In addition, several reports and dissertations from different universities were reviewed. This review also highlighted areas such as current and modern methods of preserving covered bridges as described in the following sections. Also described in detail are the Secretary of the Interior's Standard for The Treatment of Historic Properties (hereafter referred to as the SOI's Standards) which were followed for this project.

2.2. HISTORIC COVERED BRIDGES

Covered bridges represent our history frozen in time. During the 1800s, 10,000 covered bridges were built almost entirely by hand in the United States. Although covered bridges are considered an American tradition, the origins of the covered bridge can be traced to Europe. American covered bridges grew out of craft tradition, which had its roots in heavy timber construction as applied to barns, buildings, and ships. For bridges over major river crossings, the covered timber truss bridge was developed where simple trestle bridges were insufficient. The covering served the practical purpose of protecting the main truss members from the environment. Such bridges were used for local roads as well as turnpikes. Covered bridges were also used on early railway lines. The construction of covered bridges in 19th-century America led to the development of the all-metal truss bridges.

In 1950, 80 covered bridges remained in West Virginia, alone. Today, however, only 17 are left in West Virginia, 221 in Pennsylvania, 140 in Ohio, and 93 in Indiana. While this is not a promising statistic, if the proper methods are developed, all of these bridges can be saved. Emory L. Kemp sums up the battle between stabilization, repair, restoration, and replacement by saying, "The engineer's chief concern is for the safety of the traveling public and this concern is pitted against the requirement to restore these structures according to well-developed national standards for historic preservations".[2] Abba Lichtenstein warns of the issues standing between replacement and rehabilitation, "On one side of the conflict is the owner who must, with limited funds, protect the safety of the public by making sure that the structure is up to code. On the other is the preservation community whose members want to retain the bridge at any cost. Emotions run high and many issues enter this conflict."[3] Furthermore, one of the main reasons for the replacement of such bridges, instead of restoration, is the fact that few engineers have the background and experience in the design and rehabilitation of timber bridges. It is currently easier to replace a bridge than to find an alternative solution that preserves it.

One argument advanced much too often is that engineers resist restoring historic bridges because of the difficulty of the work is not always reflected in the lower fees involved. Engineers on the average usually receive 10 percent of the total construction value for design services. For

example, the new construction option might cost approximately more than three times that of a preservation alternative.[4] This is highlighted by the argument over the cost of rehabilitating the historic Norridgewock concrete arch bridge.[5] It was said by some that the engineers inflated the cost for the rehabilitation option, either because of lack of knowledge or because they wanted the new design option.[4] The latter would be very unlikely, since it would be a breach of engineering ethics.

Unless there is clear danger to the public, historic bridges should not be destroyed. Solutions for their preservation should be found, and bridge engineers/historians have a major contribution to make in this endeavor. This is where research being conducted at CFC and IHTIA at WVU and elsewhere really comes into play. Methods are being developed to save these bridges while keeping public safety and modern usages in mind.

Of the nearly 50,000 bridges nationwide that might have historical significance, approximately 1600 are listed on the National Register and 900 more are eligible for listing. Until recently, however, relatively few historic bridges have been rehabilitated to carry modern vehicular traffic. Many challenges await those engineers who have an understanding of the materials and techniques used to construct the bridges of the past. The balance between preservation principals demanding authenticity and codes requiring safety, strength and stability must be achieved by future innovations.[6] The Cultural Resource Management (CRM) lists 10 high-profile historic bridge rehabilitation projects in one of it supplements. All of the projects use external strengthening techniques or replacement of members as a method of rehabilitation. Not a single project rehabilitated and strengthened existing members using methods that would not interfere with the historic integrity of the member.

Emory L. Kemp also discusses methods of preservation other than full restoration of an existing structure.[7] For example, preservation through recording is a tool to document and study a structure that does not meet safety or use requirements; it provides a means of preservation, if only on the record. Structural stabilization, on the other hand, can temporarily make a structure safe until funding is available for a broader project or new methods are developed. Adaptive reuse is another method widely used in buildings, but not readily used in bridges. This reuse might mean removing a covered bridge from service, moving it to a park, and using it for pedestrian traffic. Partial restoration is yet another method to restore or rehabilitate portions of a structure at a time when funding is available and it becomes feasible to restore one part of the historic structure. Other parts of the structure can be restored at a later date. This method can also be used to restore only the portions of a structure that absolutely require it.

One document that offers substantial information on historic structure preservation is the Secretary of the Interior's Standard for the Treatment of Historic Properties (the "Secretary's guidelines").

2.3. THE SECRETARY OF THE INTERIOR'S STANDARDS FOR THE TREATMENT OF HISTORIC PROPERTIES

One of the goals of this project is to develop the means and methods to rehabilitate, strengthen and preserve covered bridges by complying with the Secretary of the Interior's Standards for the Treatment of Historic Properties with Guidelines for Preserving, Rehabilitating, Restoring, and

Reconstructing Historic Buildings.[8] (The SOI's Standards)While these guidelines are more for use with historic buildings than with covered bridges, as the title suggests, they nevertheless address proper stewardship in dealing with any historic property. The guidelines define rehabilitation as "the process of returning a property to a state of utility, through repair or alteration, which makes possible an efficient contemporary use while preserving those portions and features of the property which are significant to its historic, architectural, and cultural values." The use of the terms "alteration" and "contemporary" in the definition seems to indicate that major changes can be made to achieve the desired end-use of a property. This is far from the truth, however, because no changes or alterations can be made that will affect the significance of the property. In other words, placement of steel or concrete beams under an existing covered bridge does not contribute to the preservation of the historic or cultural value of the historic property. The design and construction of the original timber truss and arch members along with the siding, covering and other elements are what makes covered bridges significant. The Secretary's guidelines present ten rules for rehabilitation of historic properties. These rules have been the guiding principals for the current research project:[8]

1. A property will be used as it was historically, or be given a new use that maximizes the retention of distinctive materials, features, spaces, and spatial relationships.

2. The historic character of a property will be retained and preserved. The replacement of intact or repairable historic materials or alteration of features, spaces, and spatial relationships that characterize a property will be avoided.

3. Each property will be recognized as a physical record of its time, place, and use. Changes that create a false sense of historical development, such as adding conjectural features or element from other historic properties, will not be undertaken.

4. Changes to a property that have acquired historic significance in their own right will be retained and preserved.

5. Distinctive materials, features, finishes, and construction techniques or examples of craftsmanship that characterize a property will be preserved.

6. Deteriorated historic features will be repaired rather than replaced. Where the severity of deterioration requires replacement of a distinctive feature, the new feature will match the old in design, color, texture, and, where possible, materials. Replacement of missing features will be substantiated by documentary and physical evidence.

7. Chemical or physical treatments, if appropriate, will be undertaken using the gentlest means possible. Treatments that cause damage to historic materials will not be used.

8. Archeological resources will be protected and preserved in place. If such resources must be disturbed, mitigation measures will be undertaken.

9. New additions, exterior alterations, or related new construction will not destroy historic materials, features, and spatial relationships that characterize the property. The new work

shall be differentiated from the old and will be compatible with the historic materials, features, size, scale and proportion, and massing to protect the integrity of the property and its environment.

10. New additions and adjacent or related new construction will be undertaken in such a manner that, if removed in the future, the essential form and integrity of the historic property and its environment would be unimpaired.

2.4. PAST AND PRESENT METHODS FOR PRESERVING COVERED BRIDGES

Some past methods of strengthening historic covered bridges did not really strengthen the bridge; they turned the bridge into a timber covering over a steel or concrete deck. Steel I-beams or reinforced concrete slabs were often placed beneath a new deck to support the entire structure.[10] The original bridge members would be replaced as needed, but no longer served the purpose the designer intended. Examples of this type of preservation are commonplace; such methods have been used everywhere that covered bridges were built. Figure 3 is an example of a covered bridge that was rehabilitated with steel beams.

Figure 3. Photos. Roddy Road Covered Bridge (a) rehabilitated with steel I-beams (b), Frederick County, MD.

The Roddy Covered Bridge is a kingpost design originally constructed in 1856. The structure possesses a 12.2-meter (m) (40-foot (ft)) span, 4.9-m (16-ft) width, and 3.7-m (12-ft) clearance. The timber deck stringers were replaced with steel in 1964–65 to strengthen the structure and increase load capacity. These steel stringers were replaced again in 1979–80 because they had completely corroded and once again by galvanized steel stringers and diaphragms in 1995.

Another method used to rehabilitate is to replace original members with wood of the same type. A detailed evaluation and load rating must be conducted on the bridge to determine which members must be replaced and which ones can be salvaged. Members exhibiting moderate to heavy insect infestation, splitting, rotting, charring, weathering, and water damage are replaced.[11]

Other common methods for strengthening deteriorated wooden members include the use of steel fasteners, additional timber members, and steel components. The following describes some of these strengthening methods namely: member augmentation, and stitching, stress laminating, and epoxy repair. [11]

- Member augmentation involves the addition of material to reinforce or strengthen existing members. The added pieces, commonly wood or steel plates attached with bolts, serve to increase the effective section and thus the load capacity. The two most widely used methods of member augmentation—splicing and scabbing—while efficient, are to be avoided in restoration work. Splicing generally applies to a defined location where load transfer is to be restored at a break, split, or other defect. Traditional methods for both tension and compression splices can be augmented with glued scarf joints, lapped joints, and mortice and tenon joints, and/or the insertion of fiber-reinforced polymer (FRP) bars. In many cases, a thorough structural analysis is required to ensure the capacity of the repair and to verify stress distribution in the members. Situations that introduce eccentric loads or tension perpendicular to grain must be avoided.
  A typical problem associated with timber members is the development of longitudinal splits and checks. Checks commonly develop in sawn lumber as a member seasons. To a lesser degree, splits or checks may also develop in glued laminated (glulam) decks if delamination occurs at the glue lines, although this problem has become very rare with the introduction of waterproof adhesives. In sawn members, splits can also develop from overloads or poor design details that introduce tension perpendicular to grain at connections. When splitting is detected, it must be determined whether the splits are the result of normal seasoning or of a structural problem.

- Stitching is a strengthening operation that uses treenails to arrest cracks, splits, or delaminations in timber members. An example of stitching is shown in figure 4. These methods are most commonly used for buildings, but also apply to some bridge components, particularly truss members or other structures with a high number of small members or connections. The objective is not to close the split or check, but rather, by drawing the two parts together, to prevent further progression of splitting. Aside from fastener design requirements, there are no specific design criteria for stitching; the configuration, number, and size of treenails must be based on the magnitudes of forces to be transferred and on designer judgment, which can be site specific.[9]

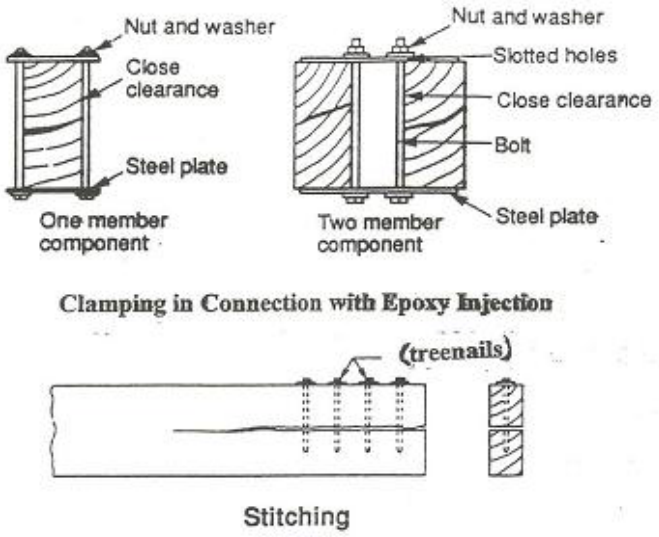

Figure 4. Illustrations. Typical clamping and stitching of timber members.

- Stress laminating is probably the most effective method for mechanical repair of existing nail-laminated decks. Such decks frequently separate and delaminate as a result of repeated loading, which causes breakup of asphalt wearing surfaces, water penetration through the deck, and loss in live-load carrying capacity. In these cases, the static strength and condition of the deck are generally maintained, but the deck's serviceability and ability to distribute loads between individual laminations is greatly reduced. In this situation, the laminations no longer act together to distribute loads, which can lead to local failures. This condition can increase the rate of deterioration, eventually leading to failures that require complete deck replacement.

- Epoxy is used for timber repair as a bonding agent (adhesive) and/or grout (filler) in structural repairs. It is commonly injected under pressure, but it is also manually applied as a gel or putty. Epoxy is most effective when used as a bonding agent to provide shear resistance between members for structural repairs in dry locations. For structural repairs, it is used to fill voids or repair bearing surfaces. Four basic types of epoxy repairs for structural repairs are typically used. These include: injection of epoxy into cracked and split members at truss joints; epoxy injection and reinforcement of decayed wood; splicing and epoxy injection of broken members; and epoxy injection of delaminated beams. Epoxy is also used for two basic types of semistructural repairs: injection into longitudinal cracks and splits in truss members away from joints; and repair of bearing surfaces using a filler combining epoxy with substances such as ground walnut shells.

2.5 INNOVATIVE METHODS FOR PRESERVING COVERED BRIDGES

The initial task of preserving covered bridges is to develop innovative and better methods of in situ evaluation. The first task of these methods is to determine if a structural member needs to be

replaced or if it has enough capacity to resist required loads. Better evaluation allows members that once would have been replaced to remain in service. One innovative method of evaluation is stress-wave timing in wooden members.[12] This method times the propagation of a stress wave through a material. Because typical stress-wave transmission times for different species at different moisture contents are known, areas of decay can thus be readily identified. This test is carried out by striking the specimen with a special hammer and using an accelerometer to measure the time it takes the wave to propagate through the specimen. This tool is especially valuable in a large member into which conventional methods can reach only short distances.

Laser scanning offers another innovative technology useful to historic preservation. A laser scanner is similar to a total station in land surveying except that the laser scanner can develop highly accurate three-dimensional drawings of structures. ("Total station" refers to the instrument used by surveyors similar to a transit.) At a range of 45.7 m (150 ft), the laser scanner is accurate within millimeters. This technology has already been used on an 1876 courthouse in northwestern Pennsylvania, one that has very intricate architecture, and on a historic bridge in Rhode Island. Laser scanning can provide some of the most accurate drawings possible. This technology can be used for recording not only historic buildings and bridges, but also historic sites.[13] With this technology, sites that in the past would have been lost due to long recording times can now be recorded in a matter of hours.

Another method of modern analysis that provides a better understanding of the historic structure is the use of finite element method (FEM) analyses.[14] FEM models can be updated by direct field measurements such as strains and deflections. An updated model can provide very accurate simulated responses and can be useful in the overall structural evaluation. The resulting analyses recount the current story of the structure, including how much load the structure is carrying, how the loads are being transferred to the ground, and what the current material strengths and properties might be. Such current data are all-important in the evaluation and decisionmaking necessary to determine if a structure can be rehabilitated.

An amazing amount of information is available through the use of nondestructive testing (NDT) methods and tools to help conduct an accurate evaluation of historic structures. NDT methods such as stress-wave timing and others can be used to uncover defects, determine material properties, locate reinforcing steel, or identify depth of foundation. These methods include ultrasonic pulse velocity, stress-wave timing, impact echo, sonic echo, infrared thermography, radar, covermeter, and electric half-cell.[15] Fiber optic borescopes can also be used to look inside walls and other cavities without removing any material.

The application of the ultrasonic NDT method has also been used widely and successfully to test historic structures. For example, CFC of WVU has developed state-of-the-art portable field instrumentation to conduct ultrasonic testing of historic bridges. CFC tested the Barrackville, WV, Covered Bridge (figures 1 and 2 of chapter 1) and the Salt Creek Covered Bridge located in Muskingum County, OH. The Salt Creek Covered Bridge, built in 1876 using white oak, is a warren truss that spans 31.7 m (104 feet). This makes it as one of the longest clear-span timber bridges in the State of Ohio (figure 5).

Figure 5. Photos. Salt Creek Covered Bridge, Muskingum County, OH.

The Salt Creek ultrasonic field testing assessed the integrity of the upper truss chords for repair and renovation. Figure 5 also shows the sensor positions for the ultrasonic through-transmission mode and the spring-loaded quick grip clamp. The results of the field testing indicated that 17 members in the bridge had defects needing immediate rehabilitation. CFC also developed an NDT manual for bridge superstructures for the West Virginia Department of Transportation (WVDOT).

The most promising innovation in preservation is the use of fiber-reinforced polymers (FRP) to strengthen structural members. FRP materials are composed of fibers embedded in a polymeric matrix. They are characterized by excellent tensile strength in the direction of the fibers, which makes them excellent as structural reinforcement. The concept of fiber reinforcement materials dates back to the Israelites in 800 B.C., when they reinforced bricks with straw.[16] The FRP matrix consists of a polymer or resin used as a binder for the reinforcing fibers. The matrix has two main functions. It enables the load to be transferred among the fibers and it protects the fibers from degradation and environmental effects. The three main types of commonly used resins include epoxy, vinylester, and phenolic. In an FRP composite material, the fibers have the role of load bearing. For structural applications, glass, carbon, and aramid fibers have been used. For infrastructural applications, glass and carbon are the most commonly used. FRPs can also be fabricated into nearly any shape imaginable. Individual fibers can be wound, pultruded, or laid up in the final shape. Filament winding entails the wrapping of resin-impregnated fibers around a mandrel. Pultrusion is the continuous production of a composite shape by pulling it through a die. Lay-up fabrication consists of the placement of multiple layers of resin-impregnated fibers or fabrics onto a designed shape. FRP composites are used in the construction industry in various forms and shapes such as:

- Sheets of fibers with resin applied in place.
- Laminates formed from sheets stacked with resin.
- Unidirectional and multidirectional sheets or fabrics with resin applied in place.

The following are just some of the reasons to consider FRP composites:[17]

- Tensile strength—FRP composites' tensile strength can range from about that of mild reinforcing steel to beyond that of prestressing steel.
- Low mass—FRPs have densities that range from 1,201 kilograms/cubic meter (kg/m^3) (75 pounds per cubic foot (lb/ft^3)) to 2,595 kg/m^3 (162 lb/ft^3), which is substantially less than that of steel, which is about 7,849 kg/m^3 (490 lb/ft^3).
- Other advantages—Ease of fabrication, custom geometry, color and coating, construction and transportation cost, reduced environmental toxicity, and resistance to corrosion. FRPs can be recycled and made from other recycled plastics.

Some of the disadvantages of FRPs are high first cost, creep, low modulus of elasticity, and shrinkage. The designs also require highly trained and specialized engineers.[17]

FRPs have been used to strengthen timber, concrete, steel, masonry, and stone structural members. Some specific applications for these materials include column-beam connections, seismic retrofitting, repair of corrosion damaged beams and columns, bridge decks, piles, precast prestressed concrete shells, chimney stacks, lighthouses, roofs, and prestressed water tanks.[18]

2.5.1. Externally Bonded Repair

FRP composites bonded externally can be used to strengthen members in several different ways. The process usually includes surface preparation, resin application, and the adhesion of an FRP sheet or fabric. The fiber direction in the FRP sheet or fabric allows for the possibility to increase mechanical properties such as strength and stiffness in different directions, depending on the application.

One of the most popular uses of FRPs is the reinforcement of bending members or FRP plate bonding. Although the application of a laminate or a fabric wrap is commonly used, in historic structures this cannot be done because of the alteration to the exterior of the member in the process of achieving the desired result. Strengthening must be accomplished in a manner that is not intrusive. In most cases, structural retrofit of timber beams by bonding FRP enhances the bending capacity by 40–100 percent in contrast to an unreinforced specimen.[19] This wide range of results can be attributed to the variability of the wood itself. Researchers have investigated the influence of factors such as FRP plate thickness, type of adhesive, and type of fibers.

When creep is an issue in a timber beam and laminates are used to reinforce the member, it does not matter which type of FRP is used. In most cases, the creep of wood and not the FRP is the dominating mechanism.[20] Furthermore, it has been shown that a small quantity of shear reinforcement can lead to substantial increases in shear capacity.[21] A crucial point in the understanding of shear reinforcement is that the theoretical capacity determined in laboratory

testing environments proved very accurate when compared to the experimental. This means that an accurate prediction can be made when designing FRP reinforcement for shear.

FRPs are very sensitive to the resin and adhesive combinations used with them. For example, the resins used in the FRP matrix must be compatible to the resin in the adhesive used, and most importantly, both of these have to be compatible to the substrate to which they are being bonded.

2.5.2. Example 1: Philippi Covered Bridge

The Philippi Bridge is a double-barreled arch-truss design having two spans, each about 42.4 m (139 ft). On February 2, 1989, in a bizarre accident, the Philippi covered bridge was heavily damaged by a gasoline fire that nearly consumed it. The State of West Virginia and the local residents of Philippi, WV, decided to rebuild the bridge to its original shape and appearance. The restoration work was undertaken by the researchers in cooperation with the West Virginia Department of Transportation/Division of Highways (WVDOT/DOH).

The engineering work primarily depended on the structural analysis of the main arch and truss members. The restoration work of the bridge was based on an extensive amount of historical research to establish both its original construction and its condition at the time of the accident. Through analysis and the use of FRPs, the bridge components were strengthened to carry adequate live loads. Furthermore, improvement of the intersection and drainage would ensure a better flow of traffic and the long-term durability of the bridge. In addition, fire sprinkler and lighting systems were installed against fire and vandalism. The entire bridge and approaches were finished in September 1991.

2.5.3. Example 2: Barrackville Covered Bridge

Another covered bridge structure restored by CFC/IHTIA is the bridge at Barrackville, WV, on the Fairmont and Wheeling Turnpike (figures 1 and 2). The bridge spans 39.9 m (131 ft) clear from spring line to spring line of abutments. The trusses are multiple kingposts sandwiched between pairs of arches framed into the trusses to create an indeterminate, composite timber structure. Because of deterioration that prevented it from carrying automated traffic, the Barrackville Bridge was being used as for pedestrians prior to restoration.

The restoration of Barrackville Bridge had two phases: development of a preservation plan and stabilization of the main bridge structure. During spring 1993, the first phase of the work was completed in cooperation with WVDOT/DOH. The information gained by a thorough inspection served as the basis for the development of plans and specifications. The second phase of the work was completed in 1999. Restored to its original capacity, the bridge's condition is stable in both the main structure and the roof and siding. The second phase of the work included removal of the sidewalk (or "wart") on the downstream side, installation of the new downstream siding, removal of extraneous floor support members that were added over time, repair of stringers, installation of a new timber deck, and renewal of the entire roof. The Barrackville Bridge was restored to its original appearance from just after the Civil War, including hand-forged bolts, as well as other materials such as bulk adhesives and FRP rebars, at a cost of $1 million.

In addition to the Philippi and Barrackville bridges, the preservation of the Meems Bottom Bridge in Virginia involved restoration techniques for members, joints, and secondary components that included consolidating cracked members using thixotropic epoxy under pressure. A mixture of epoxy and walnut shells or sawdust was used to replace areas of rot. This matched the original wood in color and texture while restoring the strength and dimensions of the original component. Critical to the restoration work was the development of splices and joints in deteriorated members, augmented with steel and FRP bars discreetly inserted into the member. Only when rot or fire damage was so severe that repairs could not be made in compliance with the best preservation techniques, without unsightly visual intrusion, were the members replaced with other wood, preferably from old structures already demolished.

Advanced methods for historic preservation have made tremendous gains over the past several years, but they still have not come far enough. The implementation of new methods and materials for structural repair and preservation is ultimately contingent upon availability of codes and the familiarity of owners, engineers, and contractors. See appendix B, "Annotated Bibliography," for more articles pertaining to the use of FRPs and innovative methods of strengthening timber bridges.

CHAPTER 3—LABORATORY EXPERIMENTS

3.1. INTRODUCTION

The laboratory experimental program carried out during this research project included internal reinforcement of wooden members with GFRP composite materials. The strengthening schemes developed and tested in this research were designed to comply with the Secretary's guidelines, as described in chapter 2. Tension specimens were developed and tested to reinforce truss members. The tests were conducted to determine the bond strength and development length of the GFRP bar adhesively bonded to wood. Bending and shear specimens were also developed and tested to improve the bending and shear capacities of floor beams and stringers. The following sections describe all the specimens tested and the experimental tests conducted for this project.

3.2. TENSION TESTS

3.2.1. Introduction

Preliminary tension tests were conducted to determine the appropriate adhesive/matrix combination and specimen preparation methods. These initial sets of experiments are described in great detail in appendix A. For this research, nine tension specimens were prepared and tested. The tension tests were conducted as a continuation of the preliminary tension tests conducted, as described in appendix A.

3.2.2. Preparation of Test Specimens

The tension specimens consisted of white oak wooden members at 8–10 percent moisture content (MC) that were air-dried at a saw mill. The test specimens were cut into a dogbone shape with dimensions prorated to American Society for Testing and Materials (ASTM) 198 test standards for tensile strength parallel to the grain. The ends of the test specimens were 3.8 by 7.6 cm (1.5 x 3.0 inches), tapering down to a constant cross section of 3.8 by 3.8 by 15.2 cm (1.5 by 1.5 by 6.0 inches), with an overall specimen length of 91.4 cm (36 inches) (figure 6).

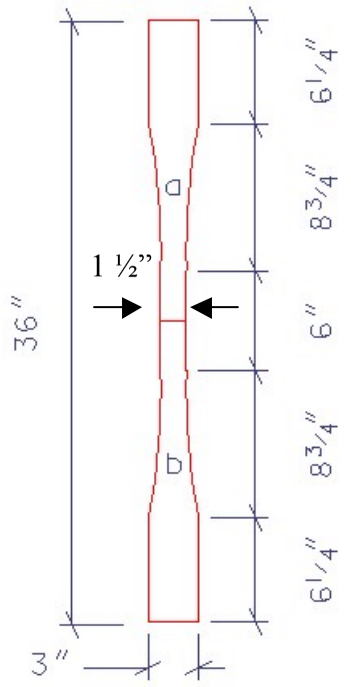

Figure 6. Illustration. Tension test specimens.

To insert the GFRP bars into the specimens, the specimens were cut in two halves (sides a and b) and holes were drilled into each end. Holes of 1.59-cm (0.625-inch) diameter were drilled to accommodate a # 4 bar (i.e., a 1.27-cm (0.5-inch) diameter). The hole size was drilled slightly larger than the diameter of the bar to allow for 0.159 cm (0.062 inch) of resin adhesive on all sides of the composite bar. To maintain alignment of the GFRP bar in wood and to ensure that the bar is fully surrounded by adhesive, a 1.27-cm (0.5-inch) countersink was drilled to the exact diameter of the bar (i.e., 1.27-cm (0.5-inch) bar diameter plus a 0.159 cm (0.062 inch) allowance for sand coating) in side a. On side b, a 2.54-cm (1.0-inch) outer diameter (O.D.) by 1.59-cm (0.625-inch) inner diameter (I.D.) by 0.318-cm- (0.125-inch-) thick washer was countersunk, as seen in figures 7 and 8.

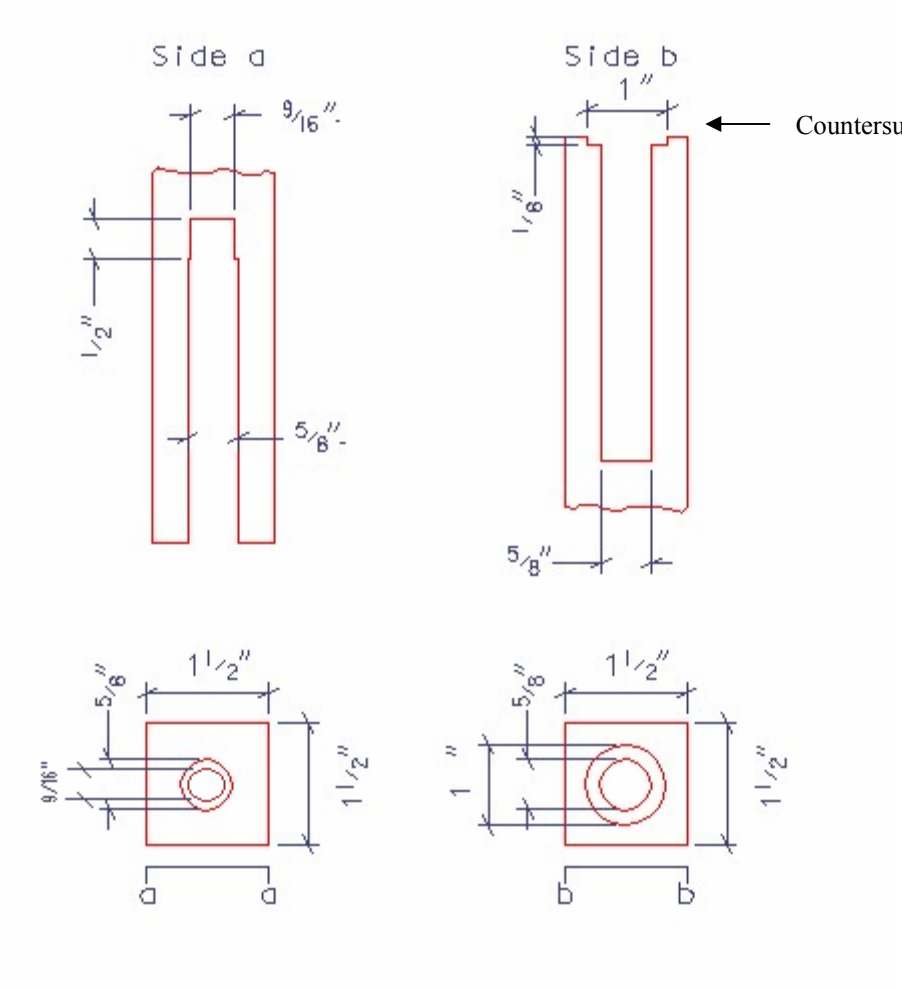

1 inch = 2.54 cm

Figure 7. Illustrations. Countersunk holes to maintain horizontal alignment.

Four different depths (2.54, 5.08, 10.16, and 20.32 cm (1, 2, 4, and 8 inches)) were also drilled into each end so that four different bond lengths (2.54, 5.08, 10.16, and 20.32 cm (1, 2, 4, and 8 inches)) could be tested. Two specimens of each bond length were tested. The GFRP bars were placed in the predrilled holes and the specimens were then clamped at the joint by a C-clamp and placed in a bar furniture clamp. The properties of the bars and adhesive used are:

Bars: Sand-coated GFRP with a vinylester matrix.
Adhesive: Urethane-based PLIOGRIP®, manufactured by the Ashland Inc.

Two 0.556-cm (0.219-inch) holes were drilled on the sides a and b (figure 8) to pressure-inject the PLIOGRIP adhesive. The specimens were left for another 48 hours to cure before testing (figure 9).

Figure 8. Photo. Tension specimens.

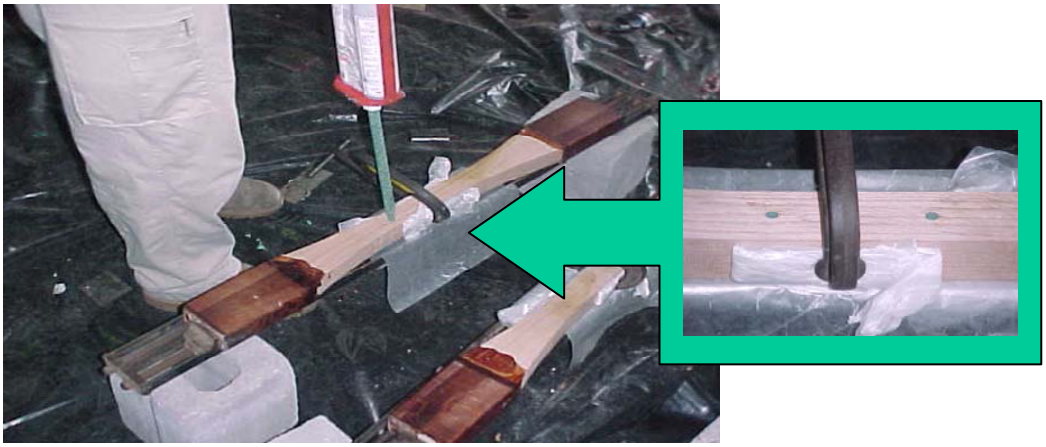

Figure 9. Photos. Injection of PLIOGRIP into tension specimen.

3.2.3. Testing Procedure

Uniaxial tension tests were performed on the GFRP reinforced wood samples, using an 889.6-kilonewton (kN) (200-kilopound (kip)) capacity Baldwin Universal Testing Machine. Strain gauges were mounted on the test specimen at midheight on both faces. Strain and load measurements were taken manually every 226.8 kg (500 lb) from the Baldwin machine. Table 1 presents the different specimens tested.

Table 1. Tension test specimens.

Specimen	Rebar Type	Rebar Diameter	Rebar Length	Bond Length
T1	None (control)	N/A	N/A	N/A
T2	Sand-coated GFRP	0.5 inch	4 inch	2 inch
T3	Sand-coated GFRP	0.5 inch	4 inch	2 inch
T4	Sand-coated GFRP	0.5 inch	2 inch	1 inch
T5	Sand-coated GFRP	0.5 inch	2 inch	1 inch
T6	Sand-coated GFRP	0.5 inch	8 inch	4 inch
T7	Sand-coated GFRP	0.5 inch	8 inch	4 inch
T8	Sand-coated GFRP	0.5 inch	16 inch	8 inch
T9	Sand-coated GFRP	0.5 inch	16 inch	8 inch

1 inch = 2.54 cm

Four different depths (2.54, 5.08, 10.16, and 20.32 cm (1, 2, 4, and 8 inches)) were also drilled into each end so that four different bond lengths (2.54, 5.08, 10.16, and 20.32 cm (1, 2, 4, and 8 inches)) could be tested.

3.3. BENDING TESTS (SMALL-SCALE)

3.3.1. Introduction

No preliminary bending tests were conducted because the adhesive and the GFRP matrix used are the same as in the tension test. The testing of bending specimens in this section was the first step in developing methods of strengthening that could be used on full-scale members, as described in section 3.4.

3.3.2. Preparation of Test Specimens

The bending specimens consisted of white oak wooden members at 8–10 percent MC that were air-dried at a saw mill. Test specimen dimensions were prorated to ASTM 198 bending test standards. A cutout section was removed to place a GFRP reinforcement plate. This method of GFRP placement was selected so that the GFRP plate might be easily hidden to comply with the Secretary's guidelines. Three 8.89- by 3.81- by 91.44-cm (3.5- by 1.5- by 36-inch) specimens were cut and surfaced. Also, a 7.94- by 1.27-cm (3.125- by 0.5-inch) section was routed for the entire length of all the specimens, as shown in figure 10.

a. Plan view (tension side) b. Cross section

1 inch = 2.54 cm

Figure 10. Illustration. Bending test specimen dimension.

One control specimen without GFRP plate reinforcement and two specimens with GFRP plate reinforcement were tested to failure. A 7.62- by 0.635-cm (3- by 0.25-inch) GFRP (E_L = 2,400 ksi with vinylester matrix plate was used to reinforce specimen B-2. One side of the GFRP plate was lightly sanded to remove a thin layer of protective coating to provide an adequate bonding surface. PLIOGRIP was applied to the wood surface and the specimen was clamped and left to cure for 2–4 days (figure 11). Specimen B-3 was reinforced using a 7.62- by 0.95-cm (3- by 0.375-inch) GFRP (E_L = 3 msi) with vinylester matrix plate. A peel ply was removed from this GFRP plate to provide an adequate bonding surface (figure 11).

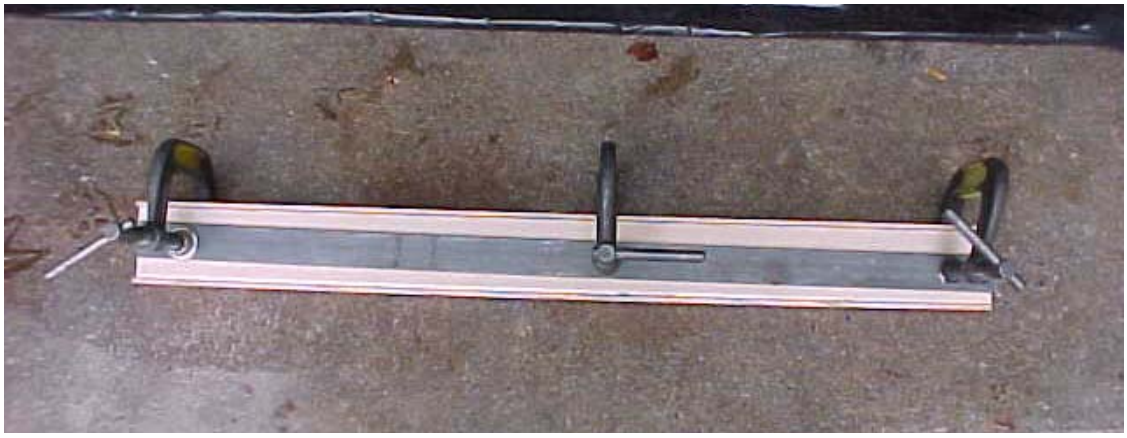

Figure 11. Photo. Bending specimen reinforcement.

3.3.3. Testing Procedure

The specimens were tested in four-point loading, as shown in figures 12 and 13. All specimens were instrumented with electrical strain gauges placed at midspan. Stress/strain curves were developed, and modes of failure were identified.

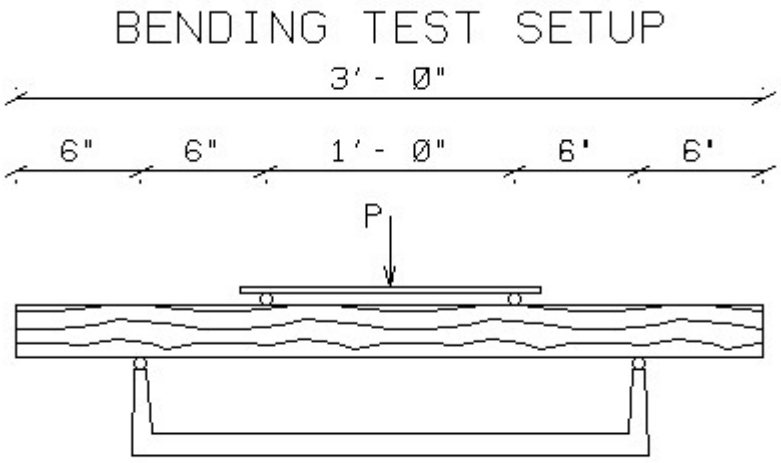

1 inch = 2.54 cm

Figure 12. Illustration. Four-point bending test setup.

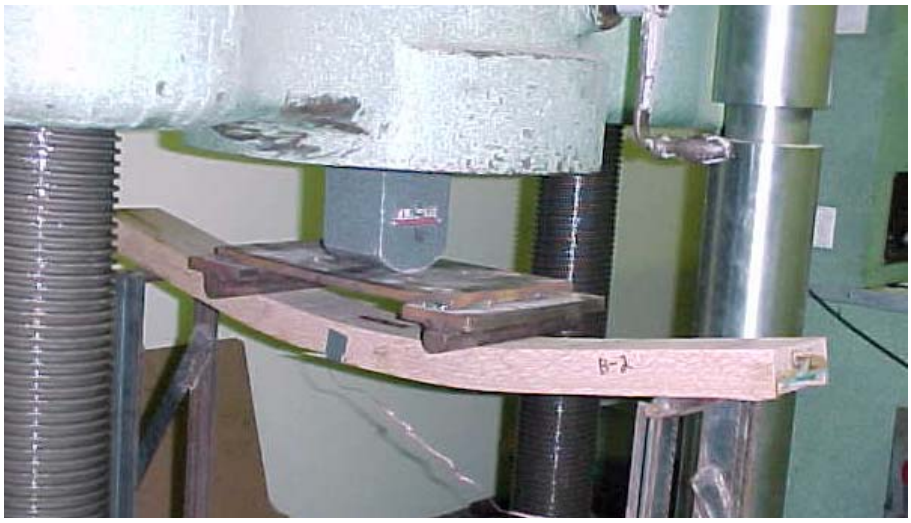

Figure 13. Photo. Specimen B-2 in four-point loading.

The control specimen test was conducted to determine the ultimate moment capacity and flexural stiffness and to identify the failure mode of the unreinforced wood. The GFRP-reinforced wood specimens (B-2 and B-3) were also tested to failure. The strain gauges on the GFRP specimens were bonded to the composite surface at midspan.

3.4. BENDING TESTS WITH GFRP PLATES (15.24 BY 29.84 CM (6 BY 11.75 INCHES))

3.4.1. Introduction

Bending tests were conducted on large-scale wooden structural members reinforced with GFRP composite plates. An additional set of bending tests on large-scale wooden members reinforced with GFRP reinforcing bars was also conducted. These tests represent a continuation of the findings and results of earlier tests to investigate the behavior of reinforcement and rehabilitation methods on field-size members. Also, tension tests were conducted to determine engineering properties of GFRP plates. In this section, tension tests of GFRP plates are presented to determine properties needed for analysis of the full-scale bending members. Description of the preparation of specimens and tests are herein presented, and preliminary findings are presented in later sections of this report.

3.4.2. Tension Tests (GFRP Plates)

3.4.2.1. Preparation of Test Specimens

Tension tests were conducted on GFRP plates used to reinforce the large-scale bending members to determine their modulus of elasticity (MOE) values. Samples were cut from the two different size plates (i.e., 0.95 and 0.64 cm (0.375 and 0.25 inches) thick). The test specimens were 0.95 by 2.54 by 30.48 cm (0.375 by 1 by 12 inches) and 0.64 by 2.54 by 30.48 by cm (0.25 by 1 by 12 inches). Additional plates were bonded at the ends of the specimen to prevent failure at the grip location, as shown in figure 14. The plates were bonded to the test specimens with the same

adhesive that was used for the large-scale bending test, as described in the following sections of this report.

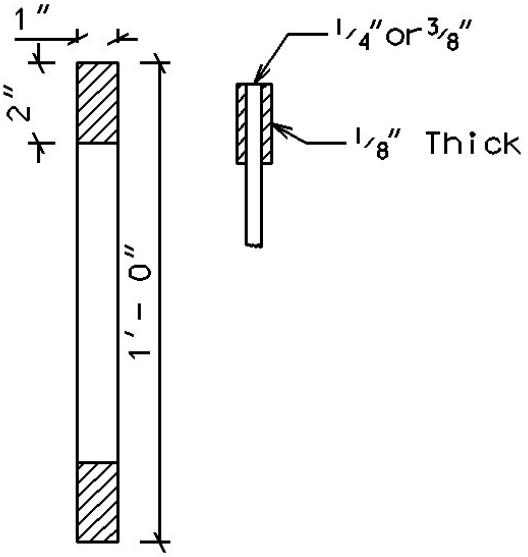

1 inch = 2.54 cm

Figure 14. Illustration. MOE tension test specimens.

3.4.2.2. Testing Procedure

Uniaxial tension tests were conducted on the GFRP plate samples using an 889.6-kN- (200-kip-) capacity Baldwin Universal Testing Machine. A strain gauge was attached at the center of the test specimen. Strain and load measurements were taken manually every 226.8 kg (500 pounds) using a strain indicator and the Baldwin machine.

3.4.2.3. Results

Since these tests were conducted to determine only the properties for analysis, they are presented in this section. The MOE values used for the transformed section analysis of the full-scale bending, presented in chapter 4, were taken as the average of the best three tests for each thickness of plates. This was determined by the mode of failure, i.e., pure tension failure in the middle of the plate. Table 2 shows the test results.

Table 2. GFRP plate MOE values.

Test	MOE (1×10^6 psi)) (0.375×1×12 inches))	MOE (1×10^6 psi)) (0.25 × 1 × 12 inches))
1	3.422	2.676
2	3.422	2.810
3	3.550	3.270
Average	3.464	2.919

* 1×10^6 pounds per square inch (psi) = 6.89×10^6 kilopascals (kPa); 1 inch = 2.54 cm

3.4.3. Preparation of Full-Scale Bending Test Specimens

The full-scale bending test specimens consisted of white oak wooden members at 8–10 percent MC that were obtained from West Virginia University Forest saw mill. These specimens were chosen to closely replicate earlier tests conducted on small-scale wooden members. The members were rough-cut cants 15.24 by 29.84 by 243.8 cm (6 by 11.75 by 96 inches) (see figure 16). Four specimens were reinforced with a GFRP plate bonded flat onto the tension side of the member. One specimen was tested without GFRP reinforcement and used as a control specimen. The plate was recessed into the member by routing an area large enough to accommodate the plate plus an additional 0.159 cm (0.0625 inch) for the adhesive and 0.159 cm (0.0625 inch) for added tolerance. Two different thicknesses of plates were used, 0.952 and 0.635 cm (0.375 and 0.25 inches) (see figure 15).

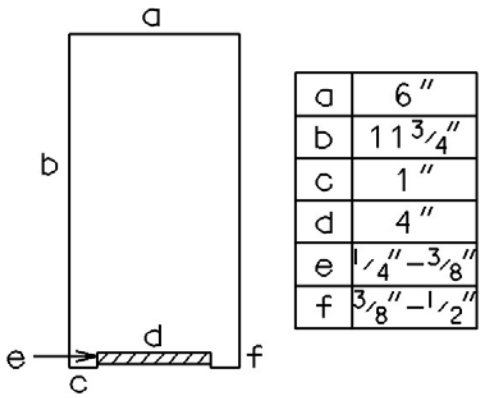

1 inch = 2.54 cm

Figure 15. Illustration. End view of test specimens.

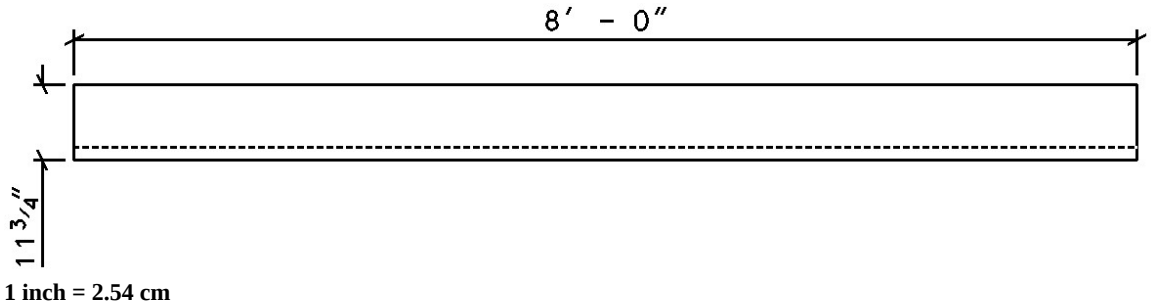

1 inch = 2.54 cm

Figure 16. Illustration. Side view of test specimens.

Typical rehabilitation of wooden beams with polymer composites uses a GFRP plate bonded directly to the tension face of the member. However, to hide the reinforcement to comply with the Secretary's guidelines, the GFRP plate had to be recessed into the member. This was accomplished by routing a 10.16- by 0.952- or 1.27-cm (4- by 0.375- or 0.5-inch) section, depending on the thickness of the GFRP plate used. The specimens were routed the entire length of the member, as shown in figure 17.

Figure 17. Photo. Routing of test specimen.

Once the routing was completed, to provide an adequate bonding surface, the protective coating was sanded from the side which was to be applied to the member. The adhesive used was the urethane-based PLIOGRIP, manufactured by Ashland Inc. After the plate was sanded, the adhesive was applied directly to the member, as shown in figure 18.

Figure 18. Photo. Applying adhesive on test member.

The plate was then placed in the recessed area and was put under pressure to ensure proper bond between the plate and wooden member (see figure 19).

Figure 19. Photo. Steel plates used as weights on test specimen.

3.4.4. Testing Procedure

The specimens were tested in four-point loading, as shown in figure 20. All specimens were instrumented with electrical strain gauges placed at the midspan, compression and tension sides, and the support on the tension side. Deflection was measured using a linear variable differential transformer (LVDT) and the loading was measured using a load cell. A data acquisition system was used for data collection. The specimens were tested to failure and stress/strain curves were developed and modes of failure were identified. One control specimen was tested with no reinforcement, two were tested with 0.64- by 10.16- by 182.9-cm (0.25- by 4-by 96-inch) GFRP plates, and two were tested with 0.95-by 10.16- by 182.9-cm (0.375- by 4- by 96-inch).

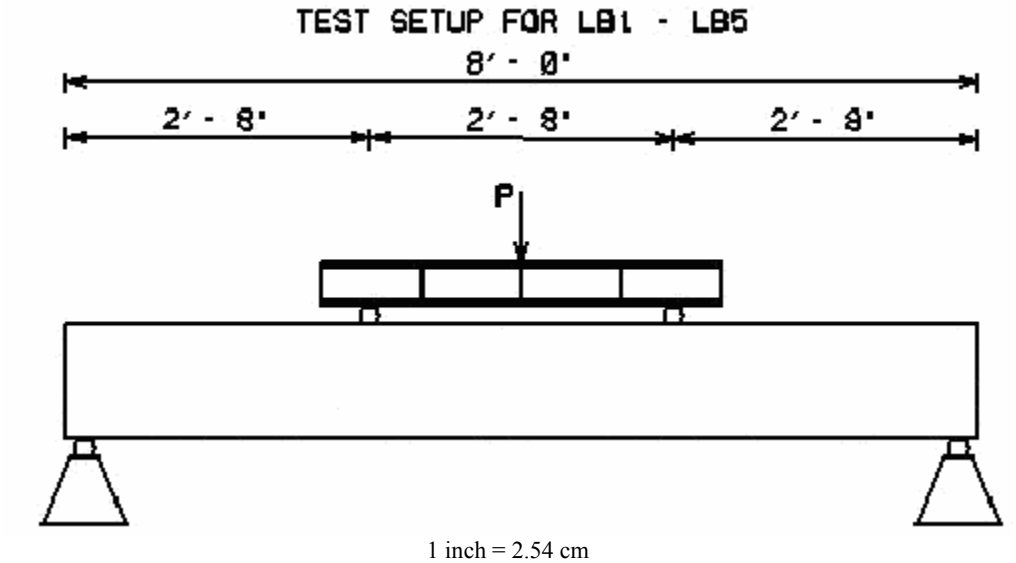

1 inch = 2.54 cm

Figure 20. Illustration. Four-point bending test setup.

3.5. BENDING TESTS WITH GFRP REINFORCING BARS

3.5.1. Introduction

The method developed for these tests was to remove only the portion of the member that was deteriorated and allow the rest of the member to remain in service. In covered bridges, the members themselves are a historic resource that must be preserved. Through the methods developed in this project, we honor the building techniques developed by previous generations by concealing the manner by which we preserve and reinforce these members.

3.5.2. Preparation of Test Specimens

The bending test specimens consisted of white oak wooden members at 9 percent MC that were obtained from West Virginia University Forest saw mill. These specimens were chosen to closely replicate earlier tests conducted on small-scale wooden members. The members were rough-cut cants 14.6 by 14.29 by 17.78 cm (5.75 by 5.625 by 7 inches). The specimens were stored in the laboratory until the desired MC of 9 percent was reached, one closely matching that of an existing covered bridge. Once the desired MC was reached, the specimens were then cut in half to develop a method useful to rehabilitating a partially deteriorated member and still allow the sound portion to remain in place. The deteriorated portion would be removed and replaced with a new piece of the same size and species of wood as the original. The pieces would then be joined together by drilling holes and inserting GFRP reinforcing bars to bridge between the new and old members. The GFRP reinforcing bars used were sand coated with a diameter of 1.429 cm (0.562 inch) and a 21.59-cm (8.5-inch) length. The bars were standard #4s, but because of the sand coating, an additional 0.159 cm (0.062 inch) was added to the diameter.

After the specimens were cut transversely into two halves, 1.59-cm- (0.625-inch-) diameter holes were drilled into the ends of the specimens. The holes were drilled in accordance with the design requirements of the *National Design Specification® (NDS®) for Wood Construction*[24], section 8.5. Two specimens were prepared and tested, BB-2 and BB-3 (see figures 21–25). BB-2 was reinforced with two GFRP reinforcing bars and BB-3, with four (see figures 21–27). After the holes were drilled to accommodate the reinforcing bars, a 0.556-cm (0.219-inch) hole was drilled into the side of the members to allow for the injection of adhesive. PLIOGRIP was used for these members. An injection process was used because, in earlier experiments conducted to determine the best method to achieve the desired bond, injection proved the best method to get to as close to perfect bond as possible. The 1.429-cm- (0.562-inch-) diameter, sand-coated GFRP bars were placed into the holes and the two pieces were joined together. Bar clamps secured the two halves in place while the adhesive was injected (see figure 28). The bar clamps were also used to provide pressure on the specimens while the adhesive had time to cure properly. The specimens were clamped for approximately 48 hours. It should be noted that BB-2 was put together with improper alignment of the holes. To avoid problems while testing, the holes on one side of the specimen were enlarged to 2.222-cm (0.875-inch) diameter. The GFRP reinforcing bars were then wrapped with a GFRP fabric that had been soaked in PLIOGRIP. The bars were then placed into the specimen in the same manner as BB-3.

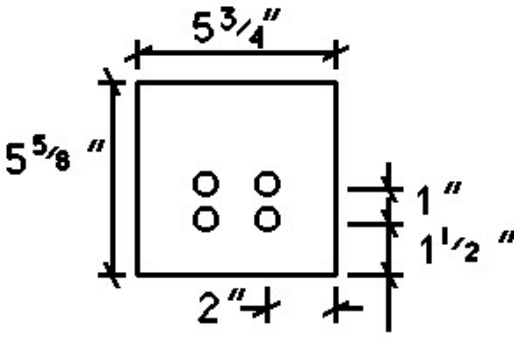

1 inch = 2.54 cm

Figure 21. Illustration. End view, BB-2.

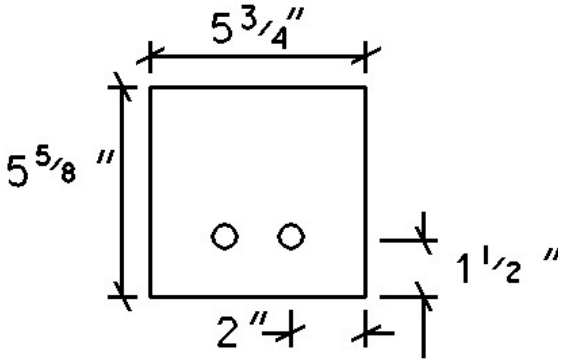

Figure 22. Illustration. End view, BB-3.

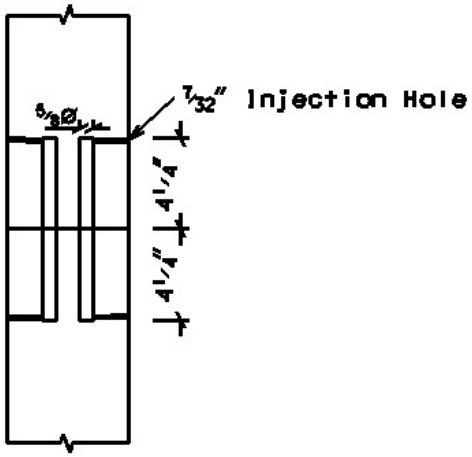

1 inch = 2.54 cm

Figure 23. Illustration. Bottom view, BB-2 and BB-3.

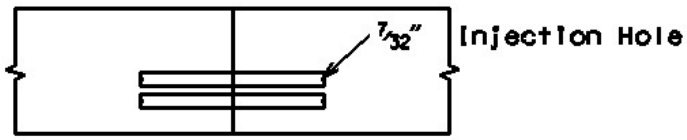

1 inch = 2.54 cm

Figure 24. Illustration. Side view, BB-2.

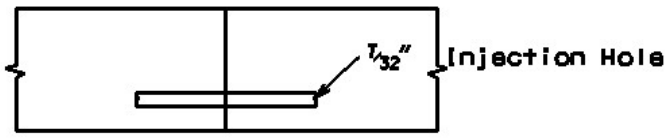

1 inch = 2.54 cm

Figure 25. Illustration. Side view, BB-3.

Figure 26. Photo. End view, BB-2.

Figure 27. Photo. Injection of adhesive.

Figure 28. Photo. Clamping of specimens.

The specimens were prepared for testing and removed from the clamps. Strain gauges were placed on the tension and compression sides of the specimens and also on the left and right sides of the joint (see figure 29).

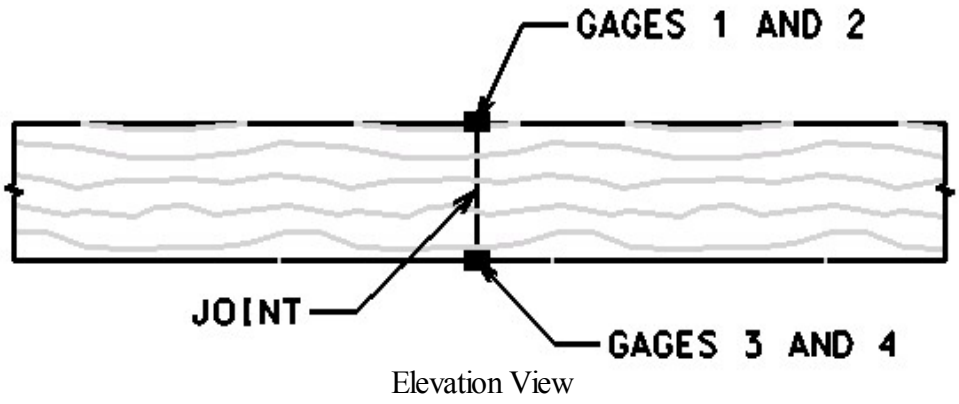

Figure 29. Illustration. Strain gauge placement, BB-2 and BB-3.

3.5.3. Testing Procedure

The specimens were tested in four-point loading, as shown in figure 30. Both specimens were instrumented with strain gauges, and deflections were measured using a dial gauge. A load cell was used to determine the applied load. The joint opening was measured with a digital caliper on the tension side of the member. A data acquisition system was used for data collection of the strain and load measurements. The specimens were tested to failure, and theoretical data were

developed to compare to the experimental data. The mode of failure was identified. Normally, a control specimen would be tested and the test specimens would be compared to a control specimen. Because of the nature of the methods used, it can easily be seen that the test specimens would not have an increase in strength and stiffness over a solid specimen. Therefore, the test data comparisons were made theoretically.

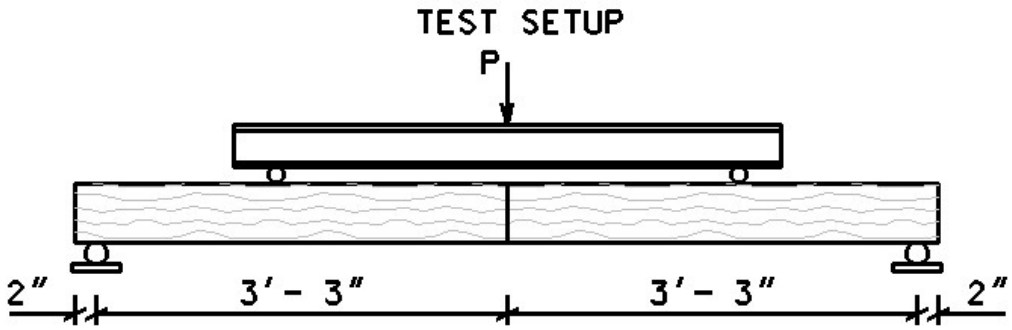

1 inch = 2.54 cm

Figure 30. Illustration. Four-point bending test setup.

3.6. BENDING TEST WITH GFRP PLATES (15.24 BY 20.32 CM (6 BY 8 INCHES))

3.6.1. Introduction

Several additional tests were conducted on full-scale wooden members reinforced with GFRP composite plates. These tests are a continuation of earlier tests to investigate the behavior of wooden members reinforced with GFRP plates bonded to the tension side. A total of three 15.24- by 20.32- by 304.8-cm (6- by 8- by 120-inch) white oak members with and without GFRP plates were tested to failure in this set of experiments.

3.6.2. Preparation of Test Specimens

The full-scale bending test specimens consisted of white oak members at 8–10 percent MC. These specimens were chosen to closely replicate earlier tests that were conducted on small-scale wooden members. The specimens were rough-cut cants, but the cross section and span length were altered to ensure bending failure and evaluate the flexural behavior of GFRP-reinforced wooden beams (see figures 31 and 32). The specimens reinforced with GFRP plates were placed flat on the tension face of the member. The shear span-to-depth ratio (a/h) for these beams was approximately 5. According to ASTM 198, if $a/h \geq 5$, a bending failure will be induced; if $a/h \leq 5$, shear failure will be induced, where the shear span is defined as the distance from the support to the loading point. In past specimens, the plates were recessed into the member by routing an area large enough to accommodate the plate plus an additional 0.159 cm (0.062 inch) for an adhesive and 0.159 cm (0.062 inch) for added tolerance. To prepare these specimens, an improved method was used that involved cutting out a recessed area of the member with a table saw (as opposed to routing) to achieve a more accurate and consistent cut, allowing 0.159 cm (0.062 inch) for adhesive. A 0.952-cm- (0.375-inch-) thick GFRP plate was used to reinforce the specimens.

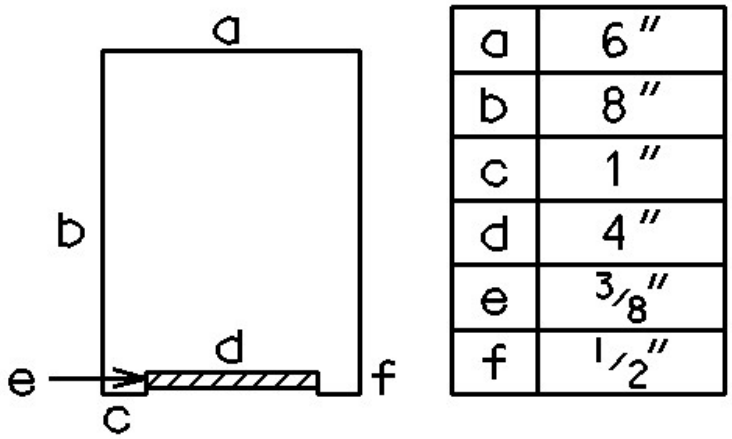

1 inch = 2.54 cm

Figure 31. Illustration. End view of test specimens.

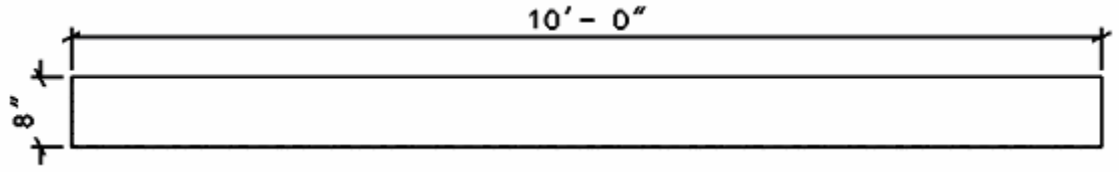

1 inch = 2.54 cm

Figure 32. Illustrations. Side view of test specimens.

A key difference between these specimens and earlier bending specimens is that after these members were obtained from the saw mill they were stored in a humidity chamber at a constant temperature and humidity level (20 degrees Celsius (°C) (68 degrees Fahrenheit (°F)) and 70 percent relative humidity) until they were ready for assembly and testing. (In such tests in the past, splits and checks developed because of excessive in situ drying in our laboratory.) Once the groove was cut, a strain gauge was placed internally at the midsection to get accurate measurements of strain on the wood beam under the adhesive. The difference of strain measurement between the wood section and the GFRP section at the same location should have indicated the slippage in the PLIOGRIP adhesive at various loads. The GFRP plates were then sanded on the side that was to be bonded to the wood member. PLIOGRIP was applied directly to the member. Once the cutout area of the member was adequately covered with PLIOGRIP to ensure proper bond, the sanded plate was placed into the cutout section. Weights were then placed on the plate to provide pressure. Past testing has shown this would create proper bond between the member and the plate. Additional strain gauges were then placed externally on the GFRP from the center of the member to the end at 30.48-cm (1-ft) intervals to observe how the strain varied along the member (figure 33).

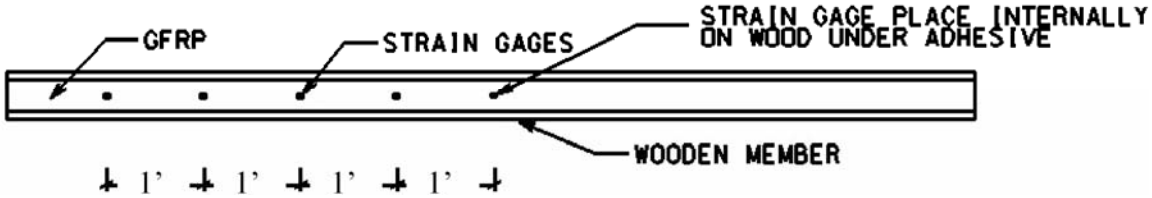

1 ft = 30.48 cm

Figure 33. Illustration. Plan view of strain gauge placement.

3.6.3. Testing Procedure

The specimens were tested in four-point loading, as shown in figure 34. All specimens were instrumented with electrical strain gauges placed at midspan, on the compression and tension sides, and at 30.48-cm (1-ft) intervals along one-half of the member on the tension side. Deflection was also measured using an LVDT and dial gauges. The applied load was measured using a load cell. A data acquisition system was used for data collection. The specimens were tested to failure. Load/deflection, load/strain, and stress/strain curves were developed and modes of failure were identified. One control specimen was tested with no reinforcement, and two specimens were tested with 0.952-cm- (0.375-inch-) thick GFRP plates. The percent reinforcement of GFRP to the total cross section of the member was 3.125 percent.

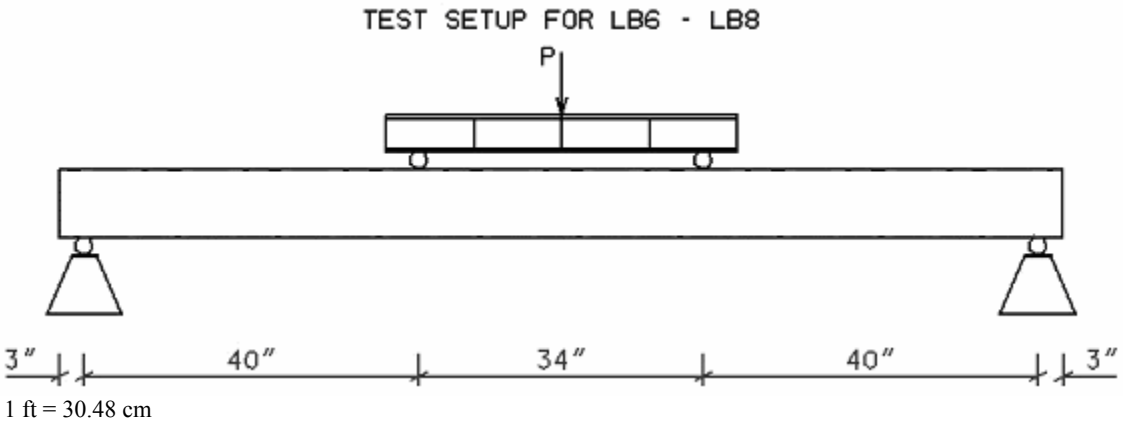

Figure 34. Illustration. Four-point bending test setup.

3.7. SHEAR TEST WITH GFRP PLATES (15.24 BY 20.32 CM (6 BY 8 INCHES))

3.7.1. Introduction

Several tests were conducted on full-scale wooden members reinforced with GFRP composite plates inserted on edge as compared to earlier tests where the GFRP plates were placed flat wise on the tension side (see figure 35). The addition of the glued-in GFRP plate makes the reinforced beam similar to the flitch beams of the past. Flitch plate beams are composite members which combine the strength and stiffness of the reinforcing material, traditionally steel, with the versatility of wood. This research will investigate the addition of a GFRP flitch plate. In the past, a steel flitch plate was sandwiched between two pieces of wood and bolted together. This research will use the structural adhesive PLIOGRIP to glue-in the GFRP plate in a notched vertical slot instead of bolting. GFRP flitch plate beams are expected to improve the shear strength and stiffness of wooden beams. The following sections describe the test conducted.

3.7.2. Preparation of Test Specimens

The full-scale bending test specimens consisted of white oak members at 7–8.5 percent MC. Three specimens (15.24 by 20.32 by 304.8 cm (6 by 8 by 120 inches) were prepared and tested. The cross section and span length of the test specimens were fabricated to ensure a shear failure

(figures 35 and 36). The specimens were reinforced with GFRP plates that were placed edgewise into a slot on the tension side of the member. The a/h for these beams was approximately 2.25. According to ASTM 198, if a/h ≥ 5, a bending failure will be induced; if a/h ≤ 5 shear failure will be induced, where the shear span is defined as the distance from the support to the loading point. The plates were recessed into the member by cutting out an area of the member with a table saw to accommodate the plate plus an additional 0.159 cm (0.062 inch) for adhesive and 0.159 cm (0.062 inch) for added tolerance. A 0.952-cm- (0.375-inch-) thick GFRP plate [0/90/45] was used to reinforce the specimens.

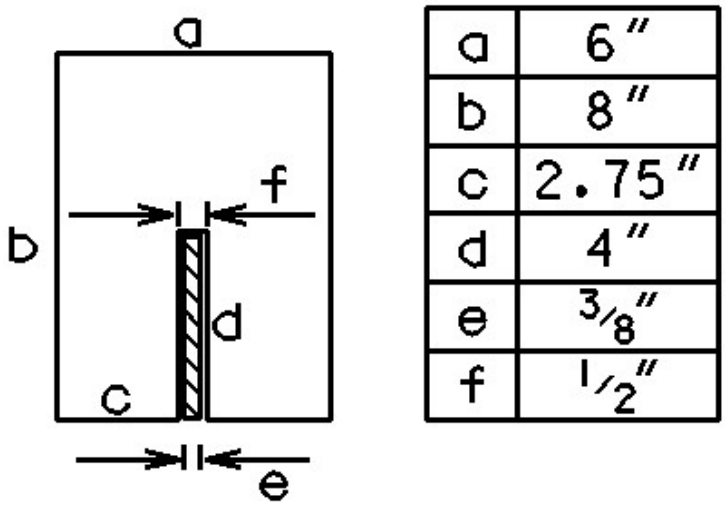

a	6″
b	8″
c	2.75″
d	4″
e	3/8″
f	1/2″

1 ft = 30.48 cm

Figure 35. Illustration. End view of test specimens.

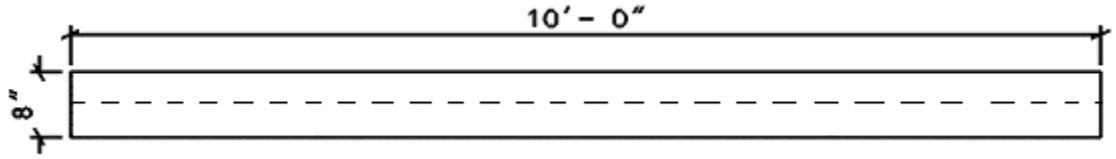

1 ft = 30.48 cm

Figure 36. Illustration. Side view of test specimens.

Splits and checks developed in the beams due to excessive and rapid in situ drying in our laboratory. Once the groove was cut, a strain gauge was placed internally at the midsection to get accurate measurements of strain on the wood beam under the adhesive. The GFRP plates were sanded on the sides that were to be bonded to the wood member. PLIOGRIP was applied directly to the member. Once the cutout area of the member was adequately covered with PLIOGRIP to ensure proper bond, the sanded plate was placed into the cutout section. Clamps were then placed on the plate to provide pressure that past testing has shown to create proper bond between the member and the plate. Additional strain gauges were then placed externally on the GFRP at the center of the member as well as a rosette strain gauge to measure shear strain at the end of the beam along its neutral axis to observe the shear strain in the beam.

3.7.3. Testing Procedure

The specimens were tested in four-point loading, as shown in figure 37. All specimens were instrumented with electrical strain gauges placed at midspan on the tension sides as well as a rosette near the end of the beam. Deflection was also measured using an LVDT and dial gauges. The applied load was measured using a load cell. A data acquisition system was used for data collection. The specimens were tested to failure. Load/deflection and load/strain curves were developed and modes of failure were identified. One control specimen was tested with no reinforcement and two specimens were tested with 0.952-cm- (0.375-inch-) thick GFRP plates. The percent reinforcement of GFRP to the total cross section of the member was 3.125 percent.

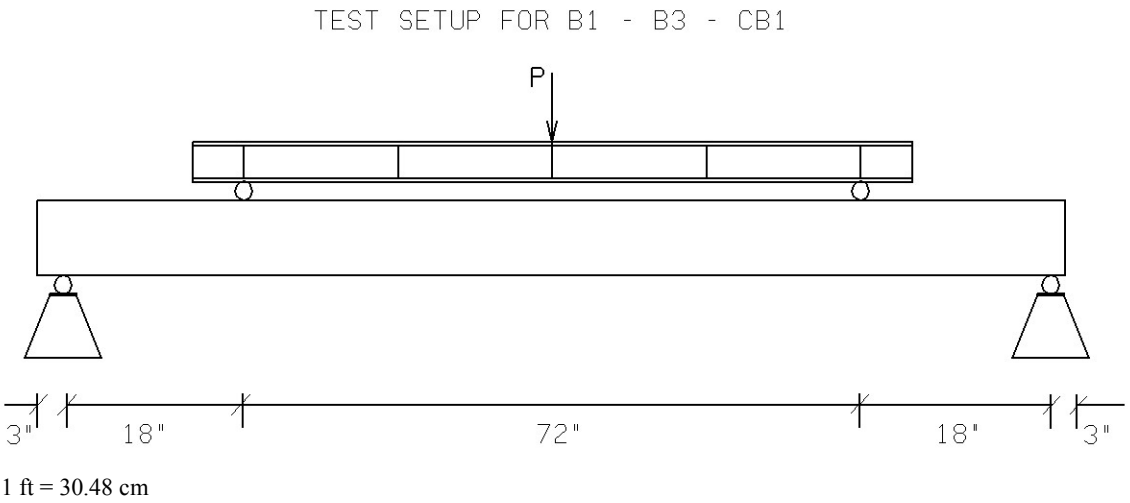

Figure 37. Illustration. Four-point bending test setup.

3.8. SUMMARY OF EXPERIMENTS

This section summarizes all experiments that are presented in this report. Table 3 presents all the experiments in summary format. Other tests conducted to determine the best combination of adhesives and methods to apply adhesives such as pressure injection are not included in table 3. Descriptions of these tests and other preliminary tests are described in appendix A. Tension tests to determine the MOE of the GFRP plates are not included in table 3.

Table 3. Summary of experiments.

Type of Test	Number of Experiments	Comments
Tension—small scale	9	Bonded-in GFRP bars; strength of tension splice and development length
Bending—small scale	3	GFRP plates flat; strength and stiffness
Bending—large scale	6	GFRP plates flat; strength and stiffness
Bending—large scale	2	GFRP bars; strength and stiffness
Shear—large scale	3	GFRP plates on edge; strength and stiffness
Total	23	

3.9. HISTORIC PRESERVATION

During these set of experiments, two different methods of concealing the reinforcement and preserving the historic integrity of the member were investigated. Both methods take advantage of routing the member in order to place the reinforcement inside of it and not on its bottom. From the top and side, the GFRP plates cannot be seen (figure 38).

Figure 38. Photo. Side view of reinforced specimen.

After concealing any view of the GFRP from the top and sides, only the bottom had to be concealed. The first method was to bond a white oak veneer to the bottom of the specimen, as shown in figure 39. The entire specimen was then stained; there are several proven methods to make new wood look old that could be used to match the existing color.

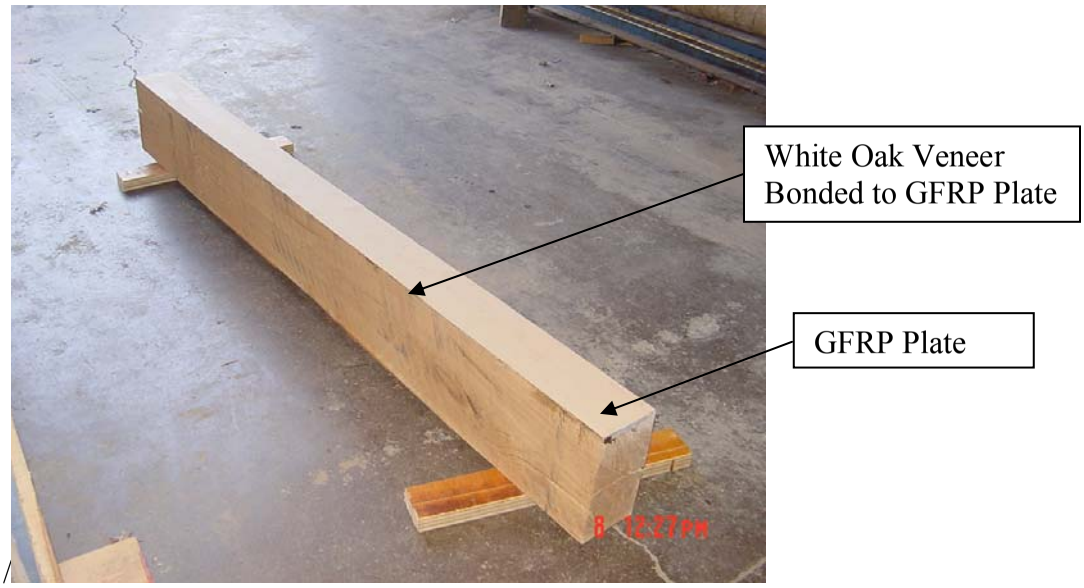

Figure 39. Photo. Specimen covered with veneer.

The next method investigated to conceal reinforcement was that of making GFRP look like wood. The idea was not to add to the GFRP a layer or ply that could degrade with time and peel off. Instead, a veil integrated at the pultrusion process was added to the GFRP plate to match existing wood or grain. A polymer composite manufacturer with whom CFC has an excellent working relationship was given a sample of a 100+-year-old wood, and using a computer-generated image, they created a veil to match the existing aged wood grain and color. Samples of the GFRP with wood grain veils are shown in the figures 40 and 41.

Figure 40. Photo. GFRP with veil.

Figure 41. Photo. GFRP with veil.

CHAPTER 4—RESULTS AND DISCUSSIONS

4.1. INTRODUCTION

This chapter presents the results of the experimental testing described in chapter 3. Also presented are analysis and discussion of these results, such as the bond strength and approximate development length of truss members, and strength and flexural rigidity improvements due to the addition of GFRP reinforcement.

4.2. TENSION TEST

4.2.1. Results

The results of the tension tests of the GFRP reinforced wood specimens revealed that there was adequate chemical cross-linking (i.e., bond) between the GFRP rebars and the wood substrate using the PLIOGRIP adhesive and the vinylester matrix of the GFRP rebar. The results of the tension tests and bond strengths are presented in table 4.

Table 4. Observed bond strength.

Specimen	Rebar Length (inch)	Bond Length (inch)	Bond Area (inch^2)	Max Load (lb)	Bond Strength (psi)
T-4*	2	1	1.571	1950	1241.25
T-5	2	1	1.571	2565	1632.72
T3**	4	2	3.142	2809	894.02
T-2	4	2	3.142	4225	1344.68
T-6*	8	4	6.284	9730	1548.38
T-7	8	4	6.284	7310	1163.27
T-8*	16	8	12.568	11900	946.85
T-9	16	8	12.568	10000	795.67

1 inch = 2.54 cm; 1 inch^2 = 6.45 cm^2; 1 lb = 0.45 kg; 1 psi = 47.9 pascals (Pa)
* = misalignment (marked red and underlined)
** = premature failure (marked red and underlined)

4.2.2. Discussion

The bond strength (i.e., shear stress) or failure is defined as load divided by the circumferential area of the embedded length of GFRP rebar in one side (the loaded end) of the test specimen; failure in the adjacent wood is defined as the load at which the specimen could not sustain any additional loading. Bond failure is defined as the failure load of the tension specimen (i.e., failure in the wood) divided by the circumferential area of the embedded length of GFRP rebar in one side of the joint.

Based on the test results, the alignment of the GFRP rebar was found to be extremely important to eliminating any eccentricity while applying tension. The countersinking and the washer were found to work well and provide the required alignment. However, several test specimens

(marked red and underlined in table 4) exhibited misalignment of the GFRP rebar as evidenced by strain gauge reading. The results from misaligned GFRP rebars and premature failure tests in specimen T-3 were not used for further analysis. Figure 42 shows the relationship between bond strength and development length. As shown in figure 42, the bond stress decreases from the end of the joint with increasing development length.

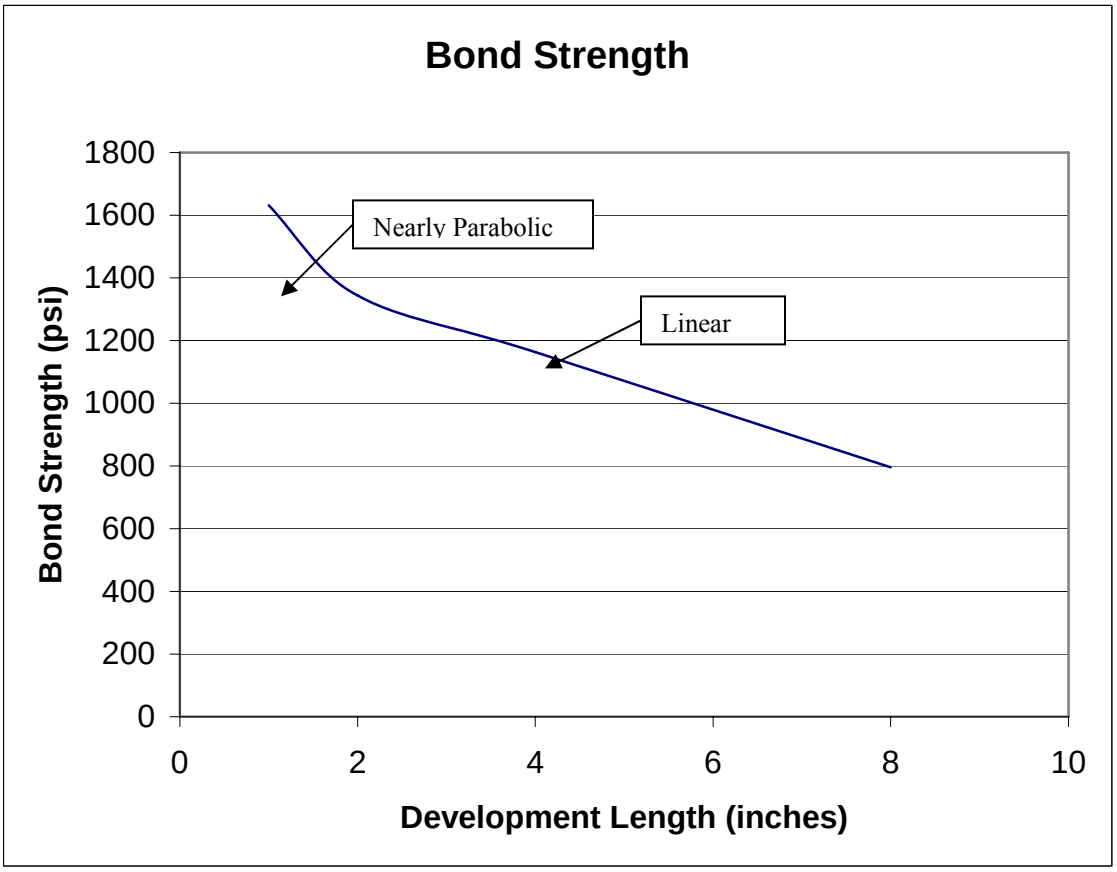

1 inch = 2.54 cm; 1,000 psi = 47.9 kPa

Figure 42. Graph. Bond strength versus development length.

4.2.3. Summary

The tension test results appear promising. In the reinforcement of wood with GFRP (as with most other types of reinforcement), more is not necessarily better. The desired bond strength can be reached in a relatively short distance; this will save immensely when it comes to the cost of materials and man-hours to conduct strengthening. Another advantage of this behavior may be that a greater-than-needed bond length can be used to improve joint ductility with a view to extending the strain to failure of the adhesive, thus avoiding a sudden joint failure. Another advantage of using GFRP reinforcement over more conventional steel is the strength-to-weight ratio. More reinforcement cannot be added to steel because of the dead load of the steel. Furthermore, the MOE values of wood and FRP are more compatible than those of wood/steel.

4.3. BENDING TESTS (SMALL-SCALE)

4.3.1. Results

The unreinforced specimen (control specimen) described in section 3.3 was tested to failure under four-point bending. As the load increased, horizontal cracks were first observed at the notched cutout located at the bottom side of the member below the loading points. A loud cracking noise occurred at 907.2 kg (2,000 lbs), and failure was sudden. The bending stress at this load level was computed as 33,094 kPa (4,800 psi). The nonlinear behavior beyond this load level was continued until failure to determine the ultimate strength or load carrying capacity as shown in figure 43. The ultimate mode of failure was a bending failure, which in a wooden beam is a tensile failure. The failure load was recorded. The initial flexural rigidity (EI) of the control specimen was computed as 272.33 kg-mm^2 (0.93 x 10^6 lb-in^2) and the ultimate strength or modulus of rupture (MOR) was computed as 38,610.6 kPa (5,600 psi). The strain at failure of the control specimen measured at the extreme fibers of the midspan tension side was 11,936 με. Due to the notched cutout of the specimen, an unintended stress concentration was introduced. A solid cross section will be used in future tests.

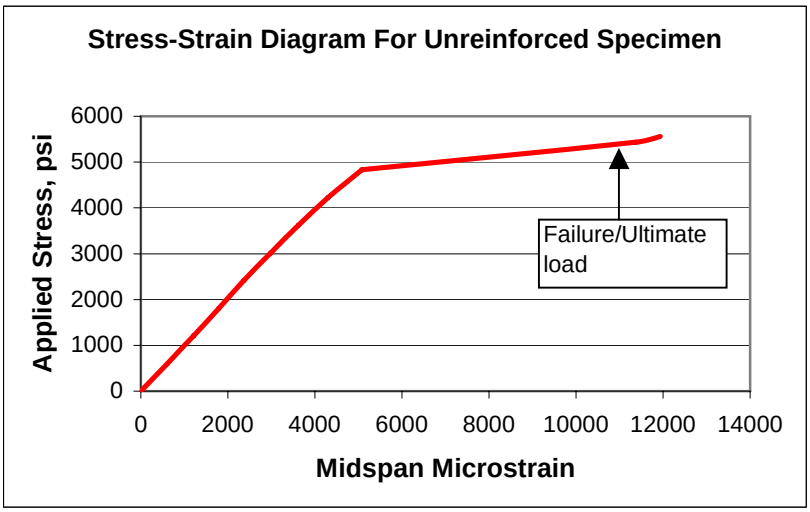

1,000 psi = 47.9 kPa

Figure 43. Graph. Stress-strain diagram for the unreinforced specimen.

To demonstrate the effectiveness of GFRP reinforcement, specimen B-2 was reinforced using a 0.64-cm- (0.25-inch-) thick GFRP plate with vinylester matrix and tested to failure. This specimen was stiffer than the unreinforced specimen and had a bilinear behavior, as clearly shown in the stress/strain curves in figure 44.

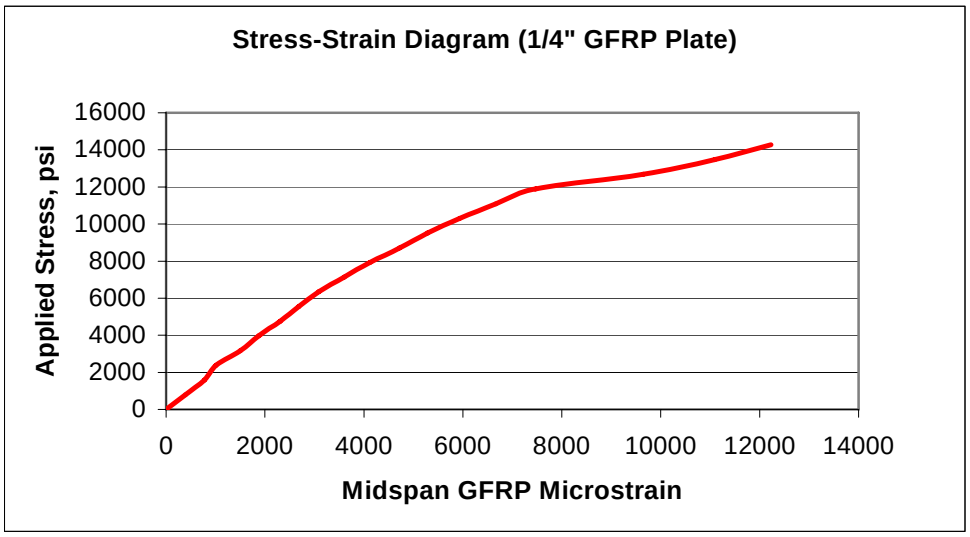

1 inch = 2.54 cm; 1,000 psi = 47.9 kPa

Figure 44. Graph. Stress-strain diagram for specimen B-2.

As the load increased, horizontal shear cracks were also first observed at the notched cutout located at the bottom side of the member, below and between the loading points, as shown in figure 45. The first linear part of the stress/strain curve was maintained to a load level of 1,723.7 kg (3,800 lbs), when there occurred a loud cracking noise; the second near-linear part of the curve was maintained until a failure load level of 2,041.2 kg (4,500 lbs). The ultimate failure mode of the specimen was a tension failure of the GFRP plate at both locations of the loads with no bond failure observed, as shown in figure 45.

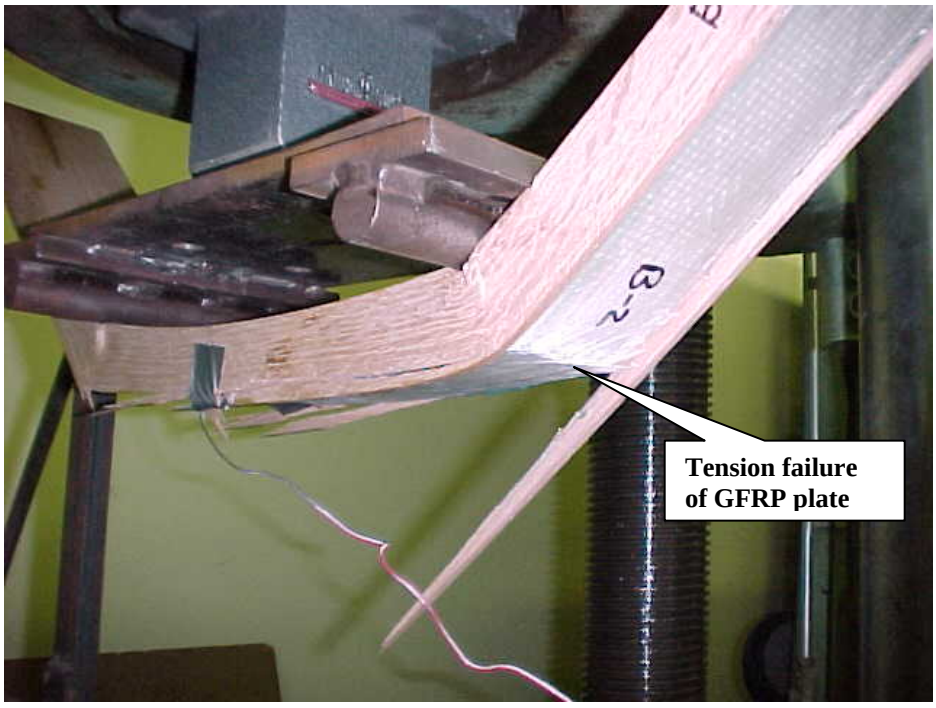

Figure 45. Photo. Failure mode of specimen B-2.

Based on the test results and a transformed section analysis, the ultimate strength (MOR) of specimen B-2 is 98,374.4 kPa (14,268 psi) or an increase of 154 percent, as compared to the unreinforced control specimen. The EI of specimen B-2 is 439kg-mm sq. (1.5 x 10^6 lb-$in^{2)}$, or a 61 percent increase over the unreinforced wood specimen. The strain at failure of specimen B-2, measured at the extreme fibers on the GFRP of the midspan tension side, was 12,231 με. The transformed and actual sections are shown in figure 46, and a transformed moment of inertia calculation is used to compute the MOR values.

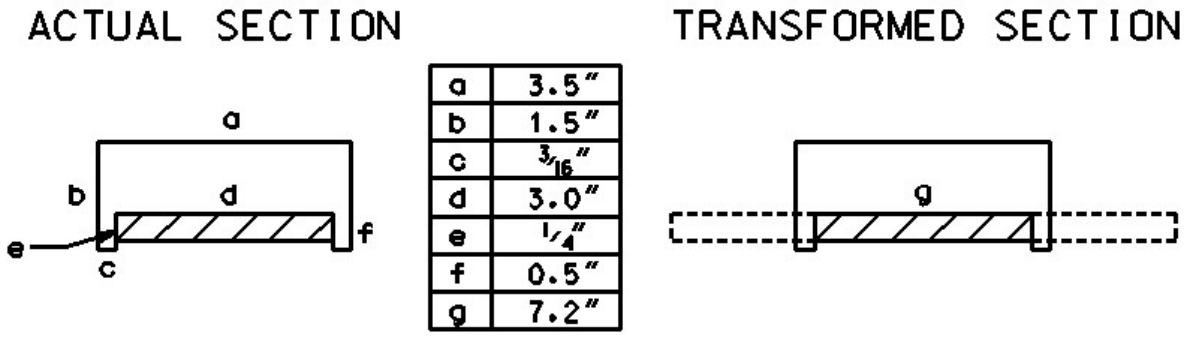

1 inch = 2.54 cm

Figure 46. Illustration. Actual and transformed sections for B-2.

Using the MOE of both wood and GFRP, a modular ratio, n, can be found:

$$n = \frac{E_{GFRP}}{E_{Wood}} = 2.411 \approx 2.4 \qquad (1)$$

The adjusted width for the 0.64- by 7.62-cm- (0.25- by 3-inch) -wide GFRP plate is: n x 3 = 183 mm (7.2”). The centroid for the transformed section is found from

$$\bar{y}_T = \frac{\Sigma \bar{y}_i A_i}{\Sigma A_i} \qquad (2)$$

Section	Area (A_i)	$\bar{y}_i$	$\bar{y}_i A_i$
1	0.09375	0.25	0.023438
2	0.09375	0.25	0.023438
3	3.5	1	3.5
4	1.8	0.375	0.675
	$\Sigma A_i = 5.4875$		$\Sigma \bar{y}_i A_i = 4.22188$

The centroid is calculated to be $\bar{y}_T$ = 19.56 mm (0.77 inches) measured from the bottom.

The transformed moment of inertia can be easily computed as:

$$I_{XT} = 2\left\{\frac{(3/16)(1/2)^3}{12} + [(3/16)(1/2)(0.77-0.25)^2]\right\} + \left\{\frac{(3.5)(1)^3}{12} + (3.5)(1)(1.5-0.77-0.5)^2\right\} + \left\{\frac{(7.2)(1/4)^3}{12} + (7.2)(1/4)(0.77-1/4-1/8)^2\right\} \quad (3)$$

$$I_{XT} = 0.05461 + 0.47682 + 0.29022 = 0.82 \text{ inches}^4$$

Specimen B-3 was reinforced using a 0.952-cm- (0.375-inch-) thick GFRP plate with vinylester matrix and tested to failure. This specimen exhibited yet a stiffer behavior when compared to specimen B-2 because of the stiffer GFRP plate used. Specimen B-3 also had a bilinear behavior, as shown in figure 47.

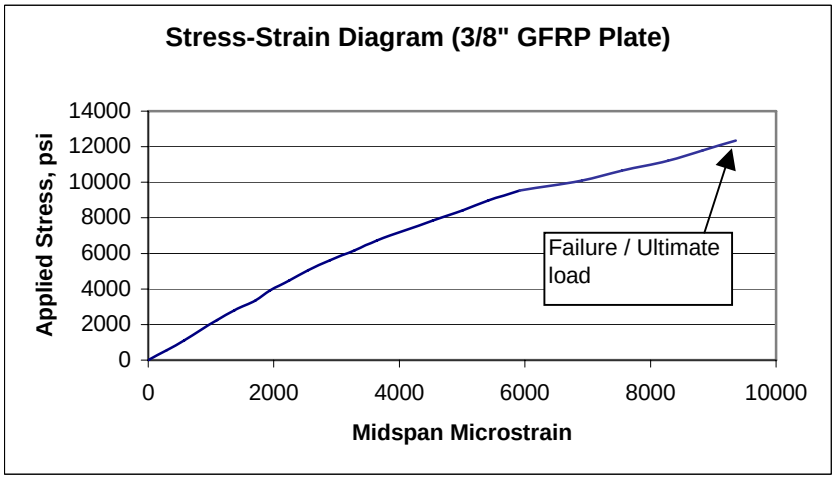

1 inch = 2.54 cm; 1,000 psi = 47.9 kPa

Figure 47. Graph. Stress-strain diagram for specimen B-3.

As the load increased, horizontal shear cracks were also first observed at the notched cutout located at the bottom side of the member below and between the loading points, as shown in figure 48. The first linear part of the stress/strain curve was maintained to a load level of 2,086.5 kg (4,600 lbs), when there occurred a loud cracking noise; the second near-linear part of the curve was maintained until a failure load level of 2,494.8 kg (5,500 lbs). The ultimate failure mode of specimen B-3 was dominated by horizontal shear failure of the wood initiated at the high moment region between the two load points, and wood failure at the bondline leading to the separation of the GFRP plate, as shown in figure 48.

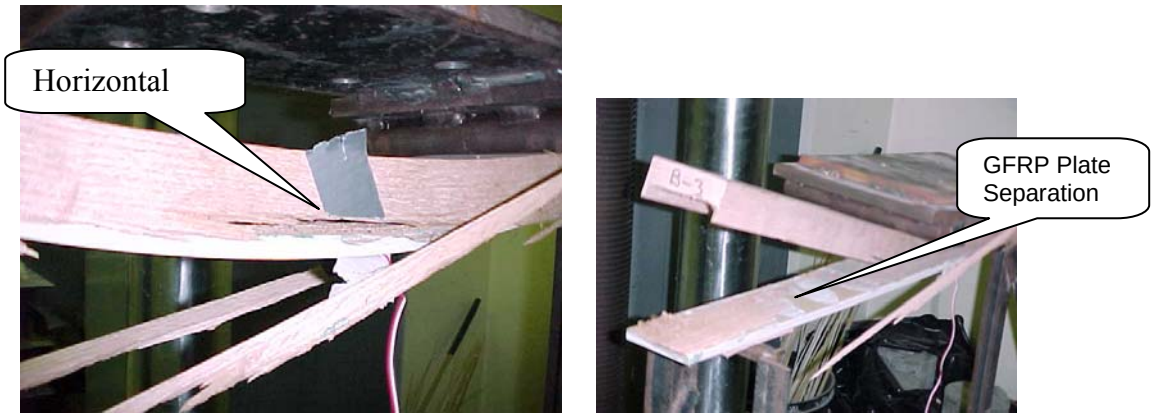

Figure 48. Photos. Failure mode of specimen B-3.

Based on the test results and a transformed section analysis, the ultimate strength (MOR) of specimen B-3 is 85,081.3 kPa (12,340 psi). The EI of specimen B-3 is 585 kg-mm sq. (2x 10^6lb-in^2.) The strain at failure of specimen B-3, measured at the extreme fibers on the GFRP of the midspan tension side, was 9,359 με. The transformed and actual section for B-3 is shown in figure 49; the method of calculation for the transformed section is the same as that of B-2.

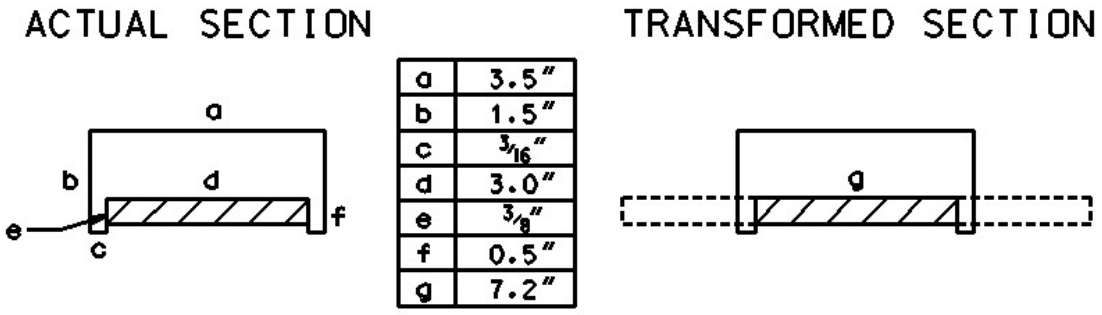

1 inch = 2.54 cm

Figure 49. Illustration. Transformed and actual section for B-3.

4.3.2 Summary

Based on the experimental results, it is evident that the use of GFRP/vinylester matrix composite with PLIOGRIP adhesive has performed very well. Two types of failures were observed: a GFRP plate tensile failure (specimen B-2) and a horizontal shear failure in the wood (specimen B-3).

The MOE of the beam with the 0.952-cm (0.375-inch) GFRP reinforcement (specimen B-3) was computed as 12.06 kPa (1.75 x 10^6 psi) (see figure 43); the MOE of the beam with the 0.64-cm (0.25-inch) GFRP reinforcement (specimen B-2) was computed as 1.82 psi. The reason for the lower MOE value appears to be the partial (less than 100 percent) bond of the 0.952-cm (0.375-inch) GFRP plate specimen (versus the 0.64-cm (0.25-inch) GFRP plate specimen). This was evidenced after careful inspection of the glue-line after the specimen failed and the GFRP plate separated (see figure 48).

The increase in strength of specimen B-2 (154 percent) was higher than the increase of strength of specimen B-3 (120 percent), in contrast to the unreinforced specimen. Also, the failure mode of specimen B-2 was a tension failure of the GFRP plate, which is more desirable than the horizontal shear failure in the wood of specimen B-3. The lower ultimate strength of specimen B-3 (with 0.952-cm- (0.375-inch-) thick GFRP plate) is also attributed to a less than perfect bond line. Furthermore, the stiffer GFRP plate appears to have induced a higher horizontal shear stress concentrated at the bond-line leading to a lower ultimate strength value.

4.4. BENDING TESTS WITH GFRP PLATES (15.24 BY 29.84 CM (6 BY 11.75 INCHES))

4.4.1. Results

The unreinforced control specimen was tested to failure under four-point bending. Loud checking sounds were heard at the onset of loading. As the load increased, horizontal checking first appeared around 11,339.8 kg (25,000 lbs). This checking continued until the specimen reached its ultimate load of 15,121.9 kg (33,338 lbs). Once the member reached this load, the load then dropped down to 10,432.6 kg (23,000 lbs). It then went back up to 14,061.4 kg (31,000 lbs) before another loud noise was heard and the load once again dropped off to 10,432.6 kg (23,000 lbs). This behavior continued for several more cycles, the load the member was carrying never went above 10,432.6 kg (23,000 lbs). The ultimate mode of failure was a combination of horizontal shear failure and tension failure due to bending. This can be seen in figure 48 and can be attributed to a low a/d ratio. This ratio must be greater than 5 to induce a bending failure following ASTM 198; if it is less than 5, horizontal shear will dominate the failure mode. For this test the a/d ratio was approximately 2.7, well below 5. The initial EI of the control specimen was computed as 125,697 kg-mm sq. (429×10^6 lb-in^2)and the ultimate strength or MOR was computed as 26,641.3 kPa (3,864 psi). The strain at failure of the control specimen measured at the extreme fibers of the midspan tension side was 2536 με. The load versus deflection curve can be seen in figure 50.

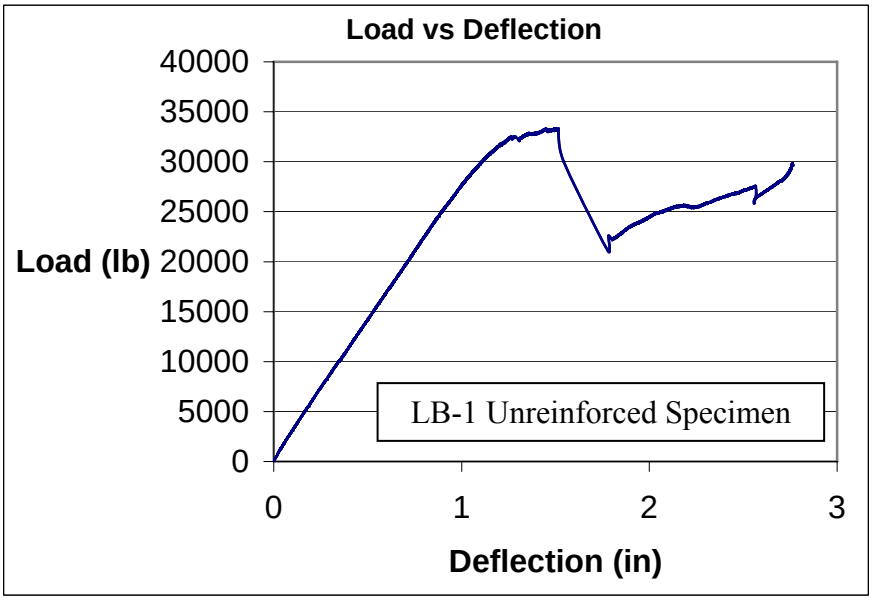

1 inch = 2.54 cm; 1 lb = 0.45 kg

Figure 50. Graph. Load versus deflection for the unreinforced specimen.

As stated earlier, two different sizes of GFRP plates were used as reinforcement. Table 6 presents MOR and EI values for all of the specimens that were tested. Table 6 also presents the percent of improvement in strength and flexural rigidity between the control unreinforced specimen and GFRP-reinforced specimens. Specimens LB-2 and LB-3 were reinforced using the 0.64-cm- (0.25-inch-) thick plate and specimens LB-4 and LB-5 used the (0.952-cm- (0.375-inch-) thick plate. The primary mode of failure for specimens LB-2, LB-3, and LB-4 was dominated by horizontal shear failure of the wood and failure in the bondline, causing a peeling action at the ends of the GFRP plate (see figure 51).

Table 6. Test results.

Specimen	Plate Thickness	EI x 106 (lb-in^2)	5% Difference	MOR (psi)
LB-1	Control	429	N/A	3864
LB-2	0.25 inch	364	-15.13	4291
LB-3	0.25 inch	478	11.47	3785
LB-4	0.375 inch	738	72.12	4913
LB-5	0.375 inch	823	91.97	4827

1 inch = 2.54 cm; 1,000 psi = 47.9 kPa

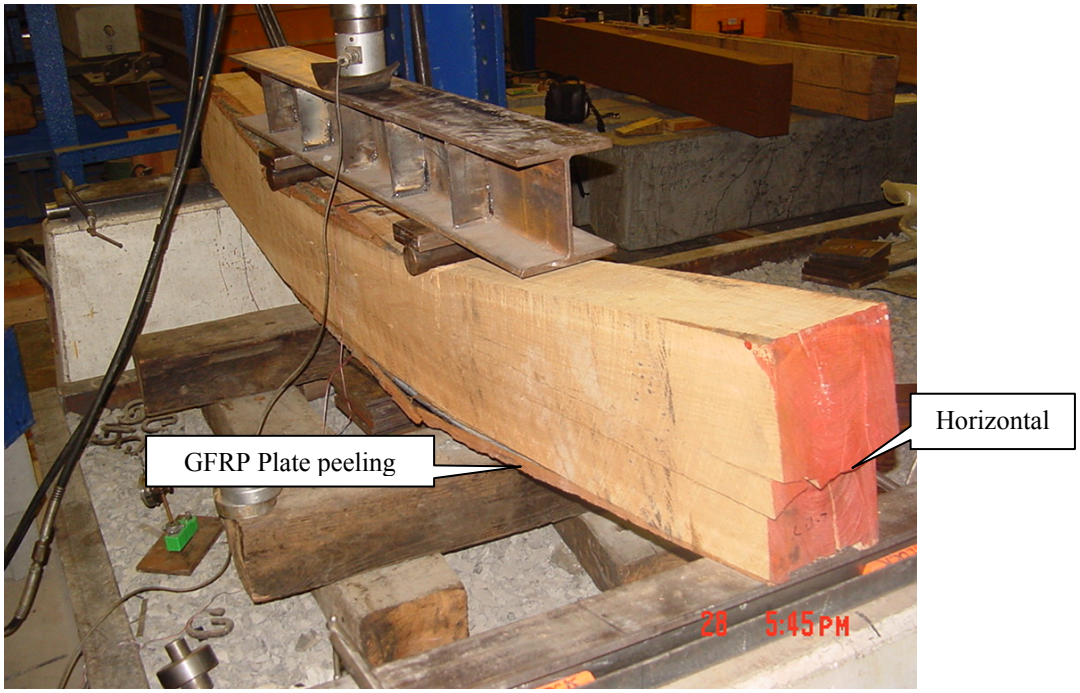

Figure 51. Photo. Failure mode of GFRP-reinforced beam.

The following computation is an example of how EI was determined:

$$\Delta_{max} = \frac{Pa/2}{24EI}(3L^2 - 4a^2) \quad (4)$$

$$EI = \frac{Pa}{48\Delta}(3L^2 - 4a^2) \quad (5)$$

Where,

L = Total length of beam between reaction points, in.
a = shear span, distance from reaction point to load point, in.
P = Total load, lb.
Δ_{max} = measured deflection at midspan, in.
EI = flexural rigidity

Because it was the only test specimen to display the desired failure mode, the detailed test results for LB-5 are described below. This specimen was tested to failure under four-point bending using the same test setup as the control specimen. Slight checking sounds were heard coming from the specimen at the onset of loading. A loud pop was heard at about 15,875.7 kg (35,000 lbs), the specimen continued to take more loading. At 18,143.7 kg (40,000 lbs) a loud pop occurred and the load dropped off to 11,339.8 kg (25,000 lbs), just as in the control specimen. A major difference between the reinforced specimen and the control specimen occurred next: The loading on the reinforced specimen continued to increase until it surpassed the point at which the loud pop was heard for the control specimen. The specimen took more loading until it reached 20,003.4 kg (44,100 lbs). The same load-stepping behavior that occurred in the control specimen occurred in specimen LB-5 when it took load until a pop was heard and the load dropped off. This continued until the load reached around 19,504.5 (43,000 lbs), at which point delamination of the GFRP plate started to occur. A tension failure occurred in the plate, as shown in figure 52. The specimen continued taking load until it completely failed at 15,875.7 kg (35,000 lbs).

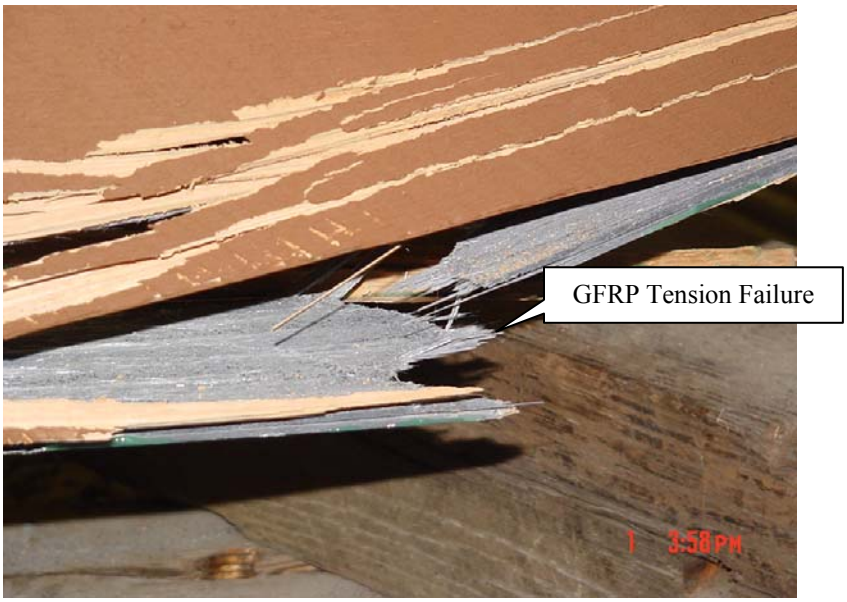

Figure 52. Photo. Failure mode of LB-5.

Figure 52 clearly shows the tension failure in the GFRP plate. Also, this specimen did not show any peeling of the GFRP at the ends. Careful inspection of all the tested specimens revealed that LB-5 was the only specimen that had no voids in the bonded surface. The authors believe that a near-perfect bond surface contributed to this failure mode in specimen LB-5.

4.4.2. Discussion

Based on the test results and a transformed section analysis (see figure 53), the ultimate strength or MOR of specimen LB-5 is found to be 33,281.0 kPa (4,827 psi), or an increase of 25 percent, in contrast to the unreinforced control specimen. The EI of specimen LB-5 is 241,139 kg-mm sq. (823 x 10^6 lb-in^2,) or a 92 percent increase over the unreinforced wood specimen. The strain at failure at the extreme fibers of the midspan tension side was 4867 με. A comparison of the load deflection diagram for specimens LB-1 and LB-5 clearly shows the improvement in flexural rigidity (see figure 54).

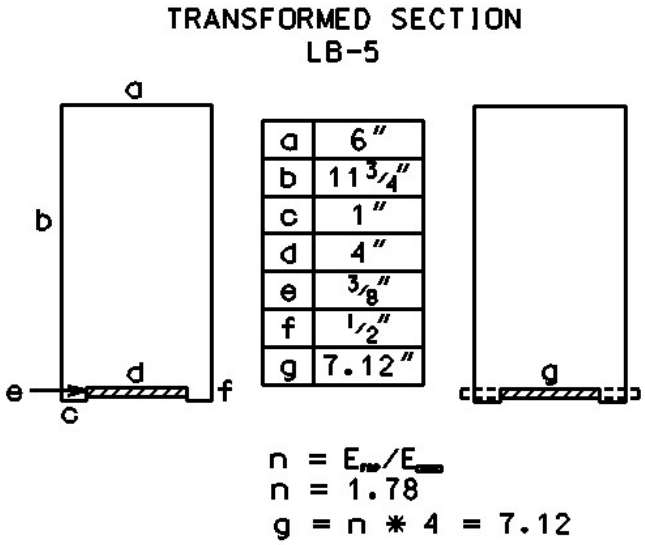

1 inch = 2.54 cm

Figure 53. Illustration. Transformed section for LB-5.

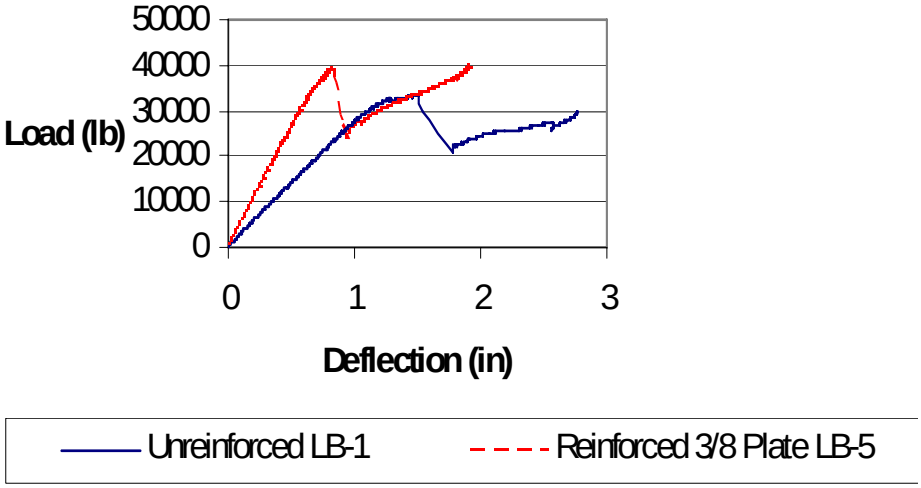

1 inch = 2.54 cm; 1 lb = 0.45 kg

Figure 54. Graph. Load versus deflection between reinforced and unreinforced beams.

4.4.2.1. Prediction of Flexural Rigidity Using Rule of Mixtures

The experimental flexural rigidity $(EI)_{exp}$ is compared to a theoretical value $(EI)_{Theo}$ by using the rule of mixtures. The rule of mixtures is a method to evaluate the structural properties of a hybrid composite/wood member based on the individual properties of its constituent materials. As an example, $(EI)_{Theo}$ was determined for specimen LB-5. This prediction assumes a perfect bond between the GFRP plate, adhesive, and wood. If there is not a perfect bond, it will show in a larger percent difference between the $(EI)_{exp}$ and the $(EI)_{Theo}$. An example of the calculation used to predict the flexural rigidity $(EI)_{Theo}$ using the rule of mixtures can be seen below:

$$(EI)_{Theo} = (EI)_{wood} + (EI)_{GFRP} \quad (6)$$

$$(EI)_{Theo} = E_{wood}\,[I_{wood} + (n \times I_{GFRP})] \quad (7)$$

$$E_{wood} = 1.8 \times 10^6 \text{ psi (determined from testing)}$$

$$I_{wood} = \frac{\mathbf{b \times d^3}}{\mathbf{12}} = \frac{\mathbf{6 \times 11.75^3}}{\mathbf{12}} = 811 \text{ in}^4 \text{ (416,231 mm to 4th power} \quad (8)$$

$$n = \frac{E_{GFRP}}{E_{wood}} = 1.78 \quad (9)$$

$$I_{GFRP} = \frac{b \times d^3}{12} = 0.0176 \text{ in}^4 \text{ (7,326 mm to 4}^{th} \text{ power)} \quad (10)$$

$$(EI)_{Theo} = 1.8 \times 10^6 [\,811 + (1.78 \times 0.0176)] \quad (11)$$

$$(EI)_{Theo} = 427{,}638 \text{ kg-mm to 4}^{th} \text{ power } (1460 \times 10^6 \text{ lb*in}^2)$$

$$\% \text{ Difference} = \frac{EI_{Theo} - EI_{exp}}{EI_{Theo}} \quad (12)$$

$$\% \text{ Difference} = \frac{\mathbf{1460 - 823}}{\mathbf{1460}} = 44\%$$

The percent difference is significant; this is an indication of less-than-perfect bond in LB-5 between the GFRP plate and the wood member.

4.4.3. Summary

The experimental results of the full-scale bending members are a further validation of earlier testing on small-scale specimens. As in the small-scale specimens, the use of GFRP/vinylester matrix composite with PLIOGRIP adhesive was used successfully to improve the strength and flexural rigidity of wooden members. Two types of failures were observed, horizontal shear failure in the

wood and tension failure in the GFRP plate. All test specimens showed an increase in strength or flexural rigidity. Specimen LB-5 showed the most significant increase in both. This can be attributed to larger bond area than the other specimens. This specimen also displayed tension failure in the plate; horizontal shear failure appeared in neither the wood nor the GFRP plate peeling at the ends.

4.5. BENDING TESTS WITH GFRP REINFORCING BARS

4.5.1. Results

Both specimens were tested to failure under four-point bending. The load versus deflection and load versus strain behavior were similar to that of earlier tension test specimens. No sounds or checking could be heard throughout the duration of the test. There was no yielding or increase in strain or deflection at constant loading (i.e., no ductility). The members did not immediately fail once the ultimate load was reached; they continued to deflect as the loading continued, but the member could not resist any more additional load (see figure 55). The ultimate mode of failure was bond failure between the PLIOGRIP and wood. The bond between the adhesive and GFRP was still intact (see figure 56). The a/d ratio for these tests was 3.2. For a bending test, this ratio should be above 5 if bending failure is desired and below 5 for shear. This ratio was irrelevant for these tests. The placement of the GFRP reinforcing bars in the specimens inhibited failure induced by horizontal shear failure.

Figure 55. Photo. Specimen after testing.

Figure 56. Photo. Specimen after testing.

The EI, MOR, and strain at failure for the test specimens are presented in tables 5 and 6. The ultimate load of BB-2 and BB-3 are respectively, 2,067.9 and 2,745.6 kg (4,559 and 6,053 lbs).

Table 7. Test results.

Specimen	MOR (psi)	EI (lb-in^2)
BB-2	2,700	4.25E+07
BB-3	3,208	4.53E+07

1,000 psi = 47.9 kPa

Table 8. Strain at failure.

Specimen	Gauge # Strain @ Failure			
	1	2	3	4
BB-2	-358	-1042	-140	-248
BB-3	-3265	-1966	-118	-98

4.5.2. Discussion

As can be seen from table 8, the strain values for gauges 1 and 2 are negative; both gauges were on the tension side of the specimen. This could be attributed to the wood pushing against the top of the reinforcing bar and the reinforcing bar pushing down onto the wood in the tension zone causing the strain reading to be negative. The strains at failure were not the maximum. The strains continued to increase even as the specimen could not take any more load. The strains increased to a point and then they went to zero as the sustained load on the specimens went to zero. The sustained load went to zero because of bond failure between the adhesive and wood. The strains also increased and decreased at different times during the test. The strains on the compression side were much higher and increased at a faster rate than those on the tension; but before the ultimate load was reached, the strains on the compression side decreased and the

strains on the tension side increased and continued to increase until well after the specimen was unable to sustain any more load.

4.5.2.1. Prediction of Flexural Rigidity Using Rule of Mixtures

EI was predicted using the rule of mixtures for specimens BB-2 and BB-3. This prediction assumes there is a perfect bond between the GFRP reinforcing bars, adhesive and the wood. If there is not a perfect bond, it will show in a larger percent difference between the $(EI)_{exp}$ and the $(EI)_{Theo}$. An example of the calculation used to predict flexural rigidity using the rule of mixtures can be seen below:

Calculation of $(EI)_{exp}$ for BB-2:

$$\Delta_{max} = \frac{Pa/2}{24EI}(3L^2 - 4a^2) \tag{13}$$

$$EI = \frac{Pa}{48\Delta}(3L^2 - 4a^2) \tag{14}$$

$$EI = \frac{18P}{48\Delta}[(3)(78)^2 - (4)(18)^2)$$

Simplifying,

$$EI = \frac{P}{\Delta}(6358.5)$$

The value of P/Δ can be found from the slope and has a value of 6683.7. Using the value in the above equation yields

$$EI = (6683.7)(6358.5)$$

producing a value of $EI = 4.25x10^7\, lb \cdot in^2$ (1245 kg-mm sq)

Calculation of $(EI)_{Theo}$:

$$(EI)_{Theo} = (EI)_{wood} + (EI)_{GFRP} \tag{15}$$

$$(EI)_{Theo} = E_{wood}\,[I_{wood} + nI_{GFRP}] \tag{16}$$

$E_{wood} = 1.8 \times 10^6$ psi (determined from testing)

$$I_{wood} = \frac{b \times d^3}{12} = 83.5 \text{ in}^4 \tag{17}$$

$$n = \frac{E_{GFRP}}{E_{wood}} = 3.11 \quad (18)$$

$$I_{GFRP} = \frac{\pi \times \mathbf{d}^4}{\mathbf{64}} \times \mathbf{2} = 0.006 \text{ in}^4 \quad (19)$$

$$(EI)_{Theo} = 1.8 \times 10^6 [\, 83.5 + (3.11 \times 0.006)] \quad (20)$$

$$(EI)_{hybrid} = 150 \times 10^6 \text{ lb-in}^2$$

$$\% \text{ Difference (BB-2)} = \frac{EI_{Theo} - EI_{exp}}{EI_{Theo}} \quad (21)$$

$$\% \text{ Difference (BB-2)} = \frac{\mathbf{150 - 42.5}}{\mathbf{150}} = 72\%$$

$(EI)_{Theo}$ for BB-3 was calculated in the same manner as BB-2.

$$(EI)_{Theo} = 150.3 \times 10^6 \text{ lb-in}^2$$

$$\% \text{ Difference (BB-3)} = \frac{EI_{Theo} - EI_{exp}}{EI_{Theo}} \quad (22)$$

$$\% \text{ Difference (BB-3)} = \frac{150.3 - 45.4}{150.3} = 72\%$$

The percent difference is significant for both of these specimens; this is another indication that there was less than perfect bond between the GFRP reinforcing bars, adhesive and the wood member.

The last measurement that was taken was the joint opening. Measurements were taken on the top of the specimen. Measurements were taken every 226.8 kg (500 lbs), the same as deflection measurements. The two specimens had about the same separation, with BB-3 having a lower amount. This was expected because BB-3 had double the amount of reinforcing bars and adhesive. Even though BB-3 had double the reinforcing material, BB-2 did not have double the joint opening distance as that of BB-3. BB-2 only separated about 7 percent more than that of BB-3. This is the same phenomenon that was displayed in earlier tension specimens and it was determined from these earlier tension tests that an increase in development length of sand-coated GFRP reinforcing bars inserted into wooden members does not improve the capacity.

The joint opening is shown in Figure 57. The trend of joint opening for both specimens is very similar. The drastic increases in joint opening are due to bond failure between the wood and adhesive.

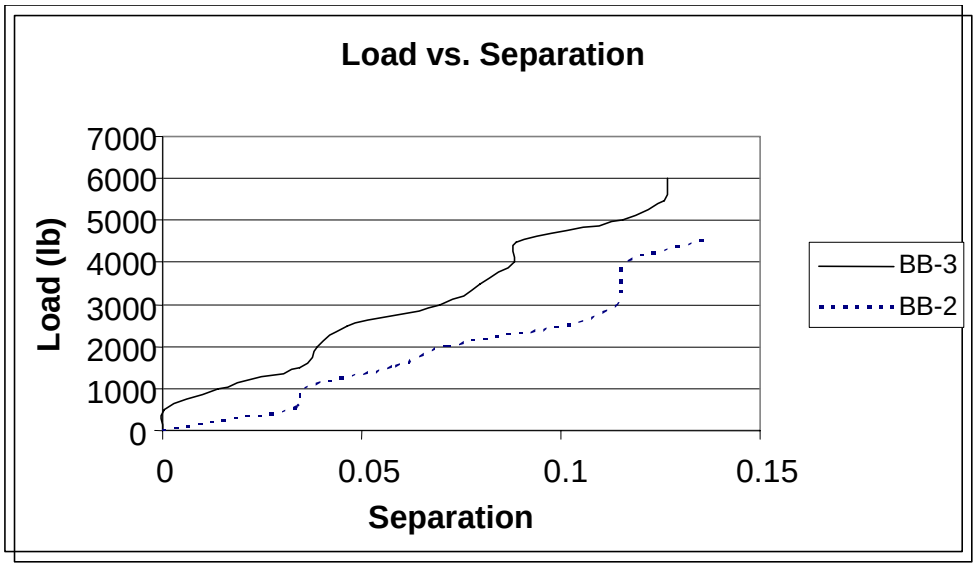

1 lb = 0.45 kg;

Figure 57. Graph. Load versus separation.

4.5.3. Summary

The experimental results of these bending specimens shows that this method of strengthening is not suited for bending members. This method would be very useful in compression members in a truss. The bars would hold the member in place and keep it from buckling. The constructability is another issue with this method. It was very difficult to drill the holes in both sides in a manner that allowed for perfect alignment. Perfect alignment could not be reached in laboratory setting and is more difficult to achieve in the field.

Figure 58 shows a detail of how a similar repair was used on the Barrackville Covered Bridge in Barrackville WV. FRP bars were used as a joint in an arch; to date, this repair is performing very well.

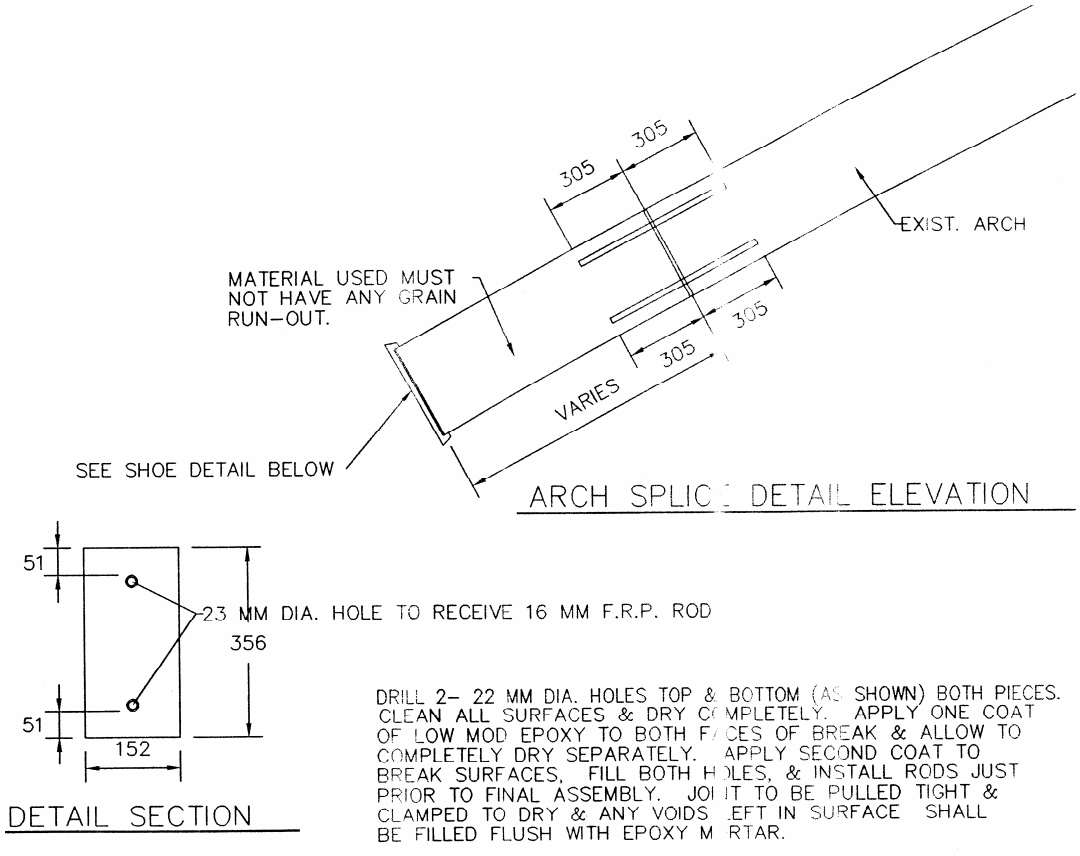

10 mm = 0.39 inch

Figure 58. Illustration. Arch splice repair detail.

4.6. BENDING TESTS WITH GFRP PLATES (15.24 BY 20.32 CM (6 BY 8 INCHES))

4.6.1. Results

The unreinforced control specimen (LB-6) was tested to failure under four-point bending to determine the ultimate moment capacity and flexural rigidity and to identify the failure mode of the unreinforced member. As the load increased, a checking sound could be heard; a loud popping noise occurred at 4,989.5 kg (11,000 lbs). Horizontal checking first appeared around 5,896.7 kg (13,000 lbs). Checking was continuous until the load reached 8,164.7 kg (18,000 lbs). Once the load reached 8,551.6 kg (18,853 lbs), another loud pop was heard, and the load then dropped down to 8,391.5 kg (18,500 lbs). This load-stepping behavior continued for several more cycles, and the load never went back above 8,391.5 kg (18,500 lbs) (see figure 59). The shear a/h ratio for this member was 5, which is adequate for the evaluation of flexural properties. Figure 60 shows the load versus deflection plot for this test. The load data in this plot do not exceed 7,257.5 kg (16,000 lbs) because the LVDT malfunctioned near the end of the test. The mode of failure was a combination of horizontal shear failure and bending failure, as seen in figure 61. The initial EI of the control specimen was computed as 899.51 kg-mm sq (3.07×10^8 lb-in^2, and the ultimate strength or MOR was computed as 40,623.9 kPa (5,892 psi). The strain at failure of the unreinforced control specimen, measured at the extreme fibers of the midspan

tension side, was 5558με. The maximum load the member sustained was 8,551.6 kg (18,853 lbs).

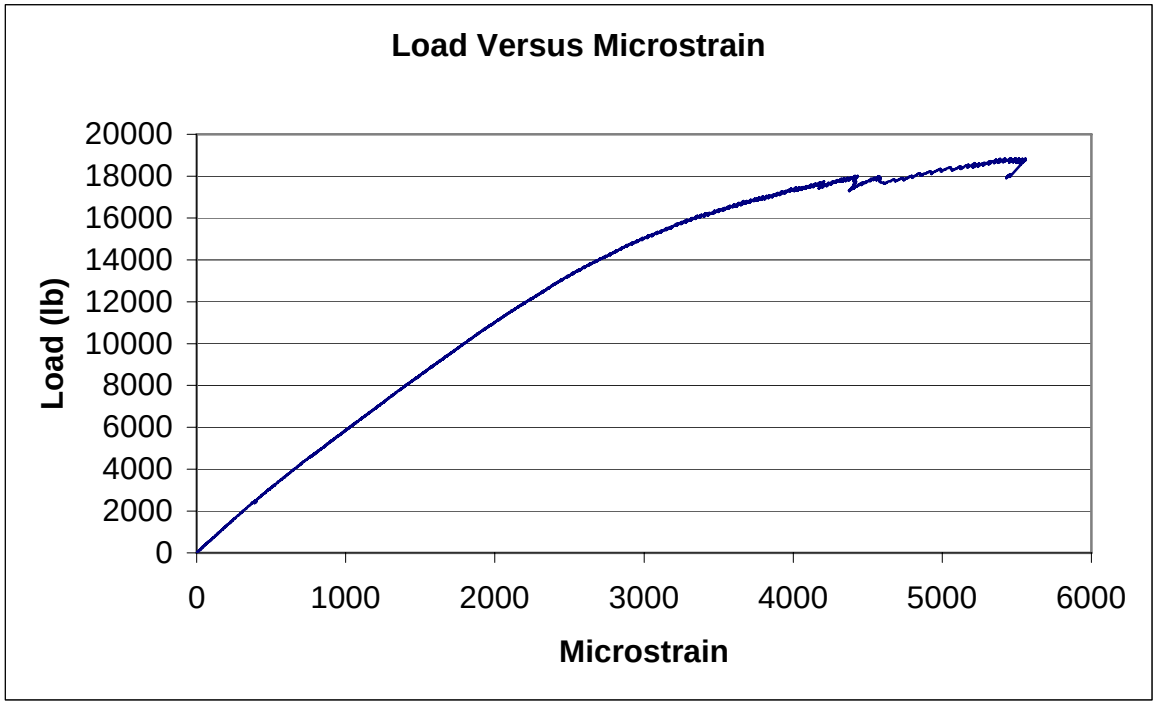

1 lb = 0.45 kg;

Figure 59. Graph. Load versus strain for the unreinforced specimen.

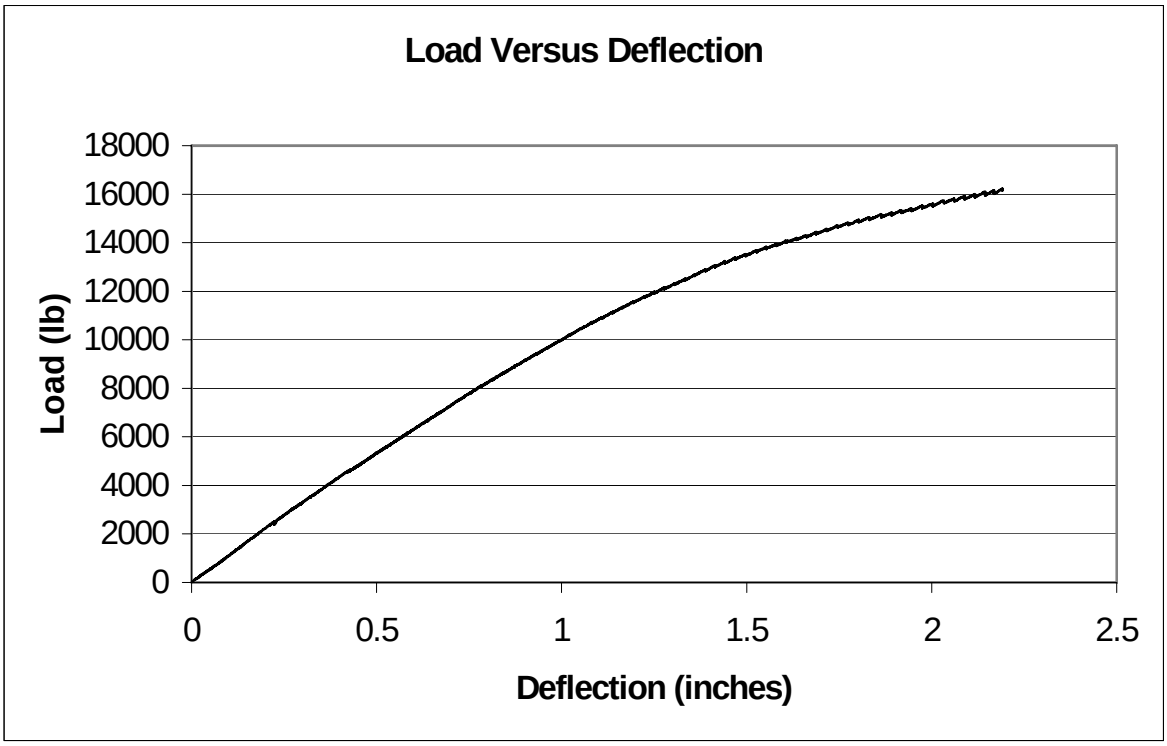

1 inch = 2.54 cm; 1 lb = 0.45 kg

Figure 60. Graph. Load versus deflection for the unreinforced specimen.

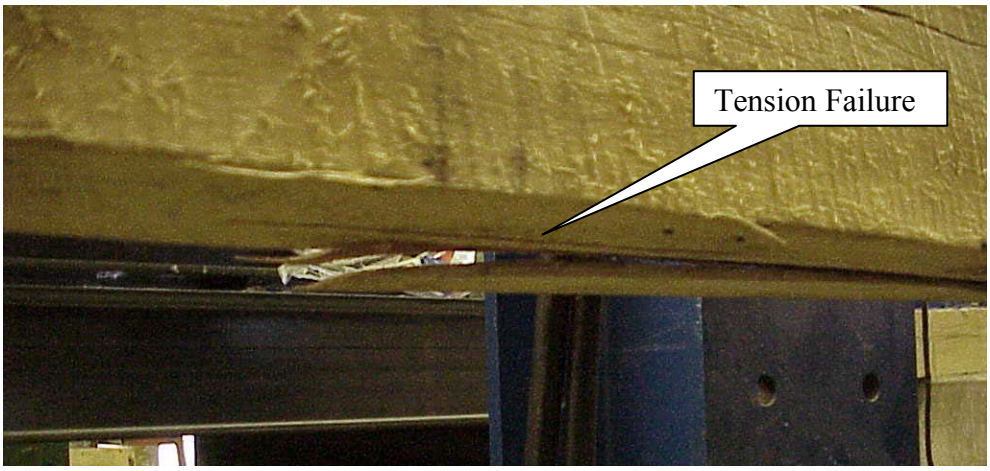

Figure 61. Photo. Failure mode of unreinforced beam.

The second specimen tested was Specimen LB-8, which was tested in the same manner as LB-6. Checking started at 5,443.1 kg (12,000 lbs). At 5,896.7 kg (13,000 lbs), a loud popping noise was heard, and dust could be seen at the same time coming from the bond line. A loud noise was heard at 6,350.3 kg (14,000 lbs) and another loud noise was heard at 6,577.1 kg (14,500 lbs). The maximum deflection of the LVDT (7.62 cm (3 inches)) was reached at 6,713.2 kg (14,800 lbs). The edges of the member on either side of the GFRP broke at 7,076.0 kg (15,600 lbs), and complete failure occurred at 7,257.5 kg (16,000 lbs). This beam's behavior was more consistent

with an unreinforced member than a reinforced one. This could be attributed to a less than perfect bond.

The primary mode of failure for LB-8 was dominated by horizontal shear failure of the wood and failure in the bondline, causing a peeling action of the GFRP plate. The full capacity of the plate was not reached in these members. The failure of the wood member in horizontal shear and the failure of the bondline occurred before the capacity of the plate could be fully used. LB-8 results demonstrate the necessity of full bond (see figure 62). A short work time adhesive (20 minutes, as suggested by the manufacturer) was used. This short work time adhesive resulted in partial bond between the plate and wood because the adhesive started to set up before the plate could be placed in the member. As seen in figure 63, there are no signs of failure in the GFRP plate in this specimen. Also, shown in figure 64, the separation of the plate was because of partial bond in the GFRP/wood.

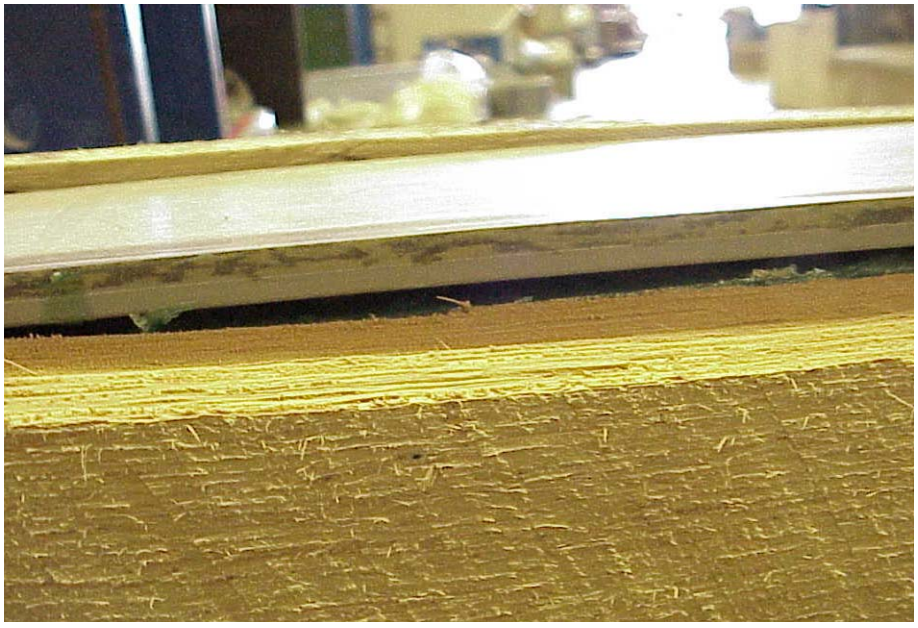

Figure 62. Photo. Bond failure of LB-8.

Figure 63. Photo. LB-8 after testing.

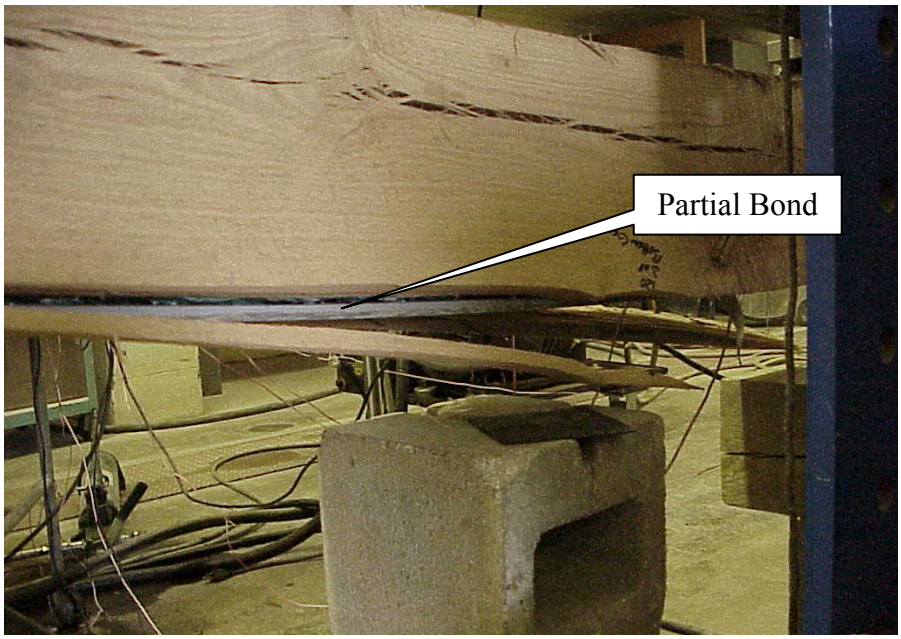

Figure 64. Photo. Partial bond in LB-8.

The third specimen tested was LB-7. This specimen was tested to failure under four-point bending on the same test setup as the other two specimens. No checking could be heard at the onset of loading. As the load increased, the load transfer between the wood member and the GFRP plate was judged adequate by monitoring the strain values from the gauges placed along the length of the member. Nonlinearity between the strain values on the compression and tension sides of the member was observed at approximately 6,803.9 kg (15,000 lbs). At 8,164.7 kg (18,000 lbs), the test member started to check, and although a loud popping noise was heard at

8,527.5 kg (18,800 lbs), the specimen continued to take more loading. The 2.54-cm- (1-inch-) wide strips (or notches) on either side of the GFRP plate failed at 9,071.8 kg (20,000 lbs) at midspan (see figure 65). Also, at this load level, a horizontal crack could be seen propagating from the center. The load then went up to 9,979.0 kg (22,000 lbs) and dropped off to 9,071.8 kg (20,000 lbs). At this time, the loading jack did not have enough travel and the member failed under creep, without any additional load being applied. This specimen also demonstrated the load-stepping behavior as seen in the other two specimens. The load-stepping behavior can be seen from the load/strain plot shown in figure 66. The key difference is that once the edge notches on this member failed, the load continued to increase. The strain at failure at the extreme fibers of the midspan tension side was 7653 με.

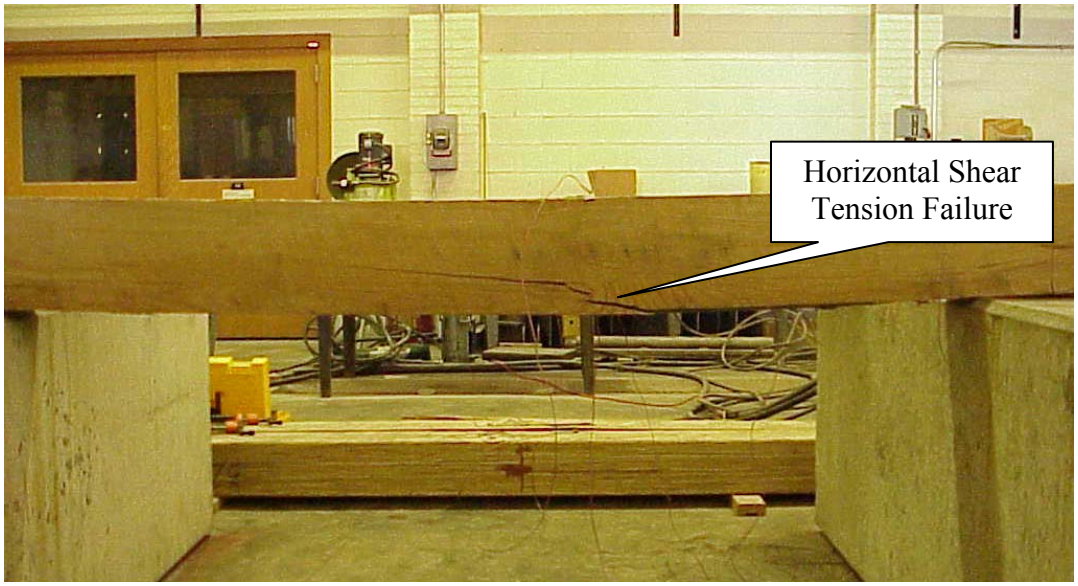

Figure 65. Photo. Failure mode of LB-7, tension side down.

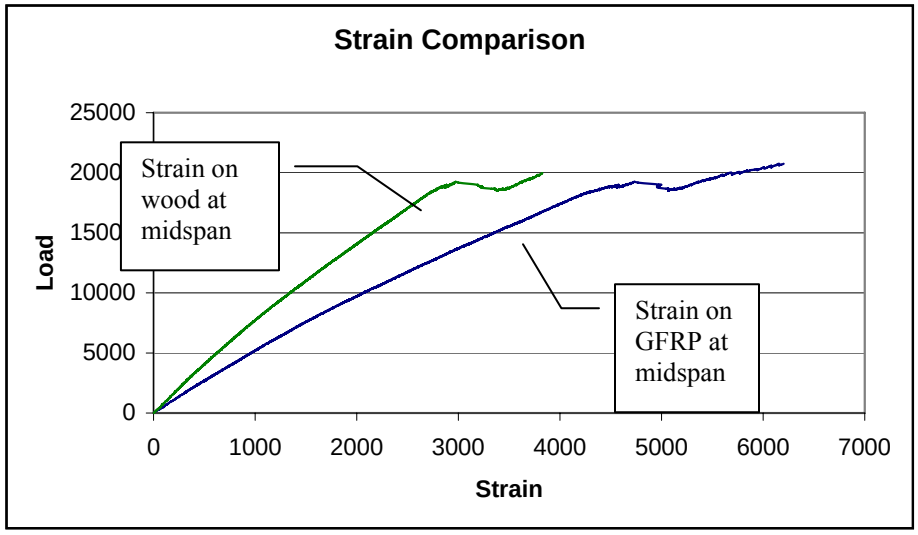

1 lb = 0.45 kg;

Figure 66. Graph. Load versus strain diagram for LB-7.

The transformed section for LB-7 is shown in figure 67. The following calculation is an example of how the neutral axis and transformed moment of inertia was determined for LB-7.

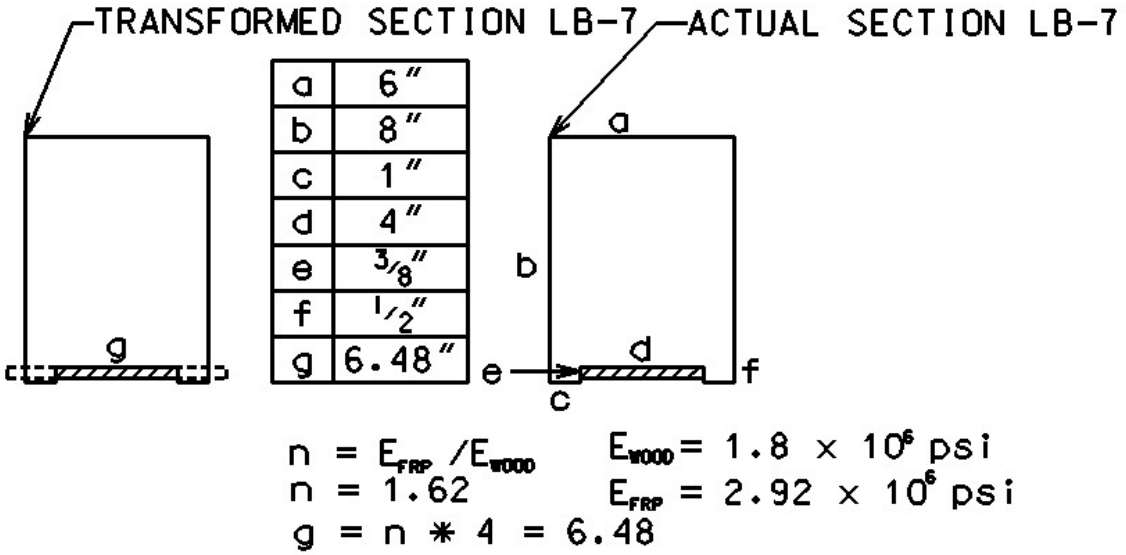

1 inch = 2.54 cm; 1,000 psi = 47.9 kPa

Figure 67. Illustration. Transformed section for LB-7.

The modular ratio, n, is calculated from the MOE values for wood and GFRP and applied to the x dimension of GFRP plate. The centroid can then be found from:

$$\bar{y} = \frac{\Sigma y_i A_i}{\Sigma A_i} \tag{23}$$

$$\bar{y} = \frac{((6 \times 7.5) \times 4.25) + ((1 \times 0.5) \times 2) + ((6.48 \times 0.375) \times 0.3125)}{48.43}$$

$$\bar{y} = 3.97 \text{ in} \uparrow$$

The transformed moment of inertia (Ix_T), with respect to the centroidal axis, can be calculated using parallel axis theorem. I_{XT} is compared to the I of the unreinforced as a check to ensure that the transformed value is larger.

$$I_{XT} = \frac{6 \times 7.5^3}{12} + [6 \times 7.5 \times 0.28^2] + \tag{24}$$
$$\frac{1 \times 0.5^3}{12} + [0.5 \times 1.0 \times 3.72^2] +$$
$$\frac{1 \times 0.5^3}{12} + [0.5 \times 1.0 \times 3.72^2] +$$

$$\frac{6.48 \times 0.375^3}{12} + [6.48 \times 0.375 \times 3.6575^2]$$

$$I_{XT} = 260.86 \text{ in}^4$$

Ix of the unreinforced section is:

$$I_X = \frac{6 \times 8^3}{12} \quad (25)$$

$$I_X = 256 \text{ in}^4$$

$$I_{XT} > I_X \therefore \text{ it's O.K.}$$

4.6.2. Discussion

As stated earlier, only one size of GFRP plate was used as reinforcement for both reinforced specimens. Table 9 shows the MOR and EI values for all of the specimens that were tested as compared to the control specimen. As presented in table 8, the flexural rigidity and strength improvement between the reinforced (LB-7) and unreinforced specimens (LB-6) are 20.4 percent and 12.03 percent, respectively. Specimen LB-8 failed prematurely because of partial bond, as described earlier.

Table 9. Test results.

Specimen	EI (lb-in^2)	% Difference	MOR (psi)	% Difference
LB-6 (control)	3.07E+08	N/A	5891.72	N/A
LB-7	3.70E+08	20.4	6600.70	12.03
LB-8 (premature failure)	1.76E+08	-42.7	4535.25	-23.04

1.0 lb-in sq = 293 kg-mm sq; 1,000 psi = 47.9 kPa

4.7. THEORETICAL MOMENT CAPACITY

In general, the bending behavior and moment capacity for a wooden beam reinforced with GFRP material can be analyzed using a basic strength of materials approach. A transformed section analysis is used to locate the neutral axis (NA) of the wood/GFRP section as described earlier. A typical moment capacity diagram is shown in figure 68. Figure 67 shows the transformed section that was used in the analysis of this test specimen. The values for modulus of elasticity for the GFRP plate and the wood member where obtained from test data.

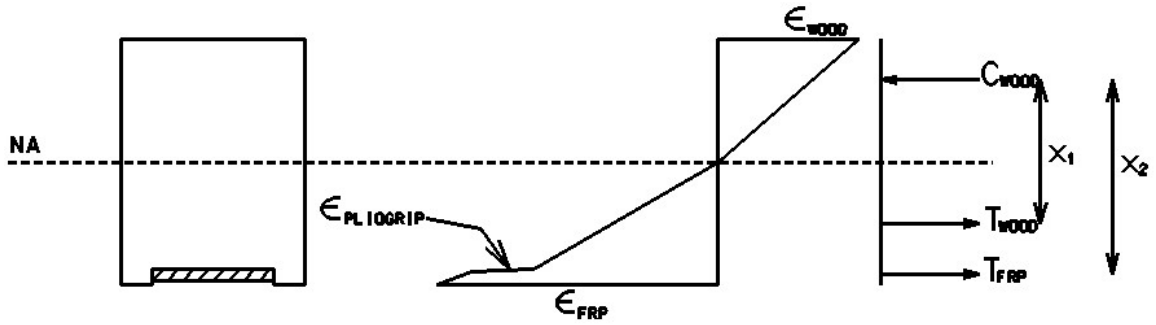

Figure 68. Illustration. Strain compatibility and internal moment equilibrium.

The theoretical moment capacity (M_{Theo}) computation is presented below and is compared to the experimental moment capacity (M_{Exp}) to determine if a theoretical moment capacity equation can be used for design purposes. The force diagram in figure 68 is used to compute M_{rTheo} The following approach is used:

T_W = Tension force of wood
ε_{WT} = Strain in wood above GFRP (midspan)
E_W = MOE of wood
A_{WT} = Area of wood in tension
T_{FRP} = Tension force of FRP
ε_{FRPT} = Strain at extreme tension fiber of FRP (midspan)
E_{FRP} = MOE of GFRP
A_{FRP} = Area of GFRP plate

The tension forces are computed as:

$$T_W = (\varepsilon_{WT} \times E_W) \times A_{WT} \quad (26)$$
$$T_{FRP} = (\varepsilon_{FRPT} \times E_{FRP}) \times A_{FRP}$$

Internal moment equilibrium, figure 68

$$M_{THEO} = (T_W \times X_1) + (T_{FRP} \times X_2) \quad (27)$$

Compare to actual moment

$$M_{EXP} = (P/2) \times a \quad (28)$$

Below is an example of the theoretical moment capacity calculation using strain compatibility and internal moment equilibrium computed at 3,175.1 kg (7,000 lbs) (see figure 69):

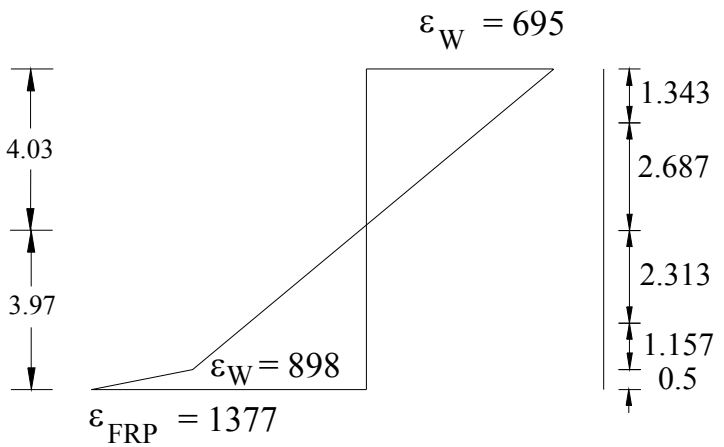

Figure 69. Illustration. Strain diagrams at 3,175.1 kg (7,000 lbs).

$$T_W = (898 \times 1.8) \times \tfrac{1}{2} (3.47 \times 6) = 16{,}827 \text{ lb} \quad (29)$$

$$T_{FRP} = (1377 \times 2.92) \times (0.5 \times 4) = 8{,}042 \text{ lb}$$

$$M_{Theo} = (T_W \times 5.0) + (T_{FRP} \times 6.157) = 134 \text{ in-kips} \quad (30)$$

$$M_{Exp} = (P/2) \times a = (7000/2) \times 40 = 140 \text{ in-kips}$$

For a 3,175.1-kg (7,000-lb) load level, the percent difference between M_{Theo}/M_{Exp} was found to be approximately 4 percent. For most of the linear range, the percent difference is less than 10 percent. However, between 6,803.9 and 8,164.7 kg (15,000 and 18,000 lbs), the percent difference converges rapidly to less than 1 percent. Figure 70 shows how the moment capacities vary with load level. As can be seen from figure 70, the moment capacity values are almost linear up to the point where failure starts to occur; then the values diverge away from each other.

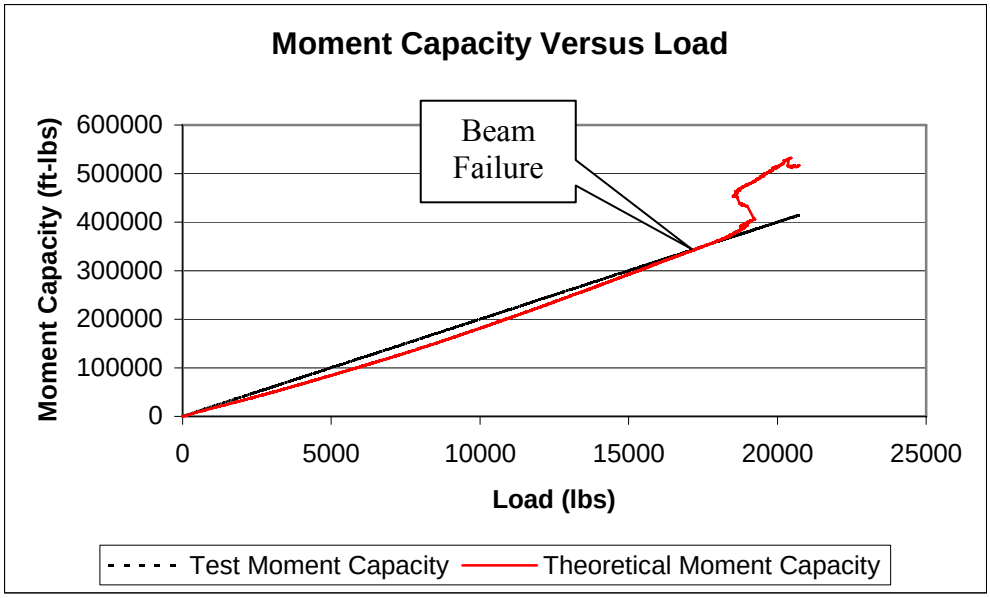

1 lb = 0.45 kg; 1 ft-lb = 1.36 joule (J)

Figure 70. Graph. Load versus M_{Theo}/M_{Exp}.

4.8. ADHESIVE STRAIN

The strain in the PLIOGRIP adhesive was determined based on the difference between the strains from the strain gauge placed on the wood internally and the strain gauge placed on the GFRP plate, as in figure 71. Also, figure 72 shows the strain elongation in the PLIOGRIP from the strain profile for a 3,175.1-kg (7,000-lb) load level.

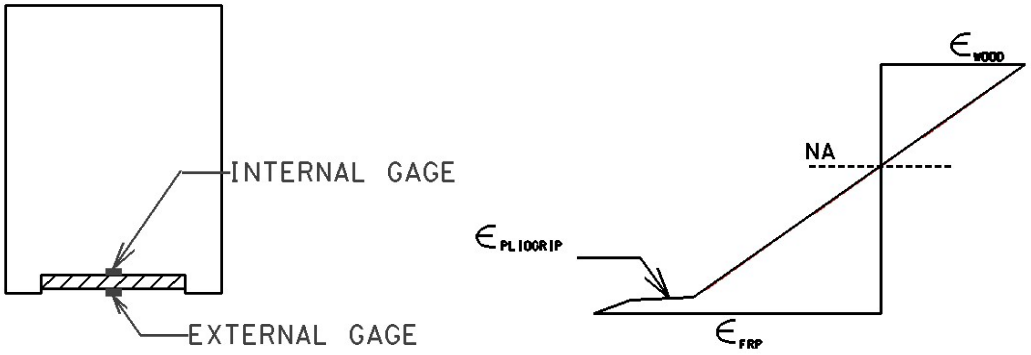

Figure 71. Illustration. Diagram of strain gauge placement and strain profile.

However, the strain in the PLIOGRIP is linear up to a certain load level (which is about 9,525.4 kg (21,000 lbs)) and then yielding of the PLIOGRIP occurs, as in figure 72. This behavior of an adhesive is extremely beneficial in terms of transferring the load to the GFRP. Other adhesives like epoxies are typically brittle and fail suddenly.

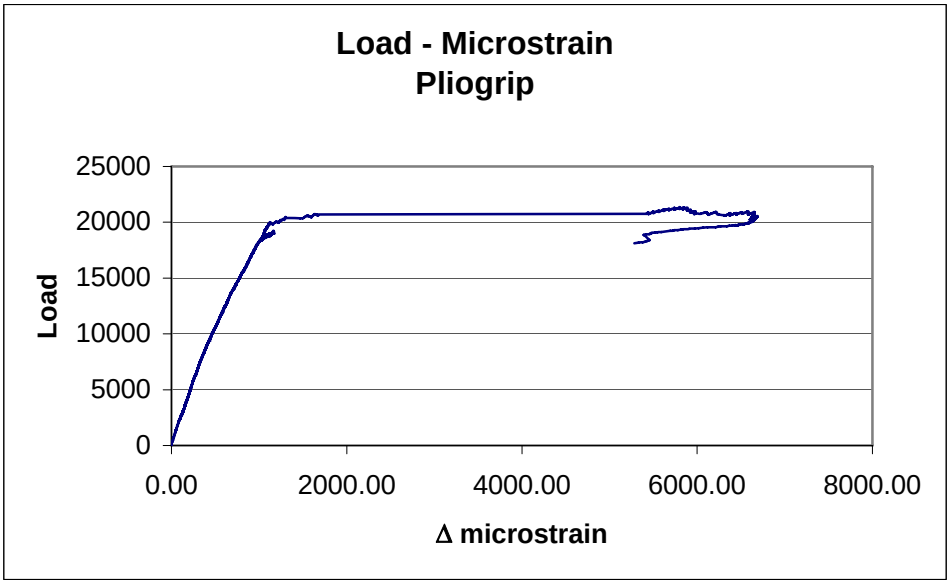

1 lb = 0.45 kg;

Figure 72. Graph. Load versus Δ microstrain (strain in GFRP minus strain in wood)

4.9. PREDICTION OF FLEXURAL RIGIDITY USING THE RULE OF MIXTURES

EI was predicted using the rule of mixtures for specimen LB-7. This prediction assumes there is perfect bond between the GFRP plate, adhesive, and wood. If there is not a perfect bond, it will show in a larger percent difference between the $(EI)_{exp}$ and the $(EI)_{hybrid}$. A detailed example of the calculation used to predict EI using the rule of mixtures can be seen in section 4.5.2.1.

EI comparison for LB-7:

$$(EI)_{hybrid} = 410 \text{ x } 10^6 \text{ lb-in}^2$$

$$\% \text{ Difference} = \frac{EI_{hybrid} - EI_{exp}}{EI_{hybrid}} \qquad (31)$$

$$\% \text{ Difference} = \frac{410 - 370}{410} = 9.8\%$$

The percent difference is under 10 percent for LB-7, an indication that there was close to perfect bond between the GFRP plate, adhesive, and wood member. This suggests composite action in the specimen, and the prediction of flexural rigidity using the rule of mixtures is accurate for this specimen.

Another issue that needs careful evaluation is the percent of GFRP in the reinforced section and the resulting stiffness.

4.10. SHEAR TEST WITH GFRP PLATES (15.24 BY 20.32 CM (6 BY 8 INCHES))

4.10.1. Results

An unreinforced control specimen (15.24 by 20.32 by 304.8 cm (6 by 8 by 120 inches) was tested to failure under four-point bending according to ASTM 198 with an a/h < 5 to induce shear failure, as described in section 3.7.2. The unreinforced specimen had a moisture content level of 20 percent and was stored in a humidity chamber at a constant temperature and humidity level (20 °C (68 °F) and 70 percent relative humidity) until testing. Small checking sounds were first heard around 4 490.6 kg (9,900 lbs) and continued throughout the test. As the load increased, the checking sounds became gradually louder and recurring. This checking continued until the specimen suddenly failed and reached an ultimate load of 22,969.0 kg (50,638 lbs). Once the member reached this load level, the load dropped down to around 11,203.7 kg (24,700 lbs) and stayed at that level for the continuation of loading. The ultimate mode of failure was sudden horizontal shear failure. This is shown in figure 73 and is attributed to a low a/h ratio. The strain at failure of the control specimen measured at the extreme fibers of the midspan tension side was 3233 με while the maximum load was 22,969.0 kg (50,638 lbs).

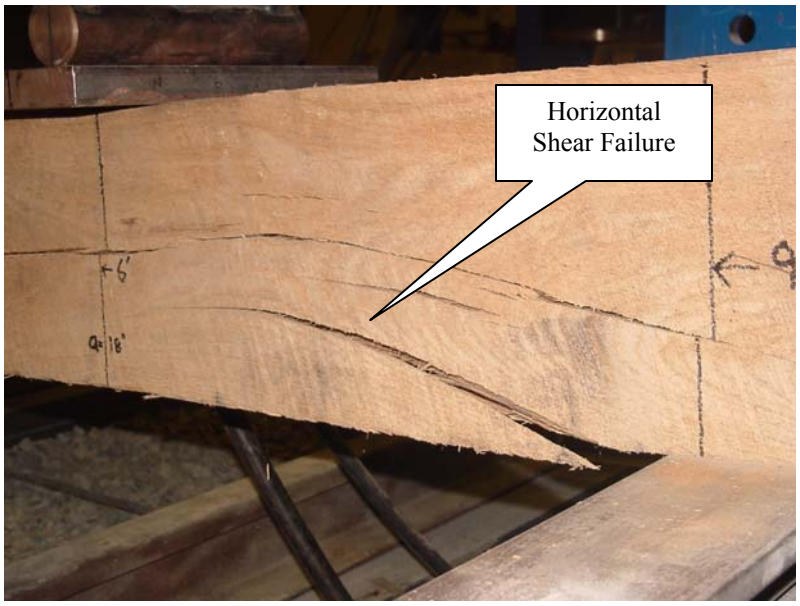

Figure 73. Photo. Horizontal shear failure of control specimen (unreinforced).

Specimen B1 was reinforced with a 0.95- by 10.16-cm (0.375- by 4.0-inch) GFRP plate, as described in section 3.7.2. This specimen was also tested to failure under four-point bending using the same test setup as the control specimen. As stated earlier, specimen B1 had several deep splits and checks because of extremely dry conditions in the lab environment. The first checking sound made under testing was around 9,979.0 kg (22,000 lbs). More checking sounds were heard around 12,927.4 kg (28,500 lbs) and then continued slightly every 907.2 kg (2,000 lbs). This continued until 17,372.6 kg (38,300 lbs), when a loud noise was heard, and dust could be seen coming from the specimen. Slight horizontal shear splits could be seen forming under one of the points where the load was being applied (see figure 74). The load dropped down to 17,327.2 kg (38,200 lbs) before increasing again. Another loud pop was heard at 18,858.1 kg

(41,575 lbs), and the load dropped down once again, this time to 17,832.1 kg (39,313 lbs). The specimen continued to split until the ultimate load was reached at 20,887.9 kg (46,050 lbs). This load-stepping behavior is shown in the load/shear strain plot in figure 75. It appears that after the wood failure, the loads were then transferred to the GFRP plate through the PLIOGRIP and the specimen could sustain loads to around 20,411.7 kg (45,000 lbs). Continual loading of the specimen then brought about tension failure in the GFRP plate, and the load decreased slightly to around 18,143.7 kg (40,000 lbs), where the test was stopped. After carefully inspecting this specimen, it was found that there were no voids in the bond surface or delamination between the GFRP and wood. We believe that a near-perfect bond surface contributed to this failure mode of specimen B1 (see figure 76).

Figure 74. Photo. Shear failure of B1 directly under loading point.

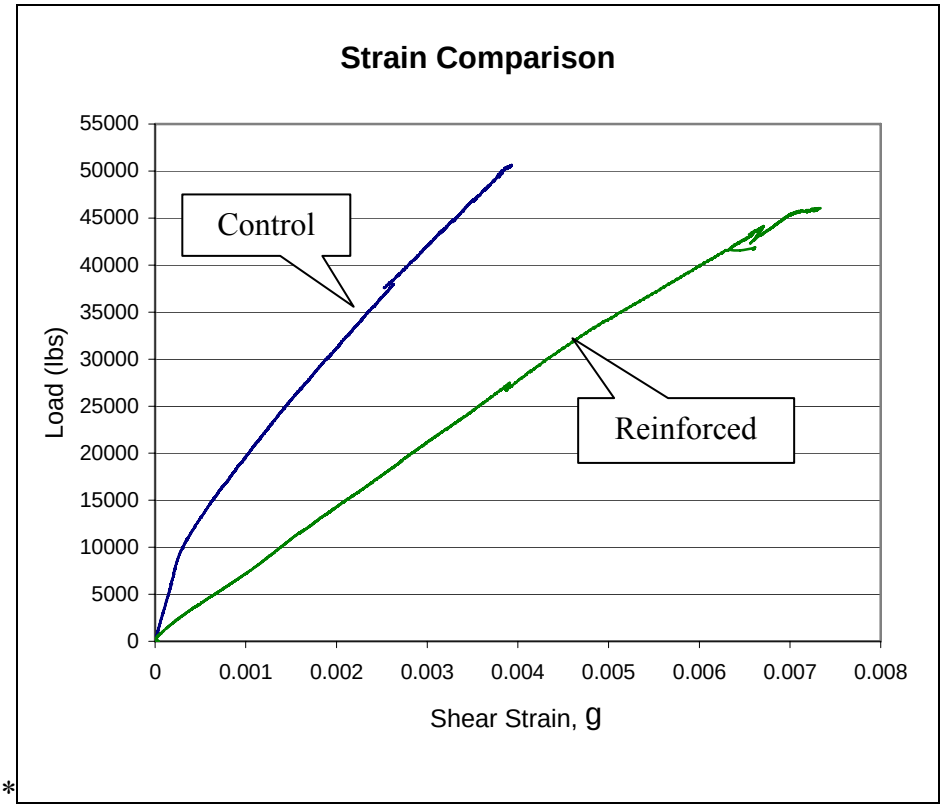

*1 lb = 0.45 kg; 1 gram = 0.035 ounce

Figure 75. Graph. Load versus strain diagram for beams tested.

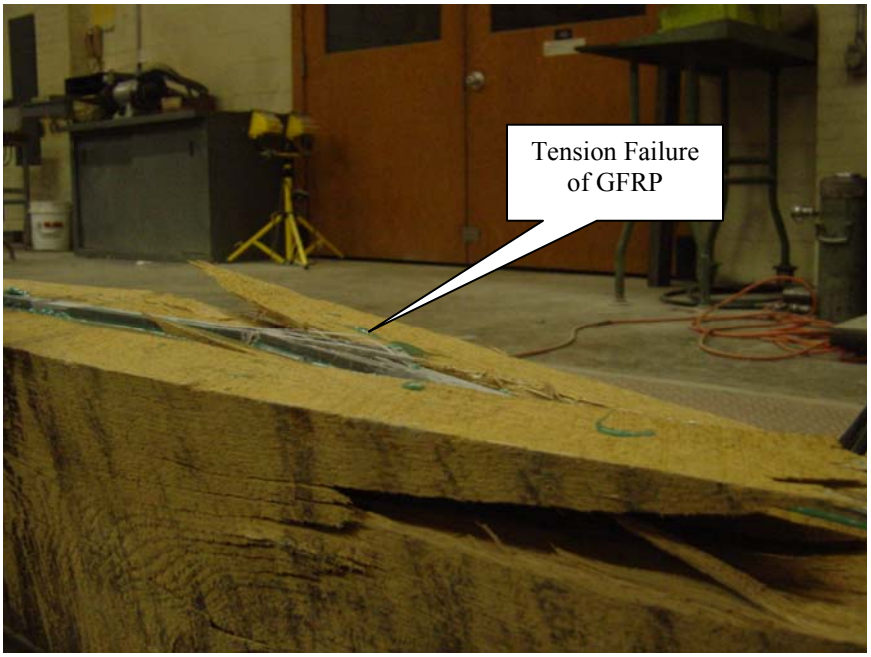

Figure 76. Photo. Tension failure of GFRP plate.

Table 10 presents shear modulus, G, and shear strain values for both specimens. Table 10 also presents the percent variation in shear strength and shear stiffness or modulus (G) between the control unreinforced specimen and GFRP-reinforced specimen.

Table 10. Shear stiffness (G) and shear strength (τ) results.

	G	Δ%	τ_{max}	Δ%
Control	536,604	N/A	791.219	N/A
Reinforced	110,422	-80	719.590	-10

The primary mode of failure for all specimens was dominated by horizontal shear failure of the wood. G was computed using the following equations:

$$\tau = G\gamma \tag{32}$$

$$\tau = \frac{VQ}{Ib} \tag{33}$$

$$Q = A\bar{y} \tag{34}$$

Where τ = Shear stress, psi
G = Shear Modulus, psi
γ = Shear strain
V = Shear load, lbs
Q = First moment of area, in^3
I = Moment of inertia, in^4
b = Beam width, in
$\bar{y}$ = Distance from centroid of area to neutral axis
A = Area, in^2

Equating the shear stresses and substituting P/2 for V yields,

$$G = \frac{P}{\gamma}\left(\frac{Q}{2Ib}\right) \tag{35}$$

where P/γ is the slope of the line from the load-shear strain diagram (see figure 75).

For the GFRP-reinforced section, transformed moment of inertia, I_t, and a transformed beam width, b_t, were computed. The reinforced section in figure 77 shows the beam width b_i, the GFRP plate width b_r, and the notch width b_v.

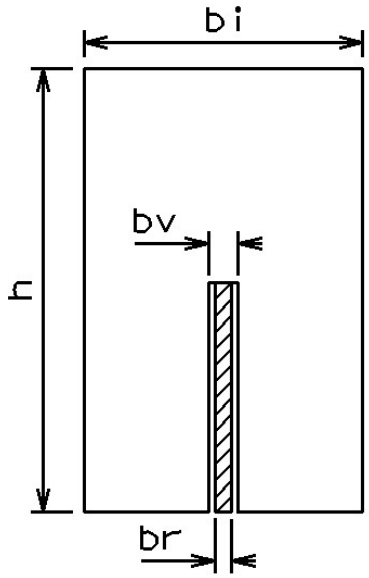

Figure 77. Illustration. Wood beam reinforced with GFRP.

The following equations were used to locate the neutral axis (N.A.) and determine the I_t and b_t.

$$\overline{y_b} = \frac{\sum_i^n \bar{y}_i A_i}{\sum_i^n A_i} \tag{36}$$

$$I_t = \sum_i^n \frac{b_i h_i^3}{12} + A_i d_i^2 \tag{37}$$

$$\mathbf{n} = \frac{\mathbf{E_{GFRP}}}{\mathbf{E_{Wood}}} \tag{38}$$

$$\mathbf{b_t = 2\left(b_i - b_v\right) + b_r * n} \tag{39}$$

Where $\bar{\mathbf{y}}_\mathbf{b}$ = Centroid of the entire beam, in
$\bar{\mathbf{y}}_\mathbf{i}$ = Centroid of each element in beam, in
A_i = Area of each element, in^2
I_t = Transformed moment of inertia, in^4
b_i = Solid beam width, in
b_v = Notch width, in
b_r = Reinforcement width, in
h_i = Height of each element, in
d_i = Distance from the centroid of the element to the neutral axis, in
b_t = Transformed beam width, in
n = Modular ratio

Plotting the shear stress along the depth of the cross section of the member (as in figures 78 and 79) shows how the stress varies along the depth of the beam. For the solid section, the shear stress is maximum at the neutral axis. This is not the case for the transformed section. Since the beam width varies from 15.24 cm (6 inches) on the top to 15.56 cm (6.126 inches) on the bottom, a shear lag develops at the interface. Figure 79 shows a transformed section with the transformed beam width. The transformed beam width along the depth of the inserted GFRP plate is 15.56 cm (6.126 inches), while the beam width above the GFRP plate is 15.24 cm (6.00 inches).

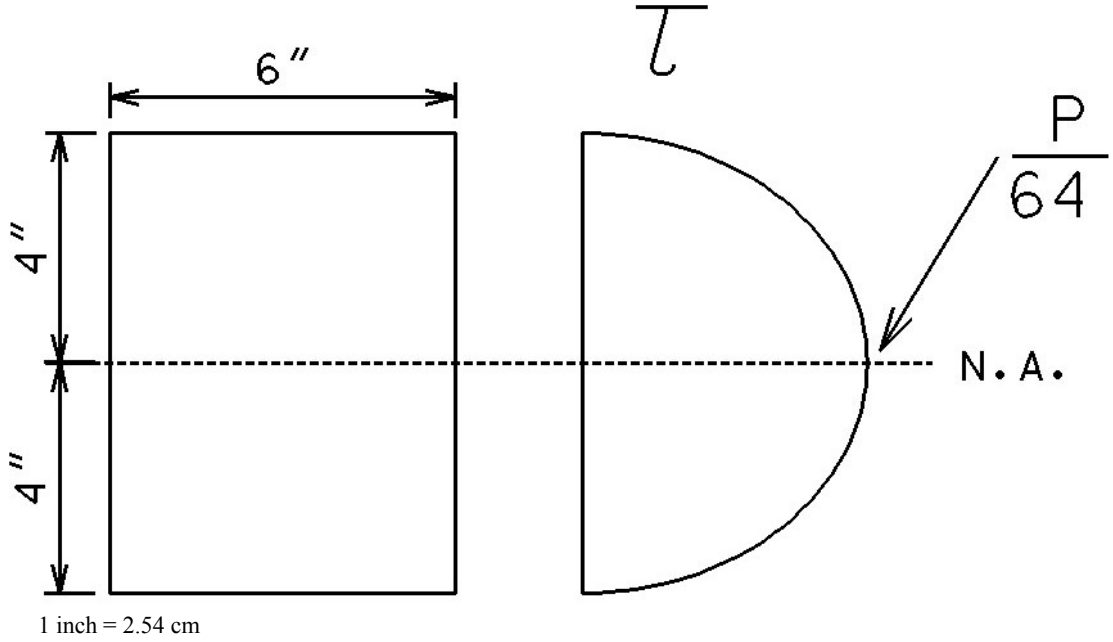

Figure 78. Illustration. Shear stress variation for solid beam.

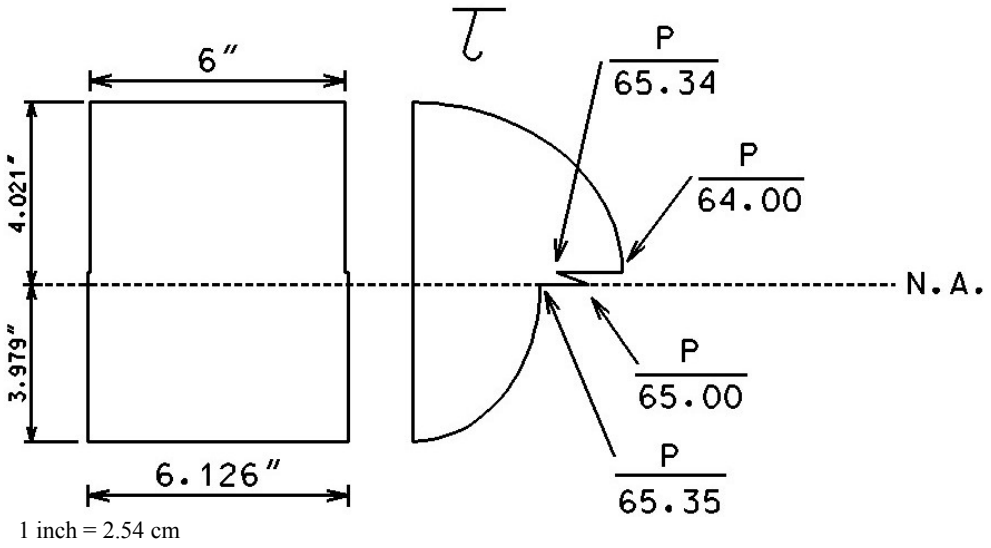

Figure 79. Illustration. Shear stress variation for GFRP transformed section.

To determine the maximum shear stress (τ) using equation 33, the transformed beam width (b_t) along with the transformed moment of inertia (I_t) are required. Several points along the shear stress diagram are established (see figure 79). These points show the slip (discontinuity) phenomenon at the NA and at the interface, as represented by varying shear stress values (see figure 78).

For example, to compute the shear stress above the GFRP plate (τ_{top}), the beam width b_i=6" is used, and τ_{top} is given as:

$$\tau_{top} = \frac{VQ}{I_t b_t} = \frac{PQ}{2I_t b_t} = \frac{P}{64.00} \tag{40}$$

To compute the shear stress just below the GFRP plate (τ_{bot}), a transformed beam width, b_t = 15.56 cm (6.126 inches), is used, resulting in a τ_{bot} = P/65.34. Since the section is no longer symmetric, the areas above and below the neutral axis are not equal, which in turn will change the value of the first moment of area, Q, resulting in two shear values (i.e., τ_{top} and τ_{bot}).

For the diagrams (figures 78 and 79), the ratios for P are given, where P is the applied load at any time during testing. The ultimate values for P were used to compute τ as presented in table 10.

Table 10 shows that τ_{max} for the reinforced specimen (B1) is actually lower than the control specimen (C1), as expected, since the reinforced specimen was heavily checked prior to testing. Future specimens will be stored in a controlled environmental chamber to minimize checking.

Figure 80 shows the shear stress/shear strain curves; figure 81 shows the load/deflection curves for the unreinforced (control) and reinforced specimens. As shown in both figures, there are several regions of load stepping behavior for the control and reinforced specimens.

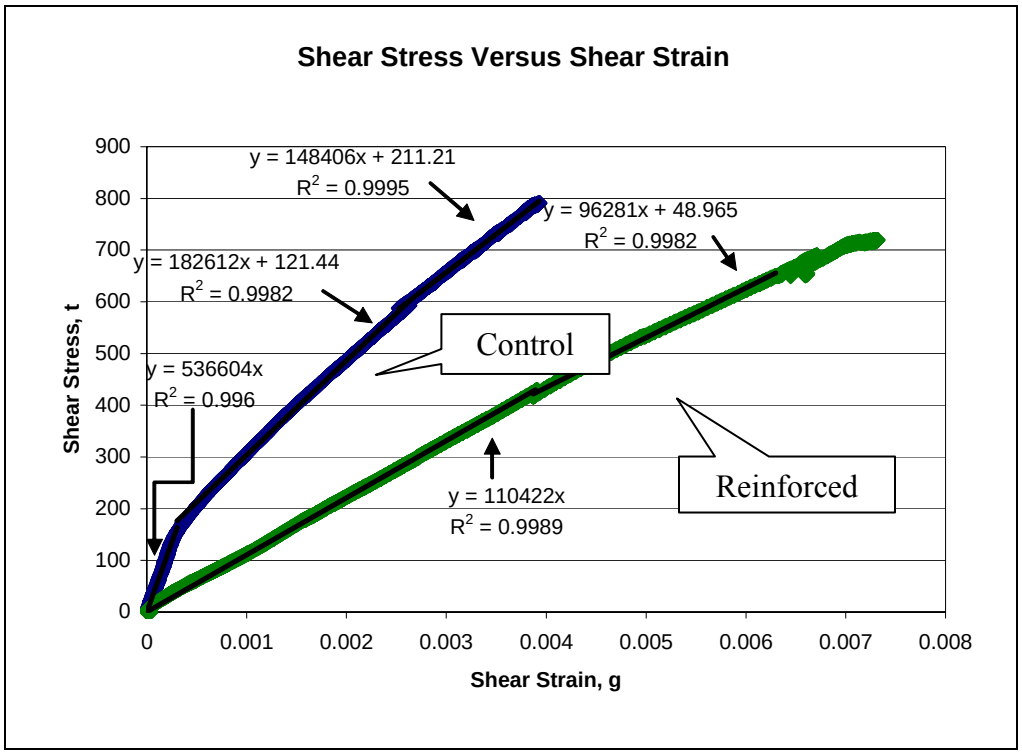

1 gram = 0.035 ounce; 1 metric ton = 1.102 U.S. ton

Figure 80. Graph. Stress versus strain diagrams for specimens.

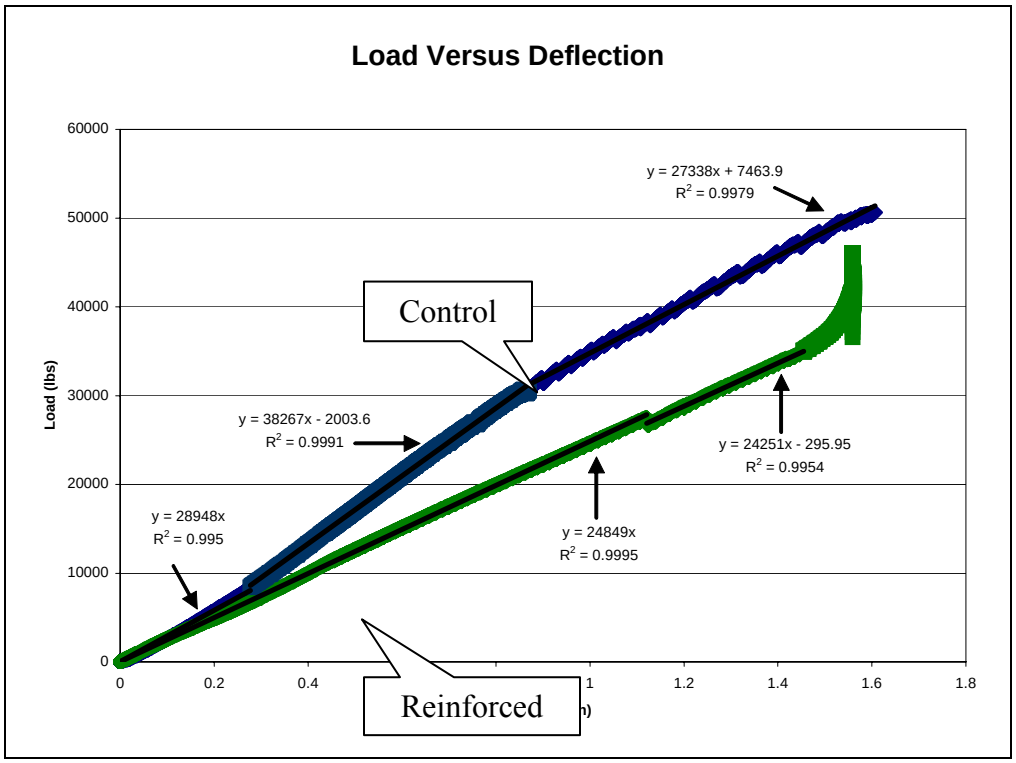

1 inch = 2.54 cm; 1 lb = 0.45 kg

Figure 81. Graph. Load versus deflection diagrams for both specimens.

4.10.2. Discussion

Since the reinforced specimen was stored in the laboratory and exposed to extreme heat conditions resulting in rapid drying, severe checking and splitting occurred prior to testing. These deep splits and checks severely degraded the horizontal shear strength of the reinforced specimen. This is one reason why the reinforced specimen did not perform as well as the control. Furthermore, because of the heat, the moisture content in specimen B1 was 7 percent compared to that of the control specimen that was kept under a controlled environment prior to testing with a moisture content of 20 percent at testing. This difference in moisture content and not having kept both beams under the same environmental conditions is a major factor in the reduction of strength in the reinforced specimen.

Future tests will be conducted with all the specimens exposed to controlled environmental conditions prior to acquiring them, during the placement of the GFRP plates, and during testing.

CHAPTER 5—CONCLUSIONS AND RECOMMENDATIONS

5.1. INTRODUCTION

Reinforcement of timber members using glass-fiber reinforcement polymers (GFRP) was evaluated during this research project. The results indicate that this type of reinforcement can be used successfully to improve the strength and stiffness of wooden members instead of using steel or stainless steel fasteners and connectors, or even custom-made steel assemblies for joining members.

The preliminary results and findings provide guidelines so that an engineer can repair and reinforce a historic timber structure. The information presented in this report provides recommendations for the use of GFRP composite materials, appropriate resins and adhesives, and methods to strengthen wooden members while complying with and supplementing the provisions of the Secretary of the Interior's Standards for the Treatment of Historic Properties.

5.2. CONCLUSIONS

Based on the research work presented, the following conclusions are drawn:

- From the experimental tests, it is evident that the use of GFRP/vinylester matrix composite with PLIOGRIP adhesive has performed very well in the case of bending and tension members. PLIOGRIP was chosen because of its high compatibility with GFRP/vinylester matrix composite and also wood.

- The tension tests established a development length for the case of sand-coated GFRP reinforcing bars embedded in wood, which was reached in a relatively short distance. Based //on the preliminary laboratory tests, the bonded-in GFRP reinforcing bar members performed well in terms of pullout force and bond strength. The chosen reinforcing bar diameter (d_b) and length did not appear to significantly affect the pullout performance and bond strength beyond a bond length of $8d_b$. The bar diameter that was used was $d_b = 1.27$ cm (0.5 inches). So the bond length was approximately equal to 10.16 cm (4 inches).

- As in the small-scale specimens, the use of GFRP/vinylester matrix composite with PLIOGRIP was successful in improving the strength and stiffness of wooden members by bonding a plate on the tension side of the member. There are, however, some limitations observed with this strengthening method. The wood surface must be prepared so that the surface is level to provide a uniform bonding area. If there is not adequate bond, the GFRP plate will peel from the member and possibly lead to a reduction in performance. The surface must be degreased and freed from loose material. The surface preparation requirements for PLIOGRIP are not as stringent as those of epoxy. In addition, for epoxy treatment, the surface temperature must be around 10 ºC (50 ºF) for all bonding applications, whereas with PLIOGRIP the work or application time is 45 minutes at 23.89 ºC (75 °F).

- The results from testing full-scale members indicate that strength and stiffness can be improved significantly, while still complying with the Secretary of the Interiors Standards for

Historic Preservation in regard to concealment of modern intrusions, and thus preserving the appearance, color, and texture of the original members.

- The experimental results conducted on bending members reinforced with bars placed at the top and bottom of the test specimens did not achieve the desired level of performance. This method, however, would be very useful with compression members in a truss. The bars would be used to hold the member in place and keep it from buckling. Constructibility is another issue with this method. It was difficult to drill the holes in both sides in a manner that allowed for perfect alignment. Perfect alignment could not be reached in a laboratory setting. A much better solution, in the authors' experience, is to use a flitched beam with a vertical GFRP plate placed in a groove in the wood. Although initial testing indicates otherwise, we believe that the shear strength can be improved by the addition of GFRP plates.

- A transformed section analysis, strain compatibility and internal moment equilibrium approach accurately predicted the moment capacity of full-scale members and can be used for design purposes.

- The ductility of PLIOGRIP, which was demonstrated experimentally, is extremely beneficial in transferring the load to GFRP. Other adhesives like epoxies fail because of brittleness and therefore do not allow the reinforcement (GFRP) to reach its full potential.

- Moisture contents and temperature of the test specimens were held as a constant for this research project. All specimens were tested at indoor ambient temperature that had very little variance. The question of degradation of the PLIOGRIP adhesive in a moist environment must be studied in the future.

- Two GFRP flitch beams were tested in shear. Although the shear capacity was expected to improve significantly with the addition of GFRP reinforcement placed on edge (resulting in a flitched beam), the shear capacity decreased slightly. The tested flitched beams were severely checked, which degraded their shear strength as compared to the solid control specimen. It is anticipated that an increase in shear strength will result when the wood samples are not heavily checked.

- A simple transformed section analysis was performed to determine the shear stresses.

5.3. RECOMMENDATIONS

The following recommendations are suggested for future research.

Performance of GFRP reinforced wood joints—Examine the feasibility of reinforcing wood at jointed connections using GFRP composite materials. Conduct, large full-scale tests on trusses, beams, and tension members to eliminate or reduce the effects of scaling.

Performance of GFRP reinforced wood members under environmental exposure—There is a need to evaluate long-term performance of bonded-in GFRP reinforcing bars in wood members subjected to tension under several varying environmental conditions.

Testing should be conducted that examines strengthening methods developed for this research project under field application conditions on existing structures.

Performance of GFRP-reinforced wood members exposed to wood preservatives—Although the Secretary of the Interior's Standard for the preservation of historic bridges does not allow the use in restoration work of wood preservatives that alter color or texture, in some cases replacing a decayed wood members with a GFRP-reinforced member that is also treated with preservatives is the ideal remedy for a particular location such as an end post resting on an exposed abutment. Therefore, another recommendation for future research would be to evaluate the long-term performance of GFRP-reinforced bridge members exposed to wood preservative chemicals and pressures.

Manual/chapter on repair and strengthening of historic covered bridges—Develop a stand-alone manual or chapter on the preservation and strengthening of historic covered bridges using GFRPs through step-by-step design procedures, including information on types of fibers and adhesives, and installation.

APPENDIX A—PRELIMINARY TESTING

A.1. INTRODUCTION

One possible method for strengthening deteriorated historic wooden members without violating the Secretary of the Interior's Standards for Rehabilitation is to internally reinforce them with glass-fiber reinforced polymer (GFRP) composite bars. To implement such rehabilitation, the nature of the bond between the composite rebar and the wood must be understood. Tension test specimens were developed and tested to determine the bond strength of the GFRP bar adhesively bonded to wood. The development of techniques used to prepare members that are internally reinforced must be developed. Achieving an acceptable bond depends on an understanding of primer and adhesive types, techniques to cut the wood and inject or pour the adhesive, and necessary bond length.

A.2. VOID TEST FOR TENSION MEMBERS

Void tests were conducted to determine the best method to apply the adhesive to the GFRP. Several different methods were developed and compared. The best method was then used to further develop the techniques to strengthen the tension members.

A.2.1. Preparation of Test Specimens

Tests were conducted to determine the best method to apply the adhesive. Because of its high compatibility with wood, phenolic formaldehyde resin was used; and the reinforcing bar was GFRP with vinylester matrix. Earlier test results showed poor results with the vinylester matrix reinforcing bars and the phenolic matrix. The test results must be validated to determine if excess voids or a bad method of preparation influenced the test response and data. The following tests were conducted to answer this question as well as determine a method to apply the adhesive and maintain proper alignment. The combination of resin/adhesive and type of FRP will be investigated in this section.

Three different methods were developed and tested. The reinforcing bars were 1.429-cm- (0.562-inch-) diameter, sand-coated GFRP 20.32 cm (8 inches) in length. The wood specimens were of white oak, 5.08 by 10.16 by30.48 cm (2 by 4 by 12 inches). The wood was cut into two pieces, and the holes were drilled as specified in the three descriptions of the test specimens (S-1, S-2, and S-3) that follow (see figure 82). A two-part phenolic resin and GFRP vinlyester reinforcing bar were used for all three specimens.

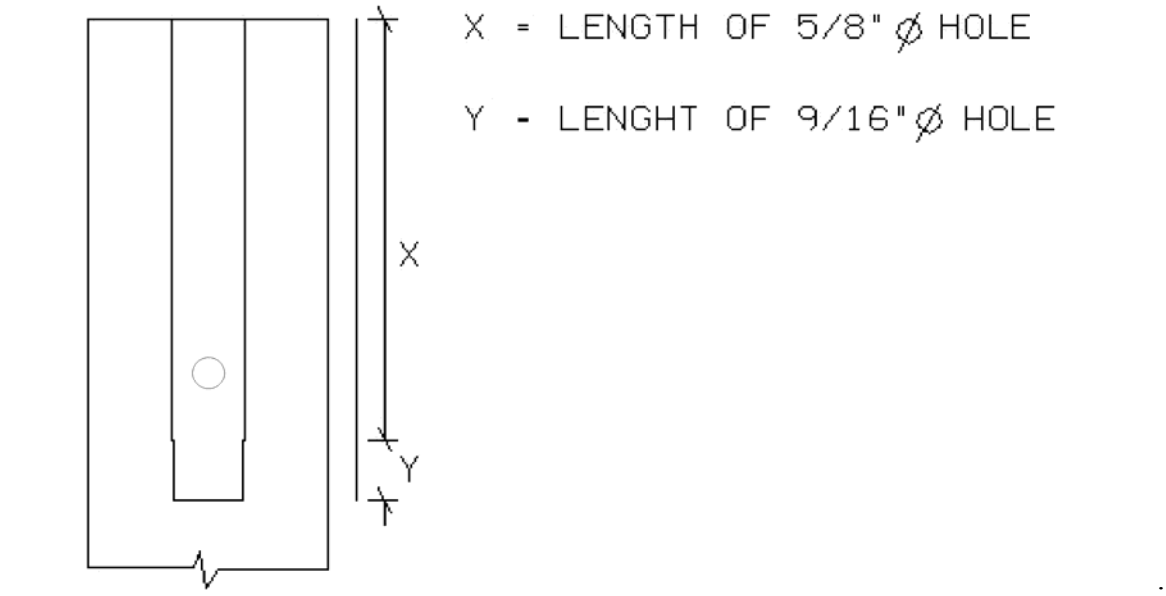

1 inch = 2.54 cm

Figure 82. Illustration. Side view of test specimens.

Specimen S-1:

x = 9.842 cm (3.875 inches)
y = 0.318 cm (0.125 inches)

A 0.556-cm (0.219-inch) bleeder/injection hole is drilled at 9.52 cm (3.75 inches) from the point where the specimen was cut into two pieces on both sides to allow for the injection of resin into the specimen and to allow for the excess to escape. The y-dimension was used to maintain proper alignment until the resin had time to cure. The following steps were used for specimen S-1:

1. Filled from one side of the specimen with resin and hardener combination.

2. Inserted GFRP bar into the side that was full of resin and removed excess resin.

3. Filled the opposite side with resin and hardener combination.

4. Inserted the side with the bar into the opposite side and clamped the specimen together, then removed excess resin.

5. After the specimen was clamped together, 10 ml (0.61 in^3)of resin and hardener were injected into the specimen. Once the resin started exiting from the bleeder hole on the opposite side, injection of the resin was discontinued.

6. Specimen was left for the resin to harden for 1 hour; at that time resin and hardener were injected into the bleeder hole. The specimen took an additional 4 ml (0.24 in^3) before it started to escape again.

Specimen S-2:

x = 8.89 cm (3.5 inches)
y = 1.27 cm (0.5 inches)

The 0.556-cm (0.219-inch) bleeder/injection holes were drilled at 8.572 cm (3.375 inches) from the point where the specimen was cut into two pieces of both sides. The following steps were used for S-2:

1. GFRP bar was inserted into the specimen and both sides were clamped together without any adhesive.

2. Resin and hardener were injected into the through the bleeder hole until the mixture started to escape through the opposite hole. Approximately 12 ml (0.73 in^3) was used to fill the cavity.

3. Specimen was left to harden for 1 hour.

4. No additional resin and hardener was needed.

Specimen S-3:

x = 9.52 cm (3.75 inches)
y = 1.9 cm (0.25 inches)

The 0.556-cm (0.219-inch) bleeder/injection holes were drilled at 8.89 cm (3.5 inches) from the point where the specimen was cut into two pieces of both sides. The following steps were used for S-2:

1. GFRP bar was inserted into the specimen and both sides were clamped together without any adhesive.

2. Resin and hardener were injected into the through the bleeder hole until the mixture started to escape through the opposite hole. Approximately 12 ml (0.73 in^3) was used to fill the cavity.

3. Specimen was left to harden for 1 hour.

4. Approximately 2 ml (0.12 in^3) of resin and hardener were injected into the specimen through the bleeder hole.

A.2.2. Discussion

The specimens were allowed to cure for 24 hours. They were then cut into varying lengths ranging from 1.27 to 4.44 cm (0.5 to 1.75 inches) thick to determine if the GFRP reinforcing bar was aligned on the inside of the specimen and the amount of voids, if any. S-1 displayed little to no voids on the cuts that were made on cross section close to the bleeder holes. There were also few voids between the resin and GFRP. When the cuts were made at the center of specimen,

voids were present and it was discovered that the bars were not aligned. S-2, on the other hand looked good, the bar was aligned the entire length of the specimen, and voids were almost nonexistent. The larger value of y was determined to be the reason the bar was aligned and the placement of the bleeder hole in the y part and not the x part was also desirable to avoid voids. The results of S-3 were very similar to those of S-1. Even though there were no voids in S-2, there appeared to be no bond between the GFRP bar and resin.

After these tests were conducted, it was determined that phenolic formaldehyde is not the most desirable resin to use for this application with the vinlyester GFRP bars. The phenolic would be the most desirable if a reinforcing bar made with a phenolic matrix could be used, but they are not readily available on the market. The purpose of developing these methods is to use them in real-world applications. Since vinlyester matrix GFRP reinforcing bars are readily available to the public, an adhesive compatible with vinlyester must be used rather than phenolic.

A.3. PRELIMINARY TENSION TESTS

The following tension tests were conducted to determine the best material combination. The same reinforcing bar was used for all tests. The adhesive was varied to determine which combination is the most desirable for this application.

A.3.1. Preparation of Test Specimens

The next set of experiments was conducted in order to determine the best material combination and expand on what was developed for S-2 in the previous experiments. Specimens were prepared using urethane, epoxy, and acrylic resins. The wood was white oak; reinforcing bars were 1.429-cm- (0.562-inch-) diameter sand-coated GFRP 15.24 cm (6 inches) in length. The wood was approximately 3.81 by 6.35 by 30.48 cm (1.5 by 2.5 by 12.0 inches). The wood was cut transversely into two pieces and the holes were drilled as specified in the following descriptions of the test specimens (S-4, S-5, S-6, S-7, S-9, and S-10).

Specimen S-4:
The resin used for this specimen was a urethane-based, two-part adhesive called PLIOGRIP, manufactured by the Ashland Inc. S-4 was drilled and prepared in the same manner as S-2. The GFRP reinforcing bar was inserted into the specimen, and it was clamped before the application of the adhesive. The PLIOGRIP was injected into the bleeder holes until it could be seen coming from the opposite bleeder hole.

Specimen S-5:
The same materials and method as used for S-4 was used on this specimen. The PLIOGRIP was inserted into the drilled hole before the GFRP reinforcing bar was inserted. It was then clamped and more adhesive was injected until it escaped from the bleeder hole.

Specimen S-6:
A two-part epoxy resin system was used for the adhesive in this specimen. The drilling of the holes was the same as S-2. The primer coat was applied to the GFRP bar and the inside of the holes and allowed to stand for 24 hours. The bar was then inserted and the specimen was

clamped without the application of the adhesive. The epoxy was then injected into the specimen by the bleeder holes until it was seen coming from the opposite bleeder hole. The epoxy adhesive used was much more viscous than the PLIOGRIP.

Specimen S-7:
This specimen was done in the same manner as S-6 with the same epoxy system.

Specimen S-9:
An acrylic resin system was used for this specimen. The specimen was drilled and put together with the same method as S-2. The adhesive did not require a primer coat.

Specimen S-10:
The urethane-based PLIOGRIP was used for this specimen. The holes were drilled in the same manner as S-2. For this specimen, a new method was used to keep the bar aligned on the inside of the specimen. A washer with an inside diameter of 1.429 cm (0.562 inch) and outside diameter of 1.588 cm (0.625 inches) was placed on the GFRP bar at the middle. The bar was then inserted into the specimen and the same procedure as S-2 was followed.

A.3.2. Discussion

Uniaxial tension tests were performed on the GFRP reinforced wood samples using a 889.6-kN (200-kip) capacity Baldwin Universal Testing Machine. No strain data were taken; the only concern was the bond strength. Load values were taken manually from the Baldwin machine. Bond strength of the specimens was determined. The bond strength or failure was defined as the load divided by the circumferential area of the embedded length of the GFRP rebar in one side (loaded end) of the test specimen, while bond failure was defined as the load at which the specimen could not sustain any additional loading. Failure was at the adhesive/timber interface. The bond strengths of the specimens are shown in figure 83.

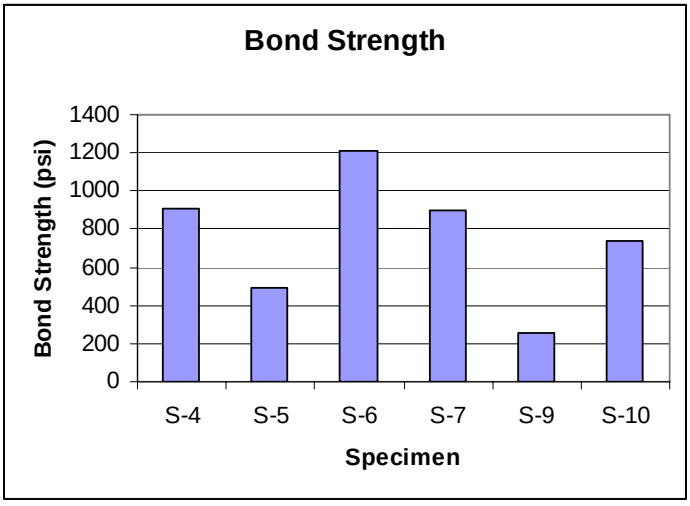

1,000 psi = 47.9 kPa

Figure 83. Chart. Bond Strength.

In figure 83, it can be seen that both of the specimens prepared with epoxy performed very well. The specimens (S-4 and S-10) that were prepared with PLIOGRIP had adequate strength as well. The acrylic did not perform as well as the PLIOGRIP and the epoxy adhesives. S-10 had near perfect alignment of the bar on the inside of the specimen, but its bond strength was lower than that of S-4. This is because of the fact that the washer did not allow the adhesive to pass freely through to allow for equal distribution. S-5 was found to have voids after inspection; the method used for S-5 will not be used again.

A.3.3. Conclusion

The best method to use is S-10; even though it did not have the highest bond strength it has the most potential for field implementation. If the adhesive can pass freely through the washer while it maintains alignment, the bond strength will be much higher. The resin to be used with the vinlyester-matrix, sand-coated GFRP bars is PLIOGRIP. Although epoxy had the highest bond strength, it was not high enough to warrant its use and for reasons to be discussed in the next section. This round of experiments has established the resin/FRP combination to use and the preferred method of application. Further test will be done to verify these test results. The following section will discuss tension tests conducted on phenolic FRP reinforcing bars with a phenolic resin and vinlyester GFRP reinforcing bars with phenolic resin.

A.3.4. Urethane Versus Epoxy

The urethane adhesive PLIOGRIP was chosen as the adhesive for all strengthening methods developed for this project. Why was PLIOGRIP chosen when the preliminary tension test results showed the greater bond strength was achieved with the epoxy adhesive? Several other factors play a major role in the choice of the right adhesive; strength alone will not achieve desired results. The first decision that needs to be made is which adhesive is most compatible to wood and vinlyester matrix GFRP. In this situation both the urethane and epoxy are compatible. The next comparison that needs to be made is the general properties and which adhesives' properties are more closely related to those of wood and the GFRP. Urethanes have higher shear strength, peel strength, and are more flexible. Epoxies have better moisture resistance and solvent resistance. The adhesives have about the same creep resistance, and urethanes are slightly better in impact strength.[23] The nature of the repairs will cause the bond line to be on the order of 0.159 to 0.318 cm (0.062 to 0.125 inch). This is acceptable for a urethane adhesive but will cause a cohesive or brittle failure in the epoxies. Due to the broad range of uses in this project, the properties of the urethane are much better suited for use with wood and GFRP.

Considering this is a historic preservation project, the impact the adhesive will have on the materials it comes into contact with is a very important factor. The epoxy tested has a very low viscosity and acts almost like paint on what it comes into contact with. Urethane, on the other hand, has higher viscosity than epoxy and can be wiped from the material it comes into contact with before it sets.

A.4 TENSION TEST

A final comparison was made between the two most desired adhesive reinforcing bar combinations. The tests were conducted on small-scale wood samples that more closely replicate tension members that would be found in a truss on an existing covered bridge.

A.4.1. Preparation of Test Specimens

The tension members consisted of white oak at 12 percent MC that was air-dried at the West Virginia University Forest saw mill. A 12 percent MC was selected to replicate MC levels typically found in timber-covered bridges (e.g., 12–15 percent). The test specimens were cut into a dogbone shape with dimensions prorated to ASTM test standards for tensile strength parallel to the grain. The ends of the test specimens were 3.17 by 8.89 cm (1.25 by 3.5 inches), tapering down to a constant cross section of 3.17 by 3.17 by 15.24 cm (1.25 x 1.25 x 6.0 inches) with an overall specimen length of 91.44 cm (36 inches).

In order to insert the GFRP bars into the specimens, the specimens were cut transversely in two halves and holes drilled into each end. Two different-sized diameter holes (1.27 and 1.59 cm (0.5 and 0.625 inches)) were drilled to accommodate two sizes of diameter bars (# 3 and # 4). The sizes of the holes were drilled slightly larger than the diameter of the bar to allow for 0.159 cm (0.062 inch) of resin on all sides of the composite bar. Two different depths (10.16 and 20.32 cm (4 and 8 inches)) were also drilled into each end so that two different bond lengths (20.32 and 40.64 cm (8 and 16 inches)) could be tested.

To prevent premature tensile failure (i.e., grip failure), the ends of the specimens were reinforced using GFRP composite fabrics. Initially, a phenolic resin was used as the adhesive and a GFRP with a vinylester matrix bar as the reinforcement. A primer coat of the phenolic resin (without the hardener or formaldehyde) was applied to the inside of the holes and allowed 24 hours to dry. The drilled holes were filled with the resin and hardener (i.e., phenol formaldehyde in a 5:1 mix ratio, respectively). After the holes were filled, the bars were soaked in the mixture and inserted into each of the cut ends of the specimens. The specimens were then clamped at the joint by a C-clamp, placed into a bar furniture clamp, and left for another 24 hours to cure before testing.

A.4.2. Testing

Uniaxial tension tests were performed on the GFRP-reinforced wood samples using a 889.6-kN (200 kip) capacity Baldwin Universal Testing Machine. Strain gauges 5.08 cm (2 inches) long were mounted on the test specimen at midheight. Initially, strain and load measurements were taken manually every 226.8 kg (500 pounds) from the Baldwin machine.

A.4.3. Results

The results of the tension tests of the GFRP-reinforced wood specimens revealed no chemical cross-linking (i.e., bond) between the phenolic resin and the vinylester matrix of the GFRP. The specimens simply separated under nominal loads (i.e., less than 228.6 kg (500 pounds)).

The reason the project used phenolic resin as an adhesive is because of its high chemical cross-linking of the resin/primer combination with wood and its resistance to degradation and harsh environment. Also, the authors' experience and high levels of success in improving the strength, stiffness, and durability of timber railroad ties and stringers in three timber railroad bridges further reinforced our approach that phenolic is an ideal resin/primer system for use with varying values of viscosity.

However, to develop adequate bond between the FRP rebar and the wood substrate, our approach included changing the adhesive type and also changing the rebar matrix type. Two additional tension tests were conducted:

1. GFRP bar with a phenolic matrix and phenolic resin.

2. Urethane-based adhesive (PLIOGRIP, manufactured by Ashland Inc.) with a GFRP bar and a vinylester matrix.

The results of the second set of tension tests using a different resin and matrix are presented in table 11. Comparisons of strength and stiffness values are made with an unreinforced (solid) wood specimen.

Table 11. Observed strength and stiffness.

Specimen	Tensile Strength (kip)	Bond Failure (ksi)	Young's Modulus (msi)
Phenolic resin/ Phenolic matrix	2.1 (953 kg)	1.35 (9.3 mPa)	N/A
PLIOGRIP resin/ vinylester matrix	2.6 (11,804 kg)	1.66 (11.4 mPa)	1.7 (11,713 mPa)

1 kip = 4.448 kN; 1 ksi = 6,890 kPa; 1 msi = 6,890 mPa

A.4.4. Discussion

GFRP bars made with the phenolic matrix and bonded with the phenolic resin exhibited a relatively high tensile strength (tensile force over full cross-sectional area of wood/GFRP, i.e., 1.35 ksi (9.3 mPa)) and eventually leading to bond failure. The 1.35 ksi value can be improved especially since the GFRP bar made with a phenolic matrix was hand-manufactured, which resulted in an uneven bar preventing an acceptable bond and force transfer. Strength using the PLIOGRIP adhesive with a GFRP bar with a vinylester matrix carried the highest tensile strength and bond failure stress (1.66 ksi (11.4 mPa)). The ultimate tensile strength of the solid wood specimen was found to be 11.54 ksi (79.51 mPa). Allowable design values (e.g., NDS) for the tensile strength of wood are of the order of 0.6 to 0.8 ksi. Therefore, the GFRP bars with phenolic matrix resulted in wood failure strength of 1.66 ksi (11.4 mPa) which is approximately 2.5 to 3 times higher than the design strength of wood. Thus the preliminary tension tests are a success. Upon further examination of the wood member cross section, we noted that the resin bonding and penetration were less than satisfactory, which are being improved in the next series

of tests. We believe that further improvements will result in tensile strengths of 3-4 ksi.(21-28mPa).

The stiffness of the solid wood specimen was measured to be 1.96 msi,(14.5 mPa) which is typical of white oak. The stiffness for the PLIOGRIP adhesive with a GFRP bar and vinylester matrix specimen was measured to be 1.7 msi (11.7 mPa) which is slightly lower than the solid wood specimen, as anticipated.

APPENDIX B—ANNOTATED BIBLIOGRAPHY

Strengthening Historic Covered Bridges To Carry Modern Traffic

Submitted as Contract Requirement for
FHWA Contract No. DTFH61-00-C-00081

B.1. INTRODUCTION

The researchers have conducted an intensive search of the available literature relevant to the strengthening historic covered bridges. The literature review was performed from various sources such as books, pamphlets, magazines, journals, Internet sites, reports, agencies, etc. The information gathered from these sources was reviewed, synthesized, and compiled for relevance to the strengthening of historic covered bridges. The search was performed under the following aspects of the project:

- Composite reinforcement of timber members.
- Durability of FRP reinforcement for wood.
- Debonding of beams reinforced with FRP plates.
- Timber joints with composites.
- FRPs in bridge applications.
- Repair of wood member.
- Nondestructive evaluation of timber bridges.

B.2. LITERATURE REVIEW STRATEGY

The literature search document was prepared using keywords on various search databases. The list of keywords is given below:

- Covered bridges.
- Historic bridges.
- Preserving historic bridges.
- Historic preservation.
- Historic preservation through modern methods.
- Bridges strengthened with FRPs.
- Strengthening historic bridges.
- Strengthening historic bridges with FRPs.
- Bridges with pultruded FRPs.
- Timber reinforced with FRPs.
- Timber with composites in bending, shear.
- Timber reinforcement.
- Timber and pultruded FRPs.
- Reinforced timber joints.

B.3. ANNOTATED BIBLIOGRAPHY

The annotated bibliography contains information such as title and authors for the source; citation of the source; a brief summary of what the paper deals with; aim, which gives the relevance of the citation; and the pros/cons of the literature reviewed.

The following section presents an annotated bibliography pertinent to the strengthening of historic covered bridges. The annotated bibliography provides a brief overview of the research conducted by various authors on several aspects related to strengthening historic covered bridges using FRPs.

B.3.1. Composite Reinforcement of Timber Members

Title: "Composite Reinforcement of Timber in Bending"

Author: K.C. Johns and S. Lacroix

Citation: *Canadian Journal of Civil Engineering*, vol. 27, 2000

Summary: A promising use for high-performance composite materials is the reinforcement of timber beams. This paper studied the use of carbon and glass fibers to reinforce sawn timber sections. Consideration was given to strength phenomena of commercial timber alone and in reinforced sections in bending and shear. It discussed anchorage length in regard to composite strips applied to the underside of simple beams. Experimental results were presented for 3 geometries of reinforcement using matched samples of 25 pairs of beams, reinforced and not. Results established that, in the composite section, the wood itself showed strength increase and that the increase in moment resistance of the reinforced beams was far greater than that predicted by simple models.

Aim: This paper showed the increases in strength that could be achieved with composite materials.

Pros/Cons: The authors show that the increase in external bond strength of sawn timber members with glass and carbon fibers show good results. This method would not be appropriate for use on historic structures; and the methods need to be tested on full-scale members. The member test size was equivalent to a 2 by 4 (5.08 by 10.16 cm).

Title: "Strengthening of Wood Beams Using FRP Composites"

Author: H.J. Dagher and R. Lindyberg

Citation: Composite Fabricators Association Conference, September 2000

Summary: The paper presented the reasons FRP reinforcement should be used over metallic reinforcement to achieve the desired strength, stiffness, and ductility. The paper showed that as little as 3 percent E glass bonded to the tension side of the beam could increase bending strength in wood laminated beams by as much as 100 percent. By using GFRP reinforcement, the wood requirements could be reduced, and in some conditions, material costs could be reduced.

Aim: This paper showed why FRPs should be used over metallic reinforcement and that high-grade glulam could be produced using low-grade wood.

Pros/Cons: The research focused on the use of glulam beams and not sawn timbers.

Title: "Strength and Stiffness Performance of FRP Reinforced White Oak"

Author: Zeno A. Martin, Joe K. Stith, and Dan A. Tingley

Citation: *Proceedings*, World Conference on Timber Engineering, Whistler Resort, British Columbia, Canada, July 31–August 3, 2000

Summary: The paper presented results of tests conducted to determine the performance characteristics of vertically laminated white oak, as used in truck trailer decks, reinforced with high-strength FRP. Significant strength and stiffness increases were shown for other such wood-FRP composites such as FRP-reinforced, glue-laminated timber, although most previous research focused on softwoods. Test results indicated that FRP-reinforced white oak decks provide many of the same benefits as FRP reinforced softwoods.

Aim: This paper showed that elastic theory was shown to predict stiffness within 15–25 percent of actual test data. The test data were higher than the predicted values.

Pros/Cons: The authors used standard data for the properties of the FRPs instead of values supplied by the manufacturer or from test data. All of the members tested showed some increase in performance over an unreinforced specimen.

Title: "Timber Beams Strengthened with GFRP Bars: Development and Applications"

Author: Chris Gentile, Dagmar Svecova, and Sami H. Rizkalla

Citation: *Journal of Composites for Construction*, vol. 6, no. 1, February 2002

Summary: Repair and rehabilitation of infrastructure is becoming increasingly important for bridges due to material deterioration and limited capacity to accommodate current load levels. An experimental program was undertaken to study the flexural behavior of creosote-treated, sawn Douglas fir timber beams strengthened with GFRP bars. The

program tested to failure 22 half-scale and 4 full-scale timber beams strengthened with GFRP bars. The percent reinforcement ratios were between 0.27 and 0.82 percent. Additional unreinforced timber beams were tested as control specimens. The results showed that using the proposed experimental technique changed the mode of failure from tension to compression; flexure strength increased by 18 to 40 percent. Research findings indicated the use of near-surface GFRP bars overcame the effect of local defects in the timber and enhanced the bending strength of the members. Based on the experimental results, an analytical model was proposed to predict the flexural capacity of both unreinforced and GFRP-reinforced timber beams.

Aim: This paper presented a method for strengthening sawn timber beams using GFRP bars on half- and full-scale members.

Pros/Cons: The percent reinforcement was only between 0.27 and 0.82 percent of the total cross-sectional area. So the percent increases in capacity compared to the percent reinforcement posed a significant weight-to-strength increase.

Title: "Wood Reinforced with Pultruded Fiber Reinforced Composites"

Author: Douglas J. Gardner, Michael P. Wolcott, and Uma M. Munipalle

Citation: *Proceedings*, Pacific Rim Bio Based Composites Symposium, November 9–13, 1992, pp. 263–269

Summary: This paper presented a way to increase strength and stiffness of glulam beams using synthetic fiber reinforcement. Pultruded composites can also be laminated with wood in glulam beams using traditional manufacturing techniques. The pultruded composite plates can replace the high-quality wood needed for the compression or tension laminates. Several different resin/composite combinations were investigated, including polyester or vinylester bonded using epoxy, resorcinol-formaldehyde, and emulsion isocyanate adhesives. The results presented in the paper showed that FRP composites could be successfully bonded to wood to increase strength and stiffness.

Aim: The paper showed that FRP could be successfully used in glulam beams.

Pros/Cons: Current tests show that phenolic adhesives are the most compatible with wood. The adhesives used for the most part are not very ductile, applications requiring wood to be bonded with vinylester will require a ductile adhesive.

Title: "Sawn and Laminated Wood Beams Wrapped with Fiber Reinforced Plastic Composites"

Author: Hota V. S. GangaRao, P.E.

Citation: *Wood Design Focus*, Fall 1997

Summary: There are many applications for FRP composites such as reinforcement of wood and creating hybrid structural components. This paper presented strength, stiffness, and accelerated-aging of sawn and laminated wood beams wrapped with woven glass FRP fabric or glass fibers bonded in place with polymeric resins. The methods used to wrap the beams were also presented. The paper showed how the failure of wrapped beams was progressive, unlike the catastrophic failure of unwrapped beams. There was also increased ductility that could be attributed to the glass fibers carrying load past the failure point of the wood core. Emphasis of this method of strengthening wood beams was characterized by selection of wrapping materials. An increase in strength and stiffness of between 40 and 70 percent was achieved.

Aim: This paper presented a method of rehabilitating and strengthening wood members that could effectively and reliably increase strength and stiffness.

Pros/Cons: Wrapping is the preferred method for strengthening timber beams, but the drawback is that it diminishes the historical integrity of the member it is reinforcing.

Title: "Strength and Stiffness Evaluations of Wood Laminates with Composite Wraps"

Author: S. S. Sonti, Hota V. S. GangaRao

Citation: 50th Annual Conference, Composites Institute, The Society of the Plastics Industry, Inc., January 30–February 1, 1995

Summary: This paper discusses the use of composite wrap on wood laminates. As part of the research, two different wrapping materials were used—glass and carbon reinforced composites. Tests were conducted on six glulam beams of either 3.05 or 6.10 m (10 or 20 ft) in length and wrapped with the glass or carbon composite. A net-like fiber architecture of the glass wrap was compared to the cloth fiber architecture. The stiffness increases were found to be relatively low compared to the relatively high increases in strength. The failure modes of the beams tended to be progressive plastic mode. The wrapping material kept the beams from failing catastrophically.

Aim: This paper presented a method of rehabilitating and strengthening wood members using different types of fibers and fiber architecture.

Pros/Cons: The stiffness increases for the beams tested in this paper were lower than what would be expected but the increases were very good. As stated earlier, wrapping is the preferred method for strengthening timber beams, but the drawback is that it diminishes the historical integrity of the member it is reinforcing.

B.3.2. Durability of FRP Reinforcement for Wood

Title: "Durability of FRP Reinforcement for Wood"

Author: Beckry Abdel-Magid, Eoin Battles, Habib Dagher, and Mohamed Iqbal

Citation: *Proceedings*, 1999 International Composites Expo; Cincinnati, OH, session 22-C

Summary: This paper examined a wood-compatible E-glass phenolic FRP system that was designed and fabricated for the reinforcement of glulam beams. In this paper, partial results were presented that showed that E-glass/phenolic FRP without surface treatment was affected by aggressive media such as moisture, alkali, and salt water. A total of 34 panels were used. The primary degradation seemed to be in the reinforcing fibers rather than in the phenolic matrix. Although the tests presented in the paper were conducted before the FRP's final processing stage, it still retained more than 80 percent of its mechanical properties.

Aim: This paper showed the durability of wood reinforced with FRP.

Pros/Cons: Although the results presented in the paper showed promising results, they were incomplete at the time the paper was published.

Title: "Durability of Wood-FRP Composite Bridges"

Author: E. Battles, H. G. Dagher, and B. Abdel-Magid

Citation: 5th International Bridge Engineering Conference; Tampa, FL; April 3–5, 2000

Summary: Although FRP composite materials offer excellent mechanical properties and corrosion resistance, their susceptibility to the synergistic effects of stress and environmental weathering is a hindrance to their acceptance as a viable alternative to traditional materials. This paper characterized the durability of a specific formulation of wood-compatible pultruded E-glass/phenolic composite. The test specimens were subjected to durability tests, per the International Conference of Building Officials'(ICBO) Acceptance Criteria 125. This criteria states that all FRP materials should retain 90 percent of their baseline strength after 1000 hours of environmental exposure, and 85 percent after 3000 hours. The test specimens narrowly missed this requirement. This indicated that the primary degradation occurred in the fibers and not in the resin matrix.

Aim: This paper showed that the durability of wood reinforced with FRP needs to be closely examined before its use in a particular project.

Pros/Cons: The performance of the test specimens did not perform to standard. This needs to be further studied and understood before this combination of FRP and adhesive can be used in a harsh environment.

B.3.3. Debonding of Beams Reinforced with FRP Plates

Title: "Significance of Midspan Debonding Failure in FRP-Plated Concrete Beams"

Author: Wendel M. Sebastian

Citation: *Journal of Structural Engineering*, vol. 127, no. 7, July 2001

Summary: Reinforced concrete beams enhanced for flexure with adhesively bonded, reinforced-polymer plates were susceptible to a brittle form of failure defined by delamination of the cover concrete attached to the adhesive that caused the plates to debond from the beam. Data from large scale experiments were presented to show that midspan debond action was triggered by high shear stresses from the plates transmitted through the adhesive to the cover concrete. These stresses arose initially from the tension stiffening in the cracked concrete. The shear span of the external load and the stiffness of the plate were cited as parameters that could influence whether end peel or midspan debond would occur in practice.

Aim: This paper described and showed how and when midspan debond would occur.

Pros/Cons: The author showed in detail two modes for which FRP plates debond from concrete. This same phenomenon of debonding occurred in timber beams with FRP plates bonded adhesively.

B.3.4. Timber Joints with Composites

Title: "Mechanical Behavior of Fiberglass Reinforced Timber Joints"

Author: Chi-Jen Chen

Citation: *Proceedings*, World Conference on Timber Engineering, Whistler Resort, British Columbia, Canada, July 31–August 3, 2000

Summary: This paper investigated the mechanical performance of dowel-type timber joints reinforced by fiberglass fabrics. Some critical characteristics such as the anisotropy of wood and splitting failure in structures and joints demand more skill and limit an engineering design. According to the paper, fiberglass reinforcements lead to a higher performance and provide a good safety factor to the timber joints.

Aim: This paper showed the improvements in dowel-type timber joints achieved by using fiberglass fabric.

Pros/Cons: Through this paper, the author showed how several design parameters can be optimized (e.g., edge distance and end distance) while optimizing the capacity of the joint.

Title: "Efficient Timber Connections Using Bonded-in GFRP Rods"

Author: J.G. Broughton and A.R. Hutchinson

Citation: *Composites in Construction*, eds., Figueiras, et al., Swets & Zeitilinger, Lisse, ISBN 90 2651 858 7, 2001, pp. 275–280.

Summary: This paper investigated a comprehensive experimental and numerical investigation into the fundamental material and joint geometry characteristics of both steel and GFRP rods bonded into structural composite lumber. Joint parameters studied included steel and GFRP rod materials, rod length, rod diameter, bond line thickness, and multiple rods with multiple spacing. In addition, the adhesive type, its performance, and the timber moisture content at the time of bonding were all studied. It was found that GFRP rods performed as well as steel rods, and epoxy adhesives outperformed all others tested.

Aim: This paper showed that GFRP rods could be used in place of steel rods in timber connections.

Pros/Cons: The paper showed that GFRP performed as well as steel, but several factors were overlooked. The authors did not try to match the properties of the GFRP rods to that of the adhesive. If this were the case, the epoxy should not have outperformed the urethane or the phenolic.

Title: "Improved Timber Connections Using Bonded-In-GFRP Rods"

Author: Kim Harvey and Martin P. Ansell

Citation: *Proceedings*, World Conference on Timber Engineering, Whistler Resort, British Columbia, Canada, July 31–August 3, 2000

Summary: This paper presented research that dealt with limited technology of bonded in rods in timber connections. In this paper, GFRP rods were used in place of steel rods. Pullout tests were conducted to characterize the bonded-in connection. Initial tests investigated the influence of rod surface preparation, bonded length, glueline thickness, and adhesive type. The results were used to determine standard sample size and fabrication method to be used in later tests. These later tests investigated the effect of moisture content, wood type, and bonding the rod perpendicular to the grain. Moment-resisting and shear joints were also tested using GFRP as the rod material. The rod surface preparation and the thickness of the glueline were found to be very important factors in determining strength of the connection.

Aim: This paper showed that GFRP rods are a very good alternate to steel rods in timber connections.

Pros/Cons: The paper showed that GFRP performs very well. The strength of the connection was limited by surface preparation, glueline thickness, bonded length, and moisture content.

B.3.5. FRPs in Bridge Applications

Title: "Advanced Fiber-Reinforced Polymer-Wood Composites in Transportation Applications"

Author: Habib J. Dagher, Melanie M. Bragdon, and Robert F. Lindyberg

Citation: Transportation Research Board 2002

Summary: This paper presented six wood-FRP composite projects that used three types of technologies developed at the University of Maine. The three types are: tension-reinforced glulam beams with preconsolidated E-glass panels, tension reinforced glulam beams and panels with wet-impregnated E-glass fabrics, and stress-laminated lumber using GFRP tendons. This paper showed that, throughout these six projects, properly designed wood-FRP composites were structurally feasible, durable, and cost effective.

Aim: This paper dealt with the use of FRP-reinforced wood in new construction.

Pros/Cons: In one of the projects highlighted in the paper, FRP was used in a stress-laminated bridge. After 2.5 years of service, the bridge retained 86 percent of its initial prestress.

Title: "FRP-Reinforced Wood in Bridge Applications"

Author: H. J. Dagher and Robert F. Lindyberg

Citation: *Proceedings*, 1st Rilem Symposium on Timber Engineering, Stockholm, Sweden, September 13–15, 1999

Summary: This paper described a probabilistic model that predicted the statistical properties of the strength and stiffness of glulam beams. The program, called ReLAM (for reinforced laminated beams), also calculated allowable bending strength and MOE. The input required was beam layup, reinforcement tensile strength and stiffness, MOE of the laminating stock, the ultimate tensile strength, and the ultimate compression strength. The accuracy of ReLAM was verified through a testing

program. The program accurately predicted the allowable strength within 6 percent and the allowable strength within 7 percent.

Also as a part of the paper, tests were conducted on 90 FRP-reinforced glulam beams that were 6.71 m (22 ft) in length. The results were to determine the accuracy of ReLAM, but they also showed that 3 percent by volume of GFRP reinforcement added to the tension side can increase allowable bending strength by 100 percent.

Aim: This paper showed that a reliable program could be developed to accurately predict strength and properties of glulam beams reinforced with FRPs.

Pros/Cons: More than 500 simulations were run using ReLAM that showed it more accurately predicted western hemlock glulam than Douglas fir.

B.3.6. Repair of Wood Members

Title: "Structural Repair of Timber Using Epoxies"

Author: Richard Avent, P.E.

Citation: *Structure*, Summer 2000

Summary: The paper discussed in detail the development of a successful repair methodology using epoxies. The procedures have been used both in the United States and abroad. The paper presented not only repair methodologies, but also a rational and reliable analysis. The analytical model was developed that corresponded to procedures by which the structural integrity of the epoxy-repaired timber could be reliably predicted. This method of epoxy repairs has been field verified for 15 years and it is very reliable in predicting the after-repair strength of the member.

Aim: This paper is a good source for developing methods of repair of timber members using epoxy.

Pros/Cons: The paper gives repair examples that walk the reader through the analytical model.

B.3.7. Nondestructive Evaluation of Timber Bridges

Title: "Nondestructive Evaluation Methods for Highway Bridge Superstructures"

Author: Udaya B. Halabe, Samer H. Petro, and Hota V. S. GangaRao

Citation: Manual submitted to the West Virginia Division of Highways

Summary: This manual described at length several nondestructive evaluation methods for use in material inspection, as well as structural components with emphasis on bridge superstructures. The manual presented some common nondestructive methods including chain drag and rebound hammer, along with several advanced methods including dynamic characterization, stress-wave techniques, ground penetrating radar, acoustic emissions, and infrared thermography. The manual also presented the advantages and limitations of each method as applied to bridge superstructures.

Aim: This manual was a good source of nondestructive testing methods that could be applied to historic covered bridges.

Pros/Cons: The manual provided the advantages and limitations of each method described.

Title: "Ultrasonic Testing of Barrackville Timber Bridge"

Author: Udaya B. Halabe, Hota V.S. GangaRao, V. Rao Hota, and Samer H. Petro

Citation: Report submitted to Dr. Emory Kemp

Summary: The report presented results on in situ ultrasonic testing of the Barrackville, WV, timber bridge. The field testing was conducted using velocity measurements. The members were tested close to the joints, and the results were used to identify deteriorated joints. The identification of the weak joints enabled the contractor to economically plan for the renovation work of the bridge leading to substantial savings.

Aim: The report was an example of in situ testing that was conducted on a historic covered bridge and was successfully used to renovate the structure.

Pros/Cons: The report was about only one bridge and used only one nondestructive testing technique.

Title: "Testing Historic Bridges with Ultrasound"

Author: David A. Simmons

Citation: *Ohio County Engineer*, no. 2, Summer 1996

Summary: This paper described how ultrasonic testing was used on the Salt Creek Covered Bridge rehabilitation project. The bridge was built in 1876 and is one of the only all wooden Warren truss bridges still standing in the United States. The past method of testing wood members was to sound them with a hammer, which was very unreliable. Researchers at the Constructed Facilities Center at West Virginia University developed a new ultrasonic technique. The system used two transducers

to send and receive sound waves transversely through the wood. The systems were verified by destructively testing a small portion of the badly deteriorated truss. With this system the researchers were able to effectively locate deteriorated portions of the member.

Aim: The paper was an excellent example of how ultrasound was used to help rehabilitate a historic covered bridge.

Pros/Cons: The paper gave a good overview of how this nondestructive method could be used on a historic bridge.

B.4. CONCLUSION

Various issues related to FRP composites and wood, as published by various researchers are summarized herein. As can be seen from the papers reviewed in chapter 2 and in this annotated bibliography, a very limited amount of literature is available on the use of FRP composites with sawn wood and very few documented sources that present results of wood members reinforced with pultruded FRP composites for a historic structure.

REFERENCES

1. Stauch, J., "Union County Covered Bridge Rehabilitation—Case History 15.4," *Timber Bridges: Design, Construction, Inspection, and Maintenance,* U.S. Department of Agriculture (USDA) Forest Service, 1990.

2. Kemp, E. L., "Covered Bridge Research," *Restructuring: America and Beyond*, vol. 2, April 2-5, 1995.

3. McFeely, D., "Bridges hang in balance Counties debate fate of old spans."

4. Crowell, A., "Historic bridge can be saved, but is cost too expensive," Kennebec *Journal*, Augusta, ME, October 23, 2002.

5. Lichtenstein, A. G., "Historic Bridges: Conflict Ahead," *Civil Engineering*, vol. 57, May 1987, pp. 64–66.

6. Jester, T. C. ,"Preserving Historic Bridges," CRM, supplement, vol. 15, no. 2.

7. Kemp, E. L., "The Rehabilitation and Restoration of Historic Bridges," *Historic Bridge Articles*, vol. 1, Emory E. Kemp Collection.

8. "The Secretary of the Interior's Standards for the Treatment of Historic Properties, with Guidelines for Preserving, Rehabilitating, Restoring & Reconstructing Historic Buildings," U.S. Department of the Interior, Washington, DC, 1995, with amendments and annotations, available online at http://www.cr.nps.gov/hps/tps/standguide/.

9. Rogers, H., "Reinforcing Historic Covered Bridges," *Proceedings*, International Bridge Conference, 1987, pp. 87–90.

10. Rich, S., "Uncovering an American Legacy Kentucky's Covered Bridges: Preserving Historical and Architectural Value," *Structure*, September 2001.

11. Ritter, M. A., "Timber Bridges: Design, Construction, Inspection, and Maintenance," USDA Forest Service, 1992, available online at http://www.fs.fed.us/na/wit/WITPages/timberbridgespub.html.

12. Ross, R. J., and M. O. Hunt, "Stress Wave Timing Nondestructive Evaluation Tools for Inspecting Historic Structures, a guide for use and interpretation," USDA Forest Service Products Laboratory General Technical Report FPL-GTR-119, 2000.

13. Pahel, J. E., "Laser Scanning: a Tale of Two Projects," *Structural Engineer*, March 2002.

14. Pullaro, J. J., "Restoring Historic Bridges Using Modern Methods," *Proceedings*, Structures Congress, 1999.

15. Davis, A. G., "Nondestructive Evaluation Helps Maintain Concrete Structures," *Structures*, September 2001, pp. 20–21.

16. Tang, B. T., "Fiber Reinforced Polymer Composites Applications in USA," *Proceedings*, Korea/USA Road Workshop, January 28–29, 1997.

17. "Engineering and Design: Composite Materials for Civil Engineering Structures," technical letter no. ETL 1110-2-548, Army Corps of Engineers, March 31, 1997.

18. Neale, K. W., "FRPs for structural rehabilitation: a survey of recent progress," *Progress in Structural Engineering Materials*, vol. 2, issue 2, August 2000, John Wiley & Sons, Ltd., 2000, pp. 133–138.

19. Lacroix, S., and K. C. Johns, "Composite reinforcement of timber in bending," *Canadian Journal of Civil Engineering*, vol. 27, no.5, 2000, pp. 899–906.

20. Plevris, N., and T.C. Triantafillou, "Creep Behavior of FRP-Reinforced Wood Members," *Journal of Structural Engineering*, vol. 121, no. 2, February 1995, pp. 174–186.

21. Triantafillou, T. C., "Shear Reinforcement of Wood Using FRP Materials," *Journal of Materials In Civil Engineering*, vol. 9, no. 2, May 1997, pp. 65–69.

22. Griggs, F. E., Jr., "Restoration of Cast and Wrought Iron Bridges," *Proceedings*, National Congress on Civil Engineering History and Heritage, September 2001, pp. 201–211.

23. Petrie, E. M., *Handbook of Adhesives and Sealants*, McGraw-Hill, 2000.

24. *National Design Specification® (NDS®) for Wood Construction*, 1997 edition, American Wood Council, Washington, DC, 1997.